Phase equilibria and semiconducting
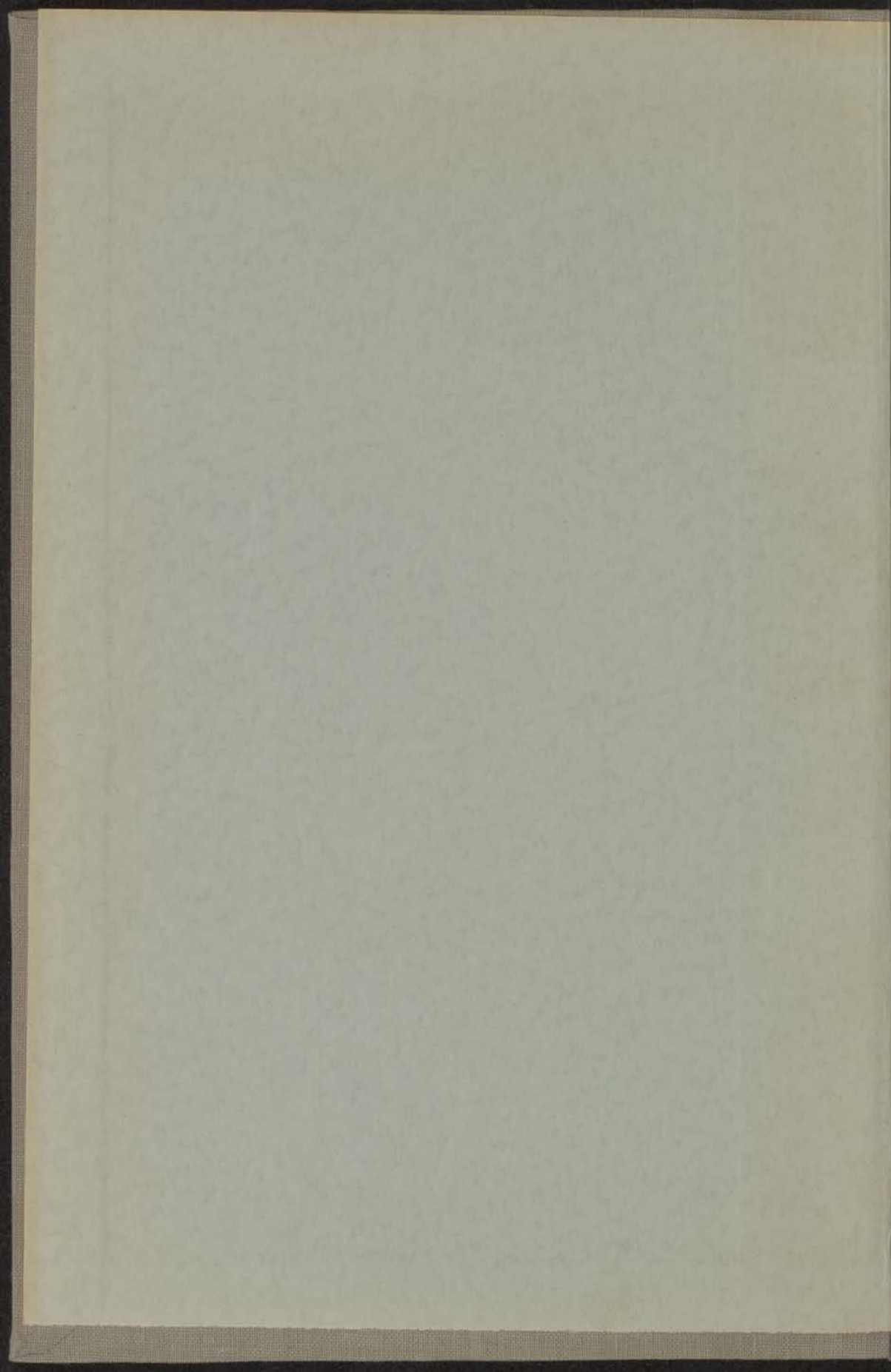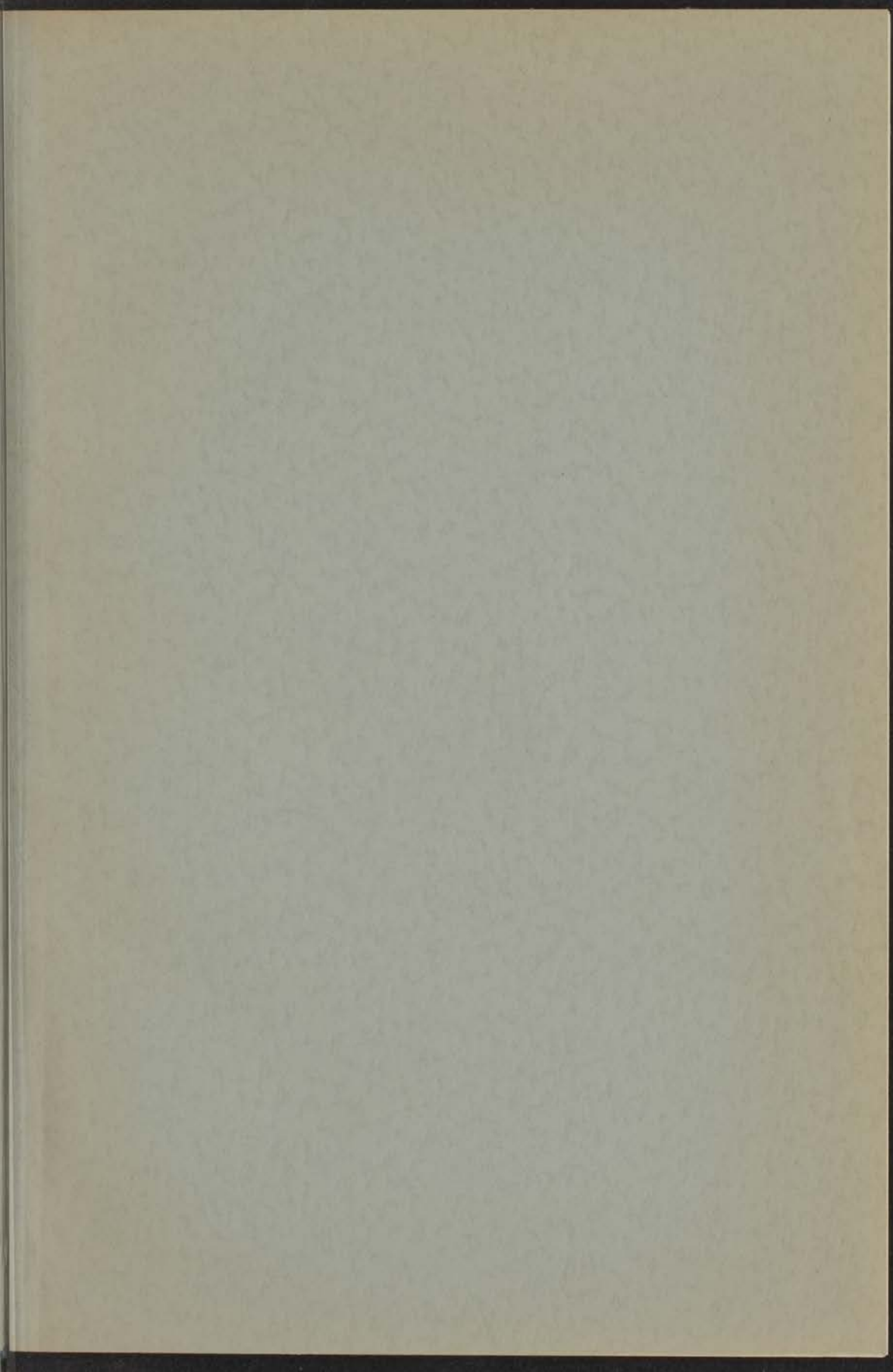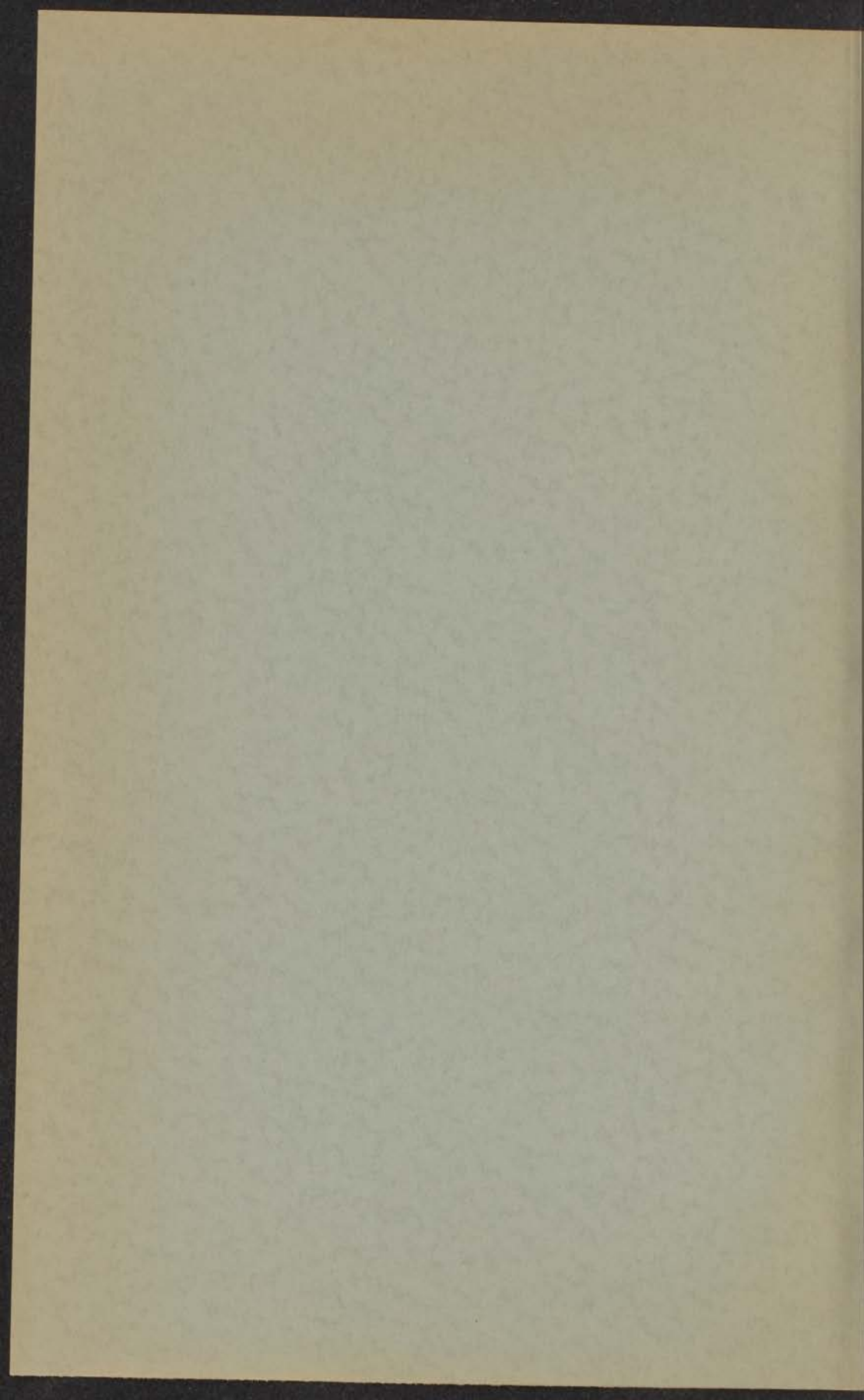# properties of cadmium telluride

D. de Nobel

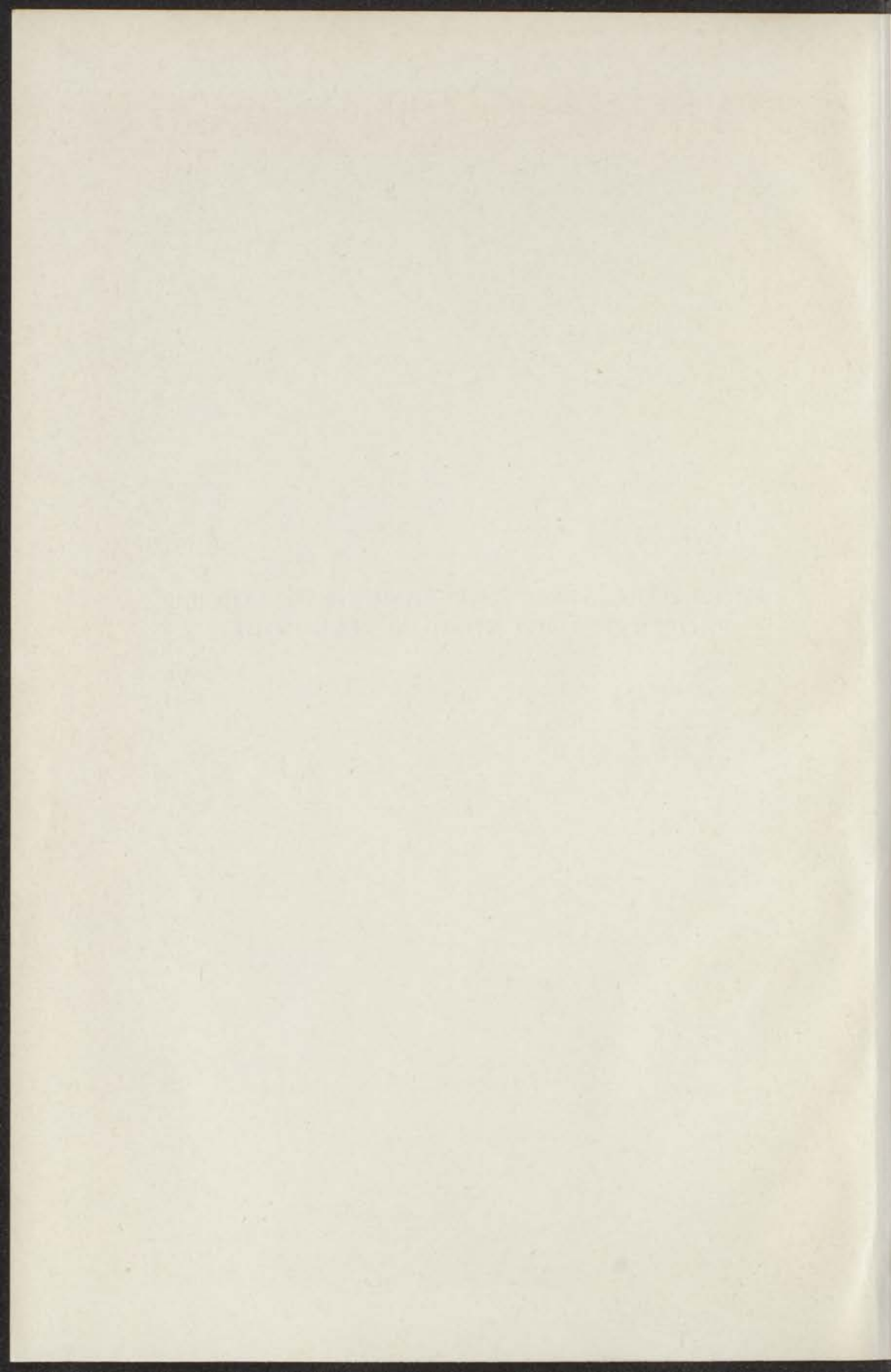# PHASE EQUILIBRIA AND SEMICONDUCTING PROPERTIES OF CADMIUM TELLURIDE

Phase equilibria and semiconducting properties of cadmium telluride

door

Dirk de Nobel

geboren te Sassenheim in 1916

Promotor: Prof. Dr A. E. van Arkel

AAN DE NAGEDACHTENIS VAN
HENDRIK SCHOTSMAN

CONTENTS

CHAPTER 3. THEORETICAL PART

INTRODUCTION

The electrical and optical properties of semiconductors depend on the presence of small concentrations of crystal imperfections, which may be either vacancies and interstitial atoms (so-called native imperfections) or foreign atoms. The concentration of these imperfections is governed by the conditions prevailing during the preparation of the crystals.

In this thesis the relation between the conditions of preparation and the electrical and optical properties will be discussed for CdTe.

Cadmium telluride is a member of the series of compounds usually indicated as the 2-6 compounds, which are compounds built up from elements of the 2nd and 6th sub-group of the periodic table. Of the other members of this group, ZnS has been studied intensively as a phosphor and CdS and CdSe have been studied as photoconductors. Yet various points are still open to discussion. It is hoped that this study will not only lead to an insight in the properties of CdTe itself but that it may also aid in more fully understanding of other substances.

The relation between the conditions of preparation and the concentration of imperfections in a crystal has been put on a quantitative basis by the fundamental work of Schottky and Wagner [1]) which was extended by Kröger, Vink and Van den Boomgaard [2]). These authors applied the theory to CdS and Bloem [3]) applied it to PbS.

Up to now only a small number of publications deal with CdTe. The earlier measurements are restricted to the determination of the phase diagram [4]) and the optical properties of evaporated layers [5]). The width of the band gap as a function of the temperature was determined by Bube [6]) from photoconductivity measurements. The influence of amounts of different foreign atoms on the electrical properties of polycrystalline samples was studied by Jenny and Bube [7]). Appel [8]) measured the temperature dependence of the specific resistance of polycrystalline samples and concluded to a transition from the sphalerite to the wurtzite structure at about 1000 °K. X-ray analysis up to 550 °C only showed the sphalerite structure.

In the following chapters first experimental results will be given regarding preparation, phase diagram, Hall effect and specific resistance as a function of the temperature, Hall effect as a function of the atmosphere over the crystals at various values of the temperature, thermoelectric power, photoconductivity and luminescence (chapter 1). These results will be interpreted in chapter 2, leading to values for the band gap and giving information about the position of various

donor and acceptor levels between the bands. In chapter 3 the equilibria governing the state of the crystals at the temperature of preparation will be discussed. Knowledge of these equilibria enables us to calculate the state of the crystals after quenching to room temperature, which calculation is followed by a comparison between calculated and experimental results. The deviations caused by association and clustering effects will be considered here too. With the aid of the equilibrium constants at high temperatures calculated in this chapter, the deviation from stoichiometry at the three-phase boundary (solidus curve in the T-x diagram) can be calculated. The temperature dependence of some of these constants enables us to calculate energies involved in the exchange of cadmium between crystal and vapour and in the transfer of cadmium from a lattice site to an interstitial position.

An estimate of the covalent and ionic character of CdTe will be given in an appendix.

CHAPTER 1

EXPERIMENTAL PART

1.1. Preparation of CdTe

CdTe was prepared from the elements. The cadmium and the tellurium used contained about 0·01% by weight of various impurities. The compound thus formed needed further purification which was carried out by the method of zone melting [9]).

The preparation of CdTe is hindered by the fact that, although the reaction between the elements already starts at 550 °C, temperatures well above 800 °C are needed in order to get complete reaction. At such temperatures, however, CdTe tends to decompose markedly and no homogeneous phase will be obtained if this decomposition is not prevented.

This can be done in two ways. First, one can prepare CdTe from cadmium and tellurium under a vapour pressure of one of its components. Then the equilibrium

$$CdTe\ (s) \rightleftarrows Cd\ (g) + \tfrac{1}{2}Te_2\ (g)$$
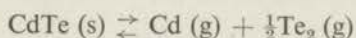
is shifted to the left and decomposition does not occur.

It is also possible to carry out the reaction by which CdTe is formed under a pressure of an inert gas. The latter method has been adopted by us. The apparatus which was used is shown in fig. 1. It consists of a graphite crucible placed inside a silica container which in its turn is placed inside a pressure bomb, the wall of which is cooled. The crucible can be heated by means of a high-frequency induction coil also present inside the bomb. The silica container is closed with a stopper supplied with a tube ending at both sides in a capillary. The perforation of the stopper is necessary in order to make it possible to maintain equal pressures in and outside the crucible.

The tube and the capillary have a double function. Firstly they slow down the diffusion of cadmium and tellurium vapour out of the crucible. Secondly the vapour of the components still escaping from the crucible will condense in the wide section of the tube between the two capillaries which has a rather low temperature. This will prevent contamination of the bomb.

For the reaction an equimolecular mixture of cadmium and tellurium is brought into the reaction vessel, a nitrogen pressure of about 50 atm is applied and then the temperature is raised to about 600 °C. The temperature is kept at this level for 5 minutes, after which the temperature is increased to a temperature slightly above the melting point of CdTe (maximum melting point 1090 °C).
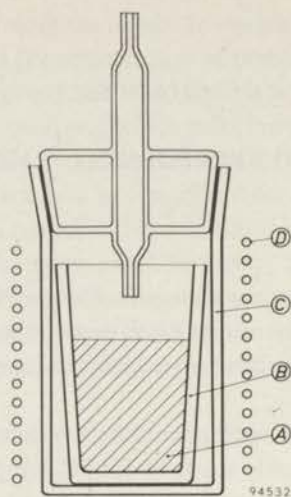
Fig. 1. Silica container (*C*) for the preparation of CdTe from a cadmium and tellurium mixture (*A*) contained in a graphite crucible (*B*). A high frequency coil (*D*) is used for heating.

After cooling down and letting off the pressure a mass of solid, polycrystalline CdTe is obtained.

Although this method can be used to prepare a large amount ($\approx$ 400 g) of CdTe in a rapid way, the growing of single crystals and the influencing of their composition is only possible by applying the other method, viz. by handling the material under definite pressures of the components. A first important question which arises now is in which way the temperature, the composition of CdTe and the partial pressures of its components are related to each other. Information about this question can be obtained by studying the equilibria between the various phases in the system Cd–Te.

1.2. The p–T–x diagram of CdTe

The T–x diagram of the system Cd–Te was determined by Kobayashi [4] (fig. 2). The diagram is rather incomplete.

In the first place no attention was paid to the exact composition of the solid phases. In the second place only points of the liquidus curve corresponding to mixtures rich in tellurium were determined. The reason was that under the conditions at which Kobayashi worked, viz. in open crucibles in a stream of CO_2, mixtures rich in cadmium tend to loose this cadmium very quickly and therefore do not give reproducible results. In order to check Kobayashi's results and to supplement them with points on the cadmium-rich side, some melting experiments were carried out in a closed and evacuated silica tube which was filled
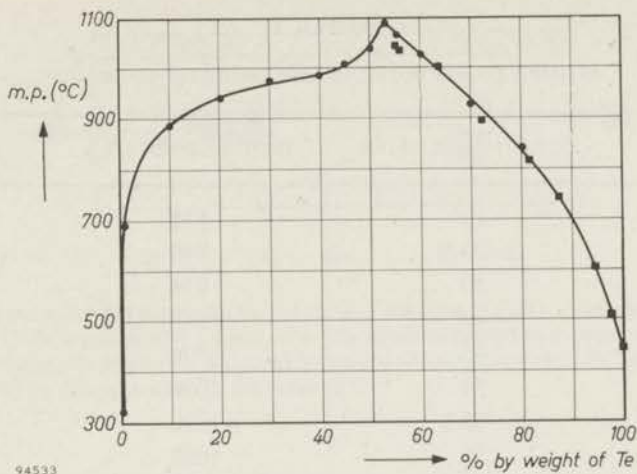
Fig. 2. The T–x diagram of CdTe (■ measurements of Kobayashi, ● our measurements).

94533
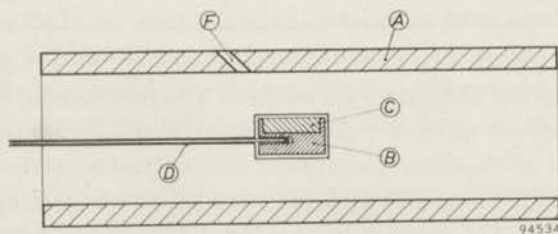
Fig. 3. Apparatus for the determination of the liquidus curve in the T–x diagram. CdTe (C) is contained in graphite crucible (B) enclosed by a silica container (D). A nichrome furnace (A) is used for heating. The temperature is measured by a thermocouple in D, the melting can be observed through a hole in the furnace (F).

with mixtures of cadmium and tellurium of known composition. The tube was filled to such an extent that the amount of material present in the gas phase at the melting temperature could be neglected (fig. 3).

The mixture was completely molten, then slowly cooled down and by observing the surface of the liquid the point at which crystals started to appear was determined. This point was the point of the liquidus curve for the given composition. The accuracy of the measurements was approximately ± 2 °C. The results are shown in table I and fig. 2.

As can be seen from this figure our results deviate from Kobayashi's results for the reasons mentioned above. For tellurium-rich mixtures this deviation is restricted to mixtures containing less than 60% by weight of tellurium. Our maximum melting point (1090 °C) is higher than the value given by Kobayashi

TABLE I

Melting points in the system cadmium-tellurium

% by weight of Te	melting point (°C)
10	885
20	940
30	974
40	983
45	1006
50	1036
53·2	1090
55	1068
60	1024
70	926
80	840

($\approx$ 1041 °C). For the cadmium-rich mixtures a sharp decrease of the melting point can be observed within 5% deviation from the stoichiometric composition (53·2% by weight of tellurium). For a larger excess of cadmium the melting point decreases gradually, falling again sharply when the composition approaches the pure cadmium side. The sharp drop near the stoichiometric composition indicates a tendency of the liquid phase to separate into two phases: one with a composition close to Cd:Te = 1:1 and one which consists mainly of pure cadmium. Though less pronounced, the same phenomenon is also indicated by the shape of the three-phase line in the p–T diagram (fig. 5), viz. close to the maximum melting point at the cadmium-rich side.

The T–x diagram is the projection of the three-phase blade on the T–x plane. One can also study the p–T diagram which is the projection of the three-phase blade on the p–T plane.

Whereas the first gives information regarding the composition in the three-phase equilibria, the latter gives information regarding the corresponding pressures.

The p–T diagram can be determined by observing the temperature at which CdTe in equilibrium with a definite cadmium or tellurium pressure starts to solidify. The experiment was performed in a double furnace system as shown in fig. 4. By placing CdTe at the left-hand side at a temperature T_1 and a piece of cadmium metal at the right-hand side at a temperature T_2, the cadmium pressure over CdTe will be equal to the cadmium pressure corresponding to T_2 if $T_2 < T_1$. As will be seen furtheron (section 1.3) this is only true if $(p_{Cd})_{T_2}$ is larger than the
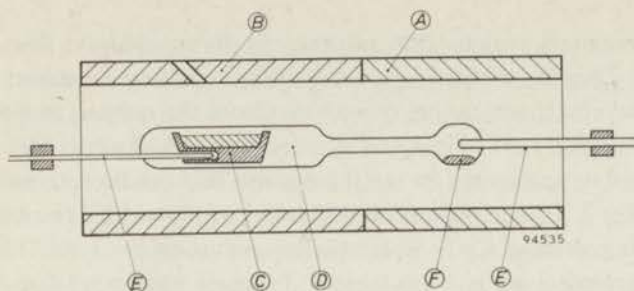
Fig. 4. Apparatus for the determination of the *p–T* diagram of CdTe. A graphite crucible (*C*) containing CdTe is enclosed in a silica tube (*D*) which is heated in a double furnace system (*A, B*). The cadmium pressure is produced by a piece of cadmium metal (*F*). The temperatures are measured by thermocouples in the tubes (*E*).

cadmium pressure of CdTe at the composition at which P_{total} ($= p_{Cd} + p_{Te_2}$) shows a minimum, provided that p_{CdTe} is so low that it can be neglected.

Maintaining a fixed cadmium pressure, the temperature T_1 is increased until melting of the CdTe occurs. Care must be taken that the condensed phases are in equilibrium with the cadmium pressure imposed. As the equilibrium liquid-gas is more readily established than the equilibrium solid-gas, the best procedure is as follows. First melt the CdTe completely and keep the melt for some time
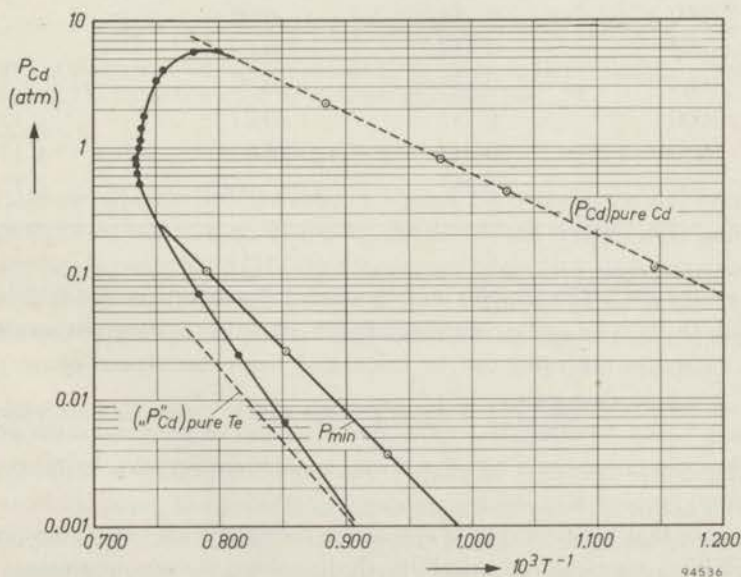
Fig. 5. The $\log p_{Cd}$ versus $10^3\ T^{-1}$ diagram of CdTe. The drawn line gives the measured melting points as a function of p_{Cd}. The vapour-pressure lines of pure cadmium and tellurium are given by dotted lines. The line marked P_{min} gives the points where the total pressure over CdTe has a minimum value.

(i.e. $\approx$ 10 minutes) at that temperature until the equilibrium liquid-vapour is established. Then lower the temperature until crystallization starts. Repeat this procedure several times, taking care to carry out the melting at a temperature as low as possible, i.e. as close to the three-phase line as possible. In this way pressures and temperatures on the three-phase line can be determined with an accuracy of $\pm 2\,°C$. The same procedure can be followed for the determination of the melting point of CdTe under various tellurium pressures. The results of these measurements are given in table II. In figure 5 the same data are given as a log p_{Cd} vs $1/T$ plot.

TABLE II

Melting points of CdTe as a function of the cadmium (tellurium) pressure

T_m (°C)	$10^3/T$ (°K^{-1})	p_{Cd} (atm)	p_{Te_2} (atm)
1009	0·780	5·60	
1049	0·756	4·00	
1058	0·759	3·20	
1081	0·740	1·75	
1084	0·738	1·13	
1086	0·737	1·00	
1090	0·734	0·80	
1090	0·734	0·63	
1088	0·735	0·50	
1000	0·785	(0·07)	0·12
950	0·817	(0·023)	0·15
900	0·852	(0·0065)	0·17

The data for the CdTe samples molten under tellurium pressures are plotted in this diagram with the corresponding cadmium pressures at the given temperature. These cadmium pressures can be calculated from the vapour-phase relation $p_{Cd}\, p_{Te_2}^{1/2} = K_{CdTe}$ (see section 1.3).

Figure 5 also contains the vapour-pressure lines of pure cadmium and pure tellurium, the latter again translated into a cadmium pressure by means of the relation $p_{Cd}\, p_{Te_2}^{1/2} = K_{CdTe}$.

It is seen that the three-phase line at the cadmium-rich side at temperatures $< 1253\,°K$ is practically identical with the line giving the vapour pressure of pure cadmium as a function of the temperature. Similarly on the tellurium-rich side at temperatures $< 1080\,°K$ the three-phase line is practically identical with the line giving the cadmium pressures which correspond to the vapour pressures of

pure tellurium as a function of the temperature. The reason is that in these ranges the liquid phase is very rich in cadmium or tellurium respectively: it is in fact molten cadmium or tellurium in which some CdTe is dissolved.

As will be seen in the following chapters it is possible to calculate the deviation from stoichiometry of solid CdTe in equilibrium with its melt at a given temperature from the knowledge of the p_{Cd} at which CdTe begins to melt at that temperature (section 3.8). In this way it is possible to construct from the $\log p_{Cd}$ vs $1/T$ diagram a T–x diagram containing the composition of both the solid and the liquid phases, which is shown in figure 6.
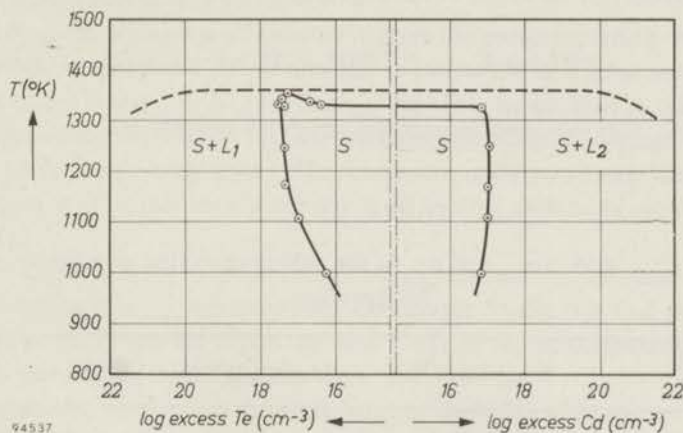
Fig. 6. The T–x diagram of CdTe. The symbols ⊙ in the figure give the calculated values of the solidus line. The liquidus is given by an arbitrary dashed line.

So far, the equilibrium between solid and liquid CdTe under various pressures of the components was studied. However, in the way the crystals were prepared the equilibrium between solid CdTe and its vapour phase also plays an important role. Therefore in the following we will discuss the equilibrium between solid CdTe and the vapour phase in the range in which no liquid phase is present.

1.3. Equilibrium CdTe (s) $\rightleftarrows$ CdTe (g) $\rightleftarrows$ Cd (g) $+ \frac{1}{2}$Te$_2$ (g)

When CdTe is heated in a closed and evacuated system at a temperature below its melting point, an equilibrium is established between the solid CdTe and cadmium, tellurium and CdTe in the vapour phase. At a given temperature definite pressures p_{Cd}, p_{Te_2} and p_{CdTe} are set up. The p_{Cd} and p_{Te_2} are not independent but are coupled by the equilibrium constant of the reaction

$$CdTe \text{ (s)} \rightleftarrows Cd \text{ (g)} + \tfrac{1}{2}Te_2 \text{ (g)}$$
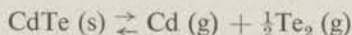
which, assuming the activity of CdTe in solid CdTe to be equal to unity and the activity of the gaseous components to be equal to the vapour pressure of these components, simplifies to

$$K_{CdTe} = p_{Cd}\, p_{Te_2}^{1/2}.$$

As no direct measurements of this constant are available the value of K_{CdTe} is calculated from thermodynamic data by means of the expression $RT \ln K_{CdTe} = -\Delta G_T^\circ$ in which ΔG_T° is the free energy of formation. The value of ΔG_T° can be approached by $\Delta G_T^\circ = \Delta H_{298}^\circ - T\Delta S_{298}^\circ$. Inserting the values of ΔH_{298}° and ΔS_{298}° (reference 10) we arrive at the expression

$$- RT \log K_{CdTe} = 71800 - 49.5\, T \text{ cal/mole.}$$

Values of K_{CdTe} at various temperatures are given in table III.

TABLE III

Values of K_{CdTe} and of p_{Cd} and p_{Te_2} at the sublimation line as a function of the temperature

T (°C)	K_{CdTe} (atm$^{3/2}$)	$(p_{Cd})_{min}$ (atm)	$(p_{Te_2})_{min}$ (atm)
700	$4.78 \cdot 10^{-6}$	$3.63 \cdot 10^{-4}$	$1.81 \cdot 10^{-4}$
800	$1.62 \cdot 10^{-4}$	$3.81 \cdot 10^{-3}$	$1.90 \cdot 10^{-3}$
900	$2.76 \cdot 10^{-3}$	$2.46 \cdot 10^{-2}$	$1.23 \cdot 10^{-2}$
1000	$3.16 \cdot 10^{-2}$	$1.26 \cdot 10^{-1}$	$0.63 \cdot 10^{-1}$

The total pressure P over solid CdTe is equal to $p_{CdTe} + p_{Cd} + p_{Te_2}$. At a definite temperature this total pressure P will change if the pressure of one of the components is varied and will reach a minimum value at a definite p_{Cd} (or p_{Te_2}). The value of this minimum total pressure and the corresponding values of p_{Cd} and p_{Te_2} can be calculated from the relations

$$p_{Cd}\, p_{Te_2}^{1/2} = K_{CdTe}, \tag{1.1}$$

$$p_{CdTe} + p_{Cd} + p_{Te_2} = P. \tag{1.2}$$

For $P = P_{minimal}$ holds $dP/dp_{Cd} = dP/dp_{Te_2} = 0$, which leads to the relation

$$p_{Cd} = 2p_{Te_2} = 2^{1/3}\, K_{CdTe}^{2/3}. \tag{1.3}$$

Thus since K_{CdTe} as a function of the temperature is known, p_{Cd} and p_{Te_2} can also be calculated. These data are also given in table III. In the $\log p_{Cd}$ vs $1/T$ projection (fig. 5) these points are also plotted. They lie on a straight line denoted as the P_{min} line.

In this consideration it was assumed that K_{CdTe} is a constant at a fixed temperature. However, K_{CdTe} will be a slowly varying function of the composition of the solid CdTe, which will change when heated under a varying cadmium pressure. As the deviation from stoichiometry is always very small ($\approx 10^{18}$ atoms per cm^3 $\approx 10^{-4}$ gram atoms per mole), the error made in calculating p_{Cd} and p_{Te_2} by using (1.3) is very small.

The P_{min} line is important, because it gives the pressures which will be finally established when solid CdTe is allowed to evaporate in a large vessel. Further we saw above that $p_{Cd} = 2p_{Te_2}$ at the P_{min} line. This means that at the minimum-pressure line the vapour has just the composition of the solid phase or, in other words, under these conditions CdTe sublimates in its own composition without decomposing. For this reason the P_{min} line is often called the sublimation line of CdTe.

In the expression for the total pressure p_{CdTe} occurs. Unfortunately, no direct measurements of p_{CdTe} are available. Goldfinger [45]) did not find molecules of CdTe in investigating the vaporization of CdTe in the mass spectrograph in the temperature region from 780–920 °K.

It is possible, however, to show that p_{CdTe} is negligible with respect to p_{Cd} and p_{Te_2} at $P = P_{min}$ and therefore p_{CdTe} may also be neglected in comparison with the greater of p_{Cd} and p_{Te_2} outside the minimum. The argument goes as follows. In the experiments in which CdTe was heated under well-defined pressures of cadmium or tellurium the following observations were made:

(a) When heating CdTe at a definite temperature in a closed system (fig. 4) no sublimation was observed in any part of the tube when working under high cadmium or tellurium pressures ($p_{Cd} \gg (p_{Cd})_{min}$ or $p_{Te_2} \gg (p_{Te_2})_{min}$, in which $(p_{Cd})_{min}$ is the value of p_{Cd} when $P = P_{min}$).

(b) When heating CdTe at the same temperature without imposing a cadmium or tellurium pressure, or at $p_{Cd} = (p_{Cd})_{min}$ or $p_{Te_2} = (p_{Te_2})_{min}$, a marked sublimation was observed.

(c) The presence of an inert gas at a pressure of the same order as the p_{Cd} or p_{Te_2} in (a) did not stop the sublimation of CdTe when no cadmium or tellurium pressure was imposed.

The rapid sublimation of CdTe as mentioned in (b) is caused by the fact that, when $P = P_{min}$, the vapour consists of almost equal molecular amounts of cadmium and tellurium; these are able to diffuse through the tube to the cooler

parts and may recombine there to solid CdTe. This causes the equilibrium CdTe (s) $\rightleftharpoons$ Cd (g) $+ \frac{1}{2}$ Te$_2$ (g) to shift to the right, resulting in further decomposition of the solid CdTe phase in the high temperature part of the tube. At 700 °C, for example, maximum sublimation occurs at $p_{Cd} = 3.63.10^{-4}$ atm. If the value of p_{CdTe} should be of this order or greater, mass transport of CdTe to cooler places of the reheating tube should also occur at higher Cd pressures as p_{CdTe} is independent of the cadmium pressure, whereas the presence of some extra atoms in the vapour phase would not hinder the diffusion (see c). However heating of CdTe during some days under high cadmium pressures ($p_{Cd} \gg (p_{Cd})_{min}$) did not produce appreciable sublimation to the cooler parts of the tube. So at 700 °C, p_{CdTe} must be much smaller than the mentioned value of $3.63.10^{-4}$ atm.

The absence of sublimation at high cadmium pressures and at high tellurium pressures is readily explained if the vapour consists mainly of Cd and Te$_2$ [11]). The reason is that sublimation of CdTe requires diffusion of cadmium as well as tellurium, the rate of diffusion of each component being proportional to its partial pressure. Therefore the smaller pressure of the two determines the rate of sublimation of CdTe. But if p_{Cd} is large, p_{Te_2} is small, and vice versa. Therefore at large values of both p_{Cd} and p_{Te_2} the sublimation is diminished.

A practical consequence of the mentioned sublimation phenomena is that a small region of cadmium pressures at both sides of the P_{min} line in fig. 5 is inaccessible for carrying out reheating experiments.

1.4 Preparation of pure crystals and crystals with foreign atoms

1.4.1. *Purification of CdTe*

The material prepared as mentioned in 1.1 was still very impure, containing about 0.01% by weight of foreign elements (see table IV). For the purification of the raw material the method of zone-refining developed by Pfann [9]) and well known in the germanium technology was used. As CdTe tends to decompose upon melting this procedure has to be carried out in a system in which a pressure of one of the components can be maintained. As shown in fig. 7 the CdTe to be purified is put into a very pure graphite or silica boat. When a silica boat is used, its surface is roughened by sandblasting and then it is covered with a layer of graphite by pyrolysis of butane at 1000 °C. The boat is placed at one end of a silica container; at the other end a piece of cadmium metal is placed. The tube then is evacuated and placed into the double furnace system, which is such that the side at which the boat is present is maintained at a certain temperature ($\approx$ 900 °C) while the cadmium is maintained at a lower temperature ($\approx$ 825 °C). The temperature of both furnaces is regulated with an accuracy of ± 1.0 °C. A small zone (1.5 – 2.0 cm) of the material can be molten by a small molybdenum furnace, which temperature is regulated making use of the temperature dependence of the molybdenum wire (accuracy about 0.2 °C at 1100 °C).
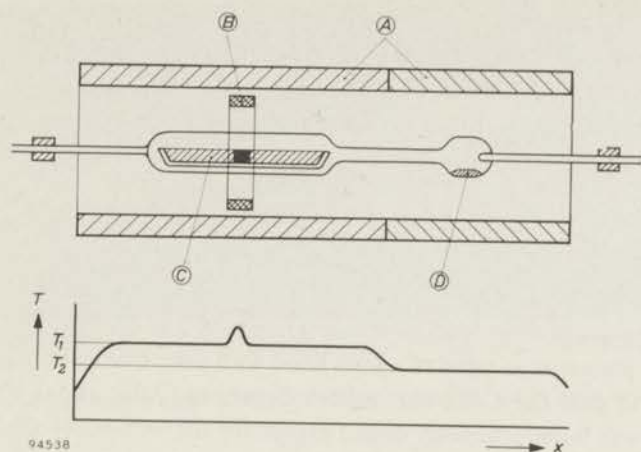
Fig. 7. Apparatus for zone-purifying and zone-levelling of CdTe. The material (*C*) is contained in a graphite boat, enclosed in a silica container. A double nichrome-furnace (*A*) and a small molybdenum furnace (*B*) are used for heating. The cadmium pressure is produced by a piece of cadmium metal (*D*). The temperature distribution is shown in a separate diagram.

TABLE IV

Spectrochemical analysis of CdTe samples taken from the end of a rod at which segregation is started.

Type of foreign atom	Concentration in the starting material (atoms/cm³)	Concentration after 6 zones (atoms/cm³)	Concentration after 40 zones (atoms/cm³)
In	$1 \cdot 5.10^{18}$	$9 \cdot 7.10^{16}$	–
Mg	$\leqslant 4 \cdot 6.10^{17}$	$\leqslant 4 \cdot 6.10^{17}$	$\leqslant 3.10^{16}$
Cu	$5 \cdot 8.10^{17}$	$5 \cdot 8.10^{16}$	$\leqslant 3.10^{16}$
Ag	$3 \cdot 5.10^{17}$	$3 \cdot 5.10^{16}$	–
Pb	$9 \cdot 0.10^{17}$	–	–
Al	$2 \cdot 7.10^{17}$	$1 \cdot 2.10^{18}$	–

At the solid-liquid interface a distribution equilibrium for the foreign atoms in CdTe sets up. The distribution coefficient $K = C_s/C_l$ is found to be smaller than unity and nearly equal to 0·5 in almost all cases; only for Al it proves to be larger than unity. By sliding the whole furnace system over the silica tube the molten zone is drawn through the material contained in the boat. In this way most of the foreign atoms accumulate at one end of the rod, aluminium only

going to the other end. After passing 6–10 zones through the material it is taken out of the tube, the impure ends are cut off and the resulting rod is subjected to another purification. As a very large number of passages (about 30–40) are necessary to obtain very pure material the purification process was partially automized. Some typical results are given in table IV.

1.4.2. *Doping of CdTe*

The pure material obtained was doped with a known amount of various foreigns atoms, viz. Cu, Ag, Au, In and Sb. This was accomplished by the zone-levelling procedure developed by Pfann [9]) in which a known amount of foreign elements is placed at one end of a boat filled with pure CdTe and a molten zone is allowed to pass the CdTe bar in both directions. After about 10 passes the whole bar was homogeneously doped except for the section of the bar where molten zone ends up.

1.4.3. *Growing of single crystals*

In making single crystals of CdTe a molten zone is allowed to traverse the material contained in a silica boat. The choice of the cadmium pressure under which single crystals are grown, the velocity at which the molten zone is traversing the material and the temperature gradient at the ends of the molten zone are found to be very important.

When the liquid CdTe has a composition which differs markedly from the composition of the solid phase which is crystallizing from it, the excess of the component present in excess is segregated at the solid-liquid interface. As in the case of CdTe both cadmium and tellurium have a large vapour pressure at the melting temperature of CdTe, the segregated excess cadmium or tellurium leads to the formation of gas bubbles at the interface. Although these will have the tendency to rise to the surface, they may easily get trapped. In that case they lead to distorted crystallization and the result is a highly porous material. It can be seen from the phase diagram that only in the maximum melting point ($T = 1090\ °C$; $p_{Cd} \approx 0.7$ atm) solid and liquid phase have the same composition. This therefore should be the ideal point to avoid the bubble effect. However, the cadmium pressure corresponding to this point is situated near to the P_{min} line, which as mentioned before leads to considerable sublimation of the material. For this reason a higher cadmium pressure ($p_{Cd} \approx 1.5$ atm) is chosen at which sublimation is negligible; by working at very low speeds of the molten zone (0.5–0.8 cm per hr) the bubble effect can be avoided. Normally the first part of the bar is polycrystalline. The number of crystals present in the bar decreases as the zone proceeds and sooner or later a state is reached in which only one crystal is left which continues through the remaining part of the bar. Therefore this part is monocrystalline, albeit that nearly always twinning occurs (see fig. 8). Laue diagrams show that the crystals grow preferentially in the (111) direction,
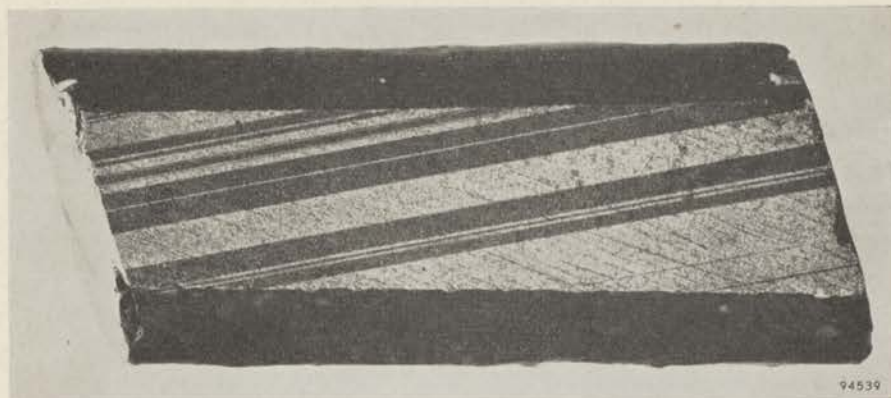
Fig. 8. A ground and etched piece of a bar of single crystalline CdTe with twinning planes. (Dimensions 40 × 15 × 8 mm).

the twin planes being [111]. Of course a piece of this material can be used as a seed crystal to obtain a monocrystalline bar out of another charge.

In cases in which doped crystals are required, the last pass of the zone as described in section 1.4.2 is carried out under the conditions described in the present section. Crystal boundaries are found to be marked potential barriers; twin boundaries, however, do not act as such (figs 9 and 10). Therefore twinned
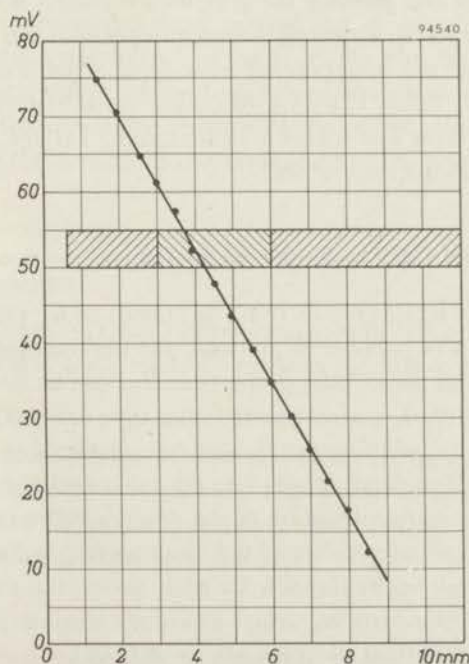
Fig. 9. Potential distribution in a piece of single crystalline CdTe with twinning planes.
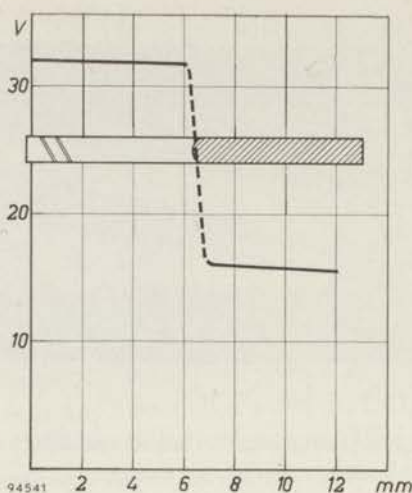
Fig. 10. Potential distribution in a piece of CdTe with a crystal barrier.

crystals were accepted for the carrying out of electrical measurements. From the monocrystalline section of the rod rectangular samples of dimensions $10 \times 1 \times 1$ mm were sawn. In order to remove the irregularities at the surface caused by the sawing and grinding the samples are etched with distilled nitric acid for 2 minutes at 30 °C. This treatment removes about 100 μ of the material. The crystals however are now covered by a layer of tellurium and tellurium oxides. Heating at $T > 60$ °C with a 10%-solution of NaOH and $Na_2S_2O_4$ in water removes this layer and leaves a clear, shining surface. The samples are now ready for reheating experiments.

1.5. Reheating of solid CdTe under pressures of one of the components

By reheating CdTe single crystals (pure or doped) under various cadmium or tellurium pressures it is possible to influence the chemical composition of the material and therewith its physical properties. This can be done by heating the sample, after being etched, in an evacuated silica tube one end of which contains a piece of tellurium or cadmium metal. This tube is placed in a double furnace system like the one described above. The crystal is embedded in some CdTe powder in order to avoid sublimation of the sample. When heating under cadmium pressures the partial pressure of tellurium corresponding to the imposed p_{Cd} is now mainly built up by the powder while the crystal remains practically unchanged. This is particularly important at lower cadmium pressures in which case a considerable tellurium pressure has to be built up in order to satisfy the vapour-phase relation $p_{Cd} p_{Te_2}^{1/2} = K_{CdTe}$.

In order to prevent reactions to take place both within the crystal (cluster effects, etc.) and between the crystal and the vapour during the cooling to room temperature, it is necessary to cool very rapidly. This can be done by rapidly taking the tube out of the furnace and rinsing it immediately with water. The speed of cooling is influenced unfavourably by the large heat resistance and the large heat capacity of the silica tube. The influence of these factors can be diminished by giving the section of the tube at which the crystal is present a very thin wall (0·2 mm) and a small diameter ($d = 1·5$ mm; see fig. 11).
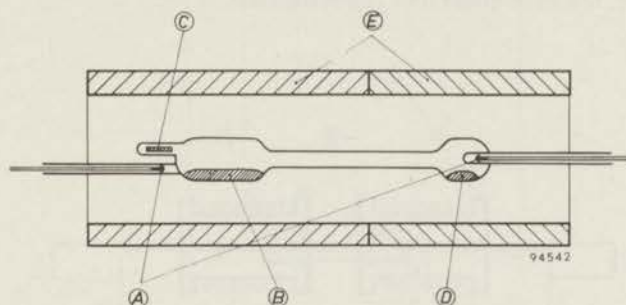
Fig. 11. Apparatus for reheating a single crystal of CdTe (C) under a definite cadmium pressure, produced by a piece of cadmium (D). Some CdTe powder is placed at B. The temperature of the double furnace system (E) is measured by two thermocouples (A).

The reheating experiments were carried out at various temperatures with CdTe single crystals containing various dopes (In, Cu, Ag, Au). Measurements of the electrical and optical properties of these crystals were carried out in order to gain insight into the relation between the various physical properties and the composition and the conditions of preparation of the crystals.

1.6. Electrical measurements

1.6.1. *Electrical contacts*

Good contacts obeying Ohm's law were necessary for accurate electrical measurements. With CdTe these could be made in the following way:

(a) *n-type samples*

Indium-plated metal probes were pressed on the crystals; then a current pulse, obtained by discharging a condensor, was passed through the crystal. Ohmic contacts could also be made by alloying small indium pellets to the *n*-type material at 550 °C in an inert atmosphere.

(b) *p-type samples*

Solutions of noble metal salts like $AgNO_3$, $AuCl_3$, $PtCl_4$, etc. when brought in contact with a CdTe sample leave a shining spot of the noble metal, which

on p-type samples gives rise to a good ohmic contact. Though the mechanism of this reaction is not completely clear, it is supposed that Cd goes into solution as a Cd^{2+} ion leaving a thin layer on the crystal with an excess of tellurium which is therefore strongly p-type. In order to maintain electrical neutrality noble metal ions are discharged at the surface, thus covering the p-type layer with the noble metal. On n-type crystals a $p–n$ junction can be produced by this method with rectifying and photoelectric properties.

The samples prepared in this way are used for measurements of the thermo-electric power, the Hall effect and the resistance.
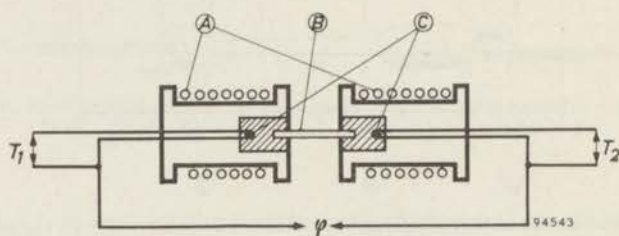
Fig. 12. Apparatus for measuring the thermo-emf. of a CdTe sample (B), enclosed between two gallium baths, heated by two furnaces (A). The temperatures T_1 and T_2 are measured by two silver-constantan thermo-couples (C); the thermo-emf. φ is measured between the silver leads.

1.6.2. *Measurement of the thermoelectric power*

The thermo-emf. measurements were performed in an apparatus consisting of two nichrome blocks, each containing a bath of gallium (fig. 12). Each block was maintained at a constant temperature with a temperature difference between the baths of about 10 °C. The temperature of the baths was measured by two silver-constantan thermo-couples inserted into the baths; the silver wires were also used as leads for measuring the thermo-emf. of the sample.

The sample to be measured was placed with its ends in the gallium baths and contact was made by melting and solidifying the gallium. This procedure guaranteed good thermal and electrical contacts to the crystal. The thermo-emf. and the temperatures were measured by a compensation method of the Poggendorff type, using a tube voltmeter with a high impedance as a zero-indicating instrument. The values of the thermo-emf. of a large number of both p- and n-type samples were measured and plotted as a function of the number of charge carriers as determined by the Hall effect. The results are shown in fig. 13 and fig. 14. These results enable us to calculate the values of the effective masses of electrons and holes (see section 2.1).
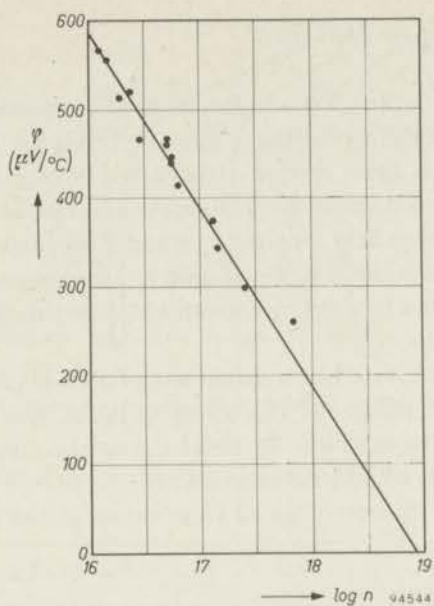
Fig. 13. The thermo-emf. of various *n*-type CdTe samples as a function of the concentration of charge carriers (electrons cm⁻³).
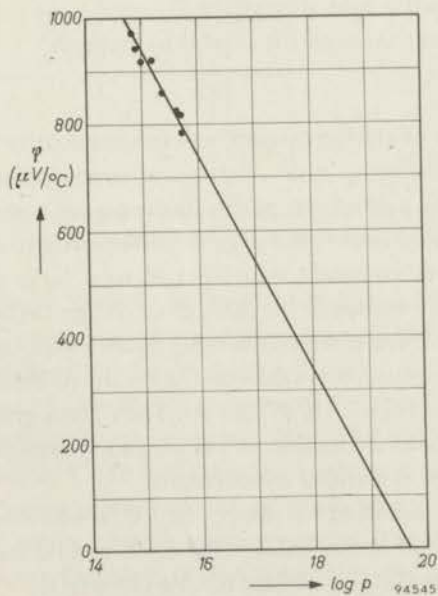
Fig. 14. The thermo-emf. of various *p*-type CdTe samples as a function of the concentration of charge carriers (holes cm⁻³).

1.6.3. *Measurement of the Hall effect*

The Hall effect of the samples was investigated by measuring at two probes placed at the sides of the crystal the voltage V_H produced by a magnetic field of strength H when a direct current i was passed through the sample. In this measurement the line connecting the probes, the direction of the current and the direction of the magnetic field form the X, Y and Z coordinates of a rectangular coordinate system. The voltage was measured by a compensation method of the Poggendorff type using a tube voltmeter with a high impedance as a zero indicating instrument.

The applied magnetic field had a magnitude of 5000 Gauss. By applying the magnetic field in both directions and reversing the current a good control of the homogeneity of the samples was obtained; at the same time perturbing, non-commuting effects could be eliminated.

The Hall constant R_H was obtained from the measured Hall voltage V_H by means of the relation

$$R_H = \frac{10^8 \, V_H b}{H i} \quad \text{cm}^3/\text{Coul},$$

with V_H = the measured Hall voltage in volts,
b = the thickness of the sample,
H = the magnetic field strength in Gauss,
i = the current through the crystal in amperes.

The concentration of charge carriers was determined by the relations: concentration of electrons $= n = -fe/R_H$ and concentration of holes $= p = +fe/R_H$, in which f is a constant, which in the case of non-degenerate samples has the value $f = 3\pi/8$, and e = charge of the electron in coulombs.

The Hall-effect measurements were applied to a large number of samples. Systematically the dependence of the number of charge carriers on the cadmium (or tellurium) pressure, under which the samples with various dopes were reheated at a definite temperature, was studied. The results of these measurements are represented in figs 15, 16, 17, 18, 19 and 20. The figures give the concentration of electrons and holes as a function of the cadmium pressure under which the samples were reheated at various temperatures.

Figure 15 gives the situation for the purest CdTe we could obtain (which, as will be shown later, still contained 2.10^{16} Cu). It can be seen that at a definite cadmium pressure the samples change from p- to n-type.

Indium-doped samples (figs 16, 17, 18) do not show p-type conductivity at all. In the range of low cadmium pressures the crystals have a high specific
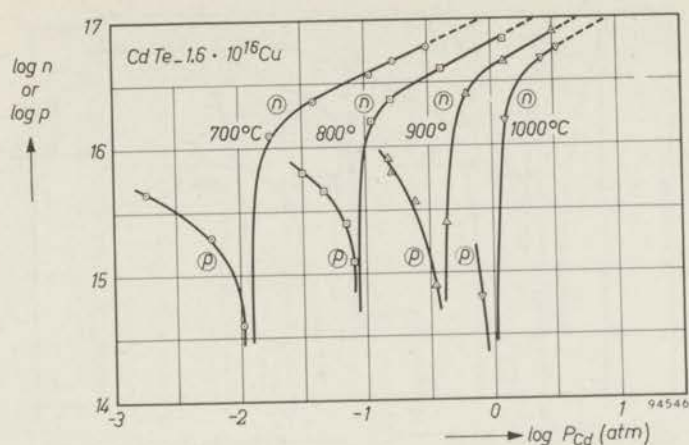
Fig. 15. The concentration of charge carriers of CdTe $- 1 \cdot 6.10^{16}$ Cu as a function of T and p_{Cd}.
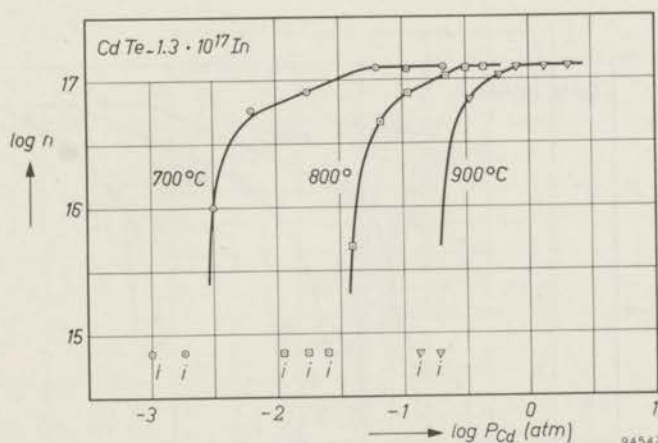
Fig. 16. The concentration of charge carriers of CdTe $- 1 \cdot 3.10^{17}$ In as a function of T and p_{Cd}. The points indicated by i denote samples with a very high specific resistance.

resistance (10^6–10^7 Ωcm). Samples prepared at higher cadmium pressures show n-type conduction. Going to higher cadmium pressures the number of free electrons first nearly satisfies the relation d $\log n$/d $\log p_{Cd} = \frac{1}{2}$. At a definite p_{Cd}, however, the number of free electrons becomes independent of the cadmium pressure and equal to the concentration of indium. This region is called the region of controlled conductivity. CdTe with the highest indium dope ([In] $= 5.10^{17}$ cm^{-3}) shows a marked influence of the velocity of quenching to room temperature of the samples after reheating at high temperature. The dotted line in fig. 18 shows the result of slow quenching, the full drawn line the result of rapid quenching. This phenomenon, which is ascribed to clustering effects, will be treated in section 3.7.
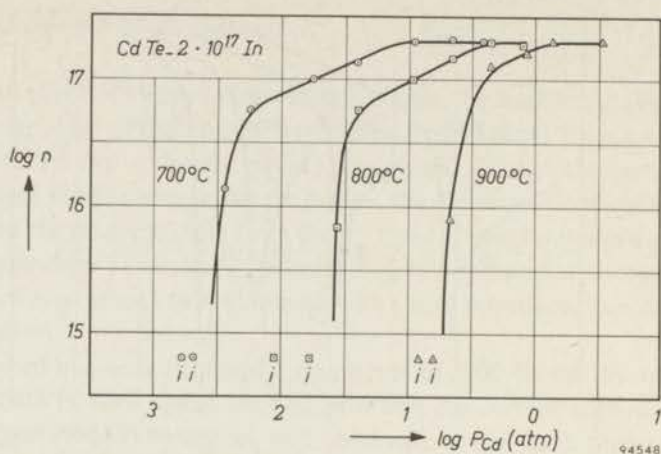
Fig. 17. The concentration of charge carriers of CdTe – 2.10^{17} In as a function of T and p_{Cd}. The points indicated by i denote samples with a very high specific resistance.
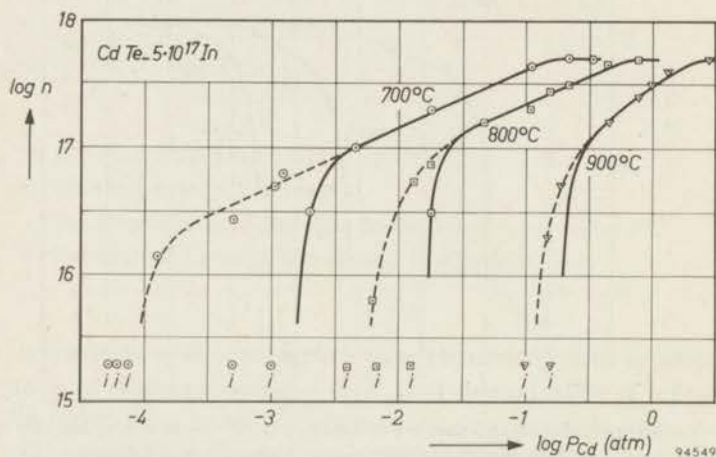
Fig. 18. The concentration of charge carriers of CdTe – 5.10^{17} In as a function of T and p_{Cd}. The points indicated by i denote samples with a very high specific resistance. The drawn lines give the situation after very rapid quenching of the samples from high temperature to room temperature, the dotted lines after less rapid quenching.

Gold doped samples prepared at low values of p_{Cd} show p-type conduction. At a certain value of p_{Cd} the conductivity suddenly changes to n-type. Samples containing 5.10^{16} Au cm^{-3} show a range in which the concentration of holes is independent of p_{Cd}, i.e. a range of controlled conductivity similar to that observed with n-type CdTe – In (fig. 19). Only part of this range can be covered experimentally due to the fact that it is situated in the vicinity of P_{min}, which fact causes sublimation of the samples (see 1.3). In samples containing gold in a higher
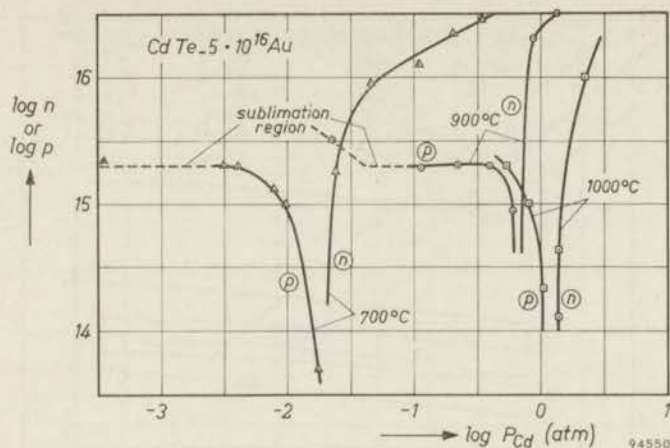
Fig. 19. The concentration of charge carriers in CdTe − 5.10^{16} Au samples as a function of T and p_{Cd}.
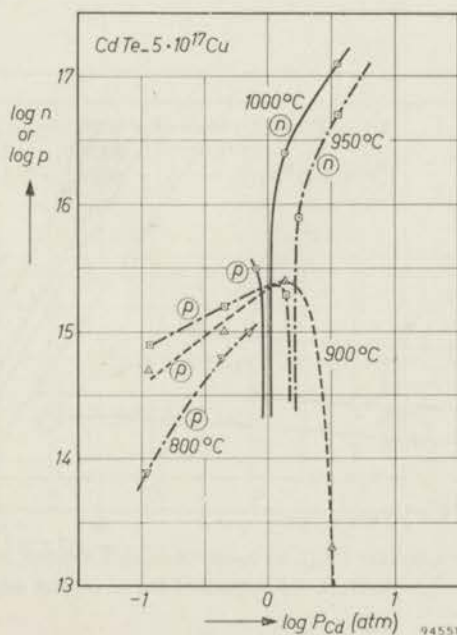
Fig. 20. The concentration of charge carriers in CdTe − 5.10^{17} Cu samples as a function of T and p_{Cd}.

concentration, viz. 4.10^{17} cm^{-3}, a range of controlled conductivity can not be found. The crystals show non-reproducible behaviour in the p-type region, which is ascribed to cluster effects of the gold centres (see 3.7). Only the cadmium pressure at which the conductivity of the samples changes of sign can
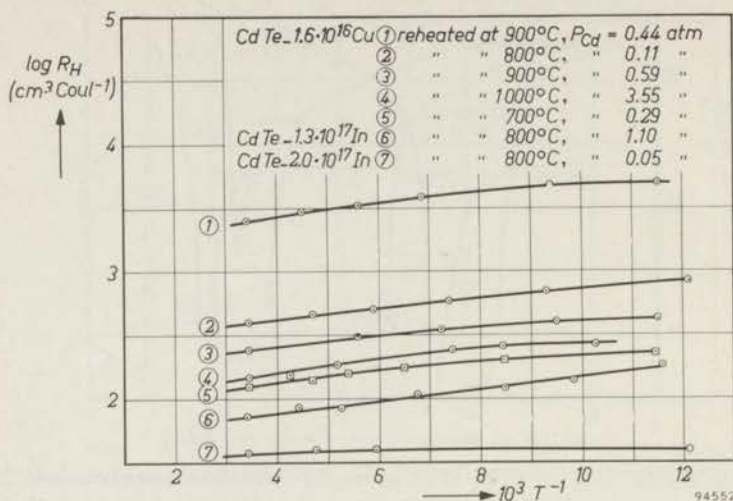
Fig. 21. Temperature dependence of R_H of various n-type samples.
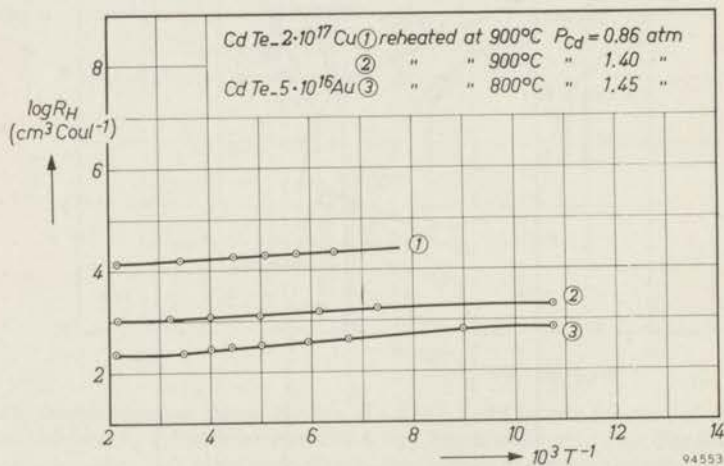
Fig. 22. Temperature dependence of R_H of various n-type samples.

be reproduced. For 700 °C this occurred at $p_{Cd} = 0.4$ atm; for 800 °C at $p_{Cd} = 1.3$ atm and for 900 °C at $p_{Cd} = 3.2$ atm.

Experiments with copper, silver and antimony dopes show the same features as samples highly doped with gold in the p-type region (see fig. 20). Introduction of the alkali metals offers large difficulties because of the evaporation of the dope from CdTe during the prolonged heating at high temperatures.
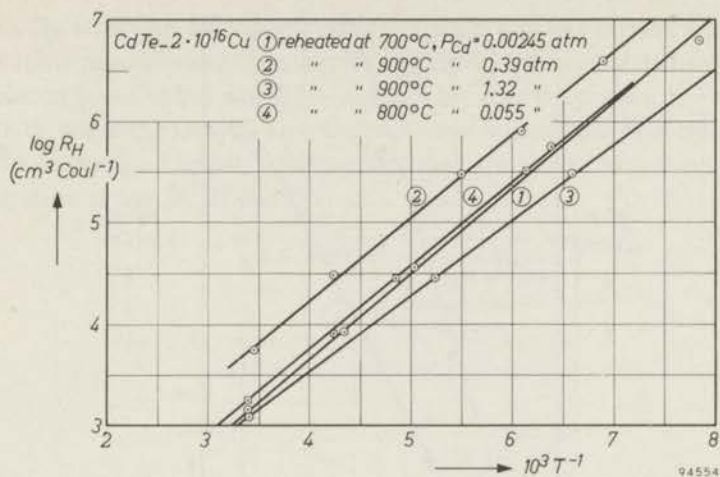
Fig. 23. Temperature dependence of R_H of various p-type samples.
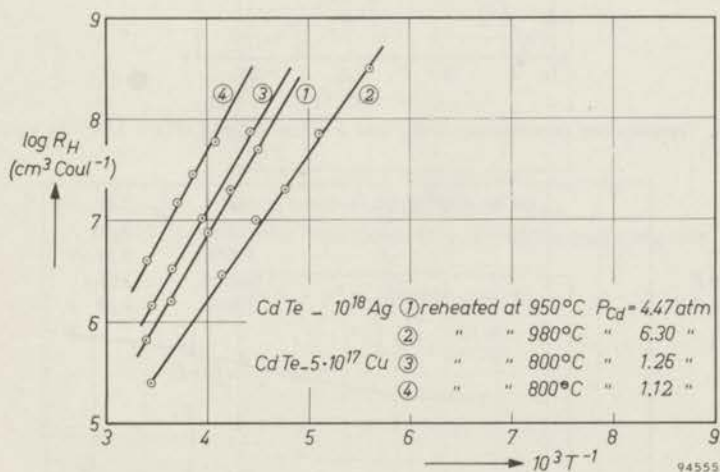
Fig. 24. Temperature dependence of R_H of various p-type samples.

As will be seen in chapter 3 of this study much information can be drawn from $\log n$ (or p) vs $\log p_{Cd}$ diagrams.

In order to obtain information about the ionization energy of the centres responsible for the n- or p-type conductivity the Hall effect of a large number of samples with various dopes was measured as a function of the temperature. The results are represented in figs 21, 22, 23, 24 and 25; these results are interpreted in section 2.2.
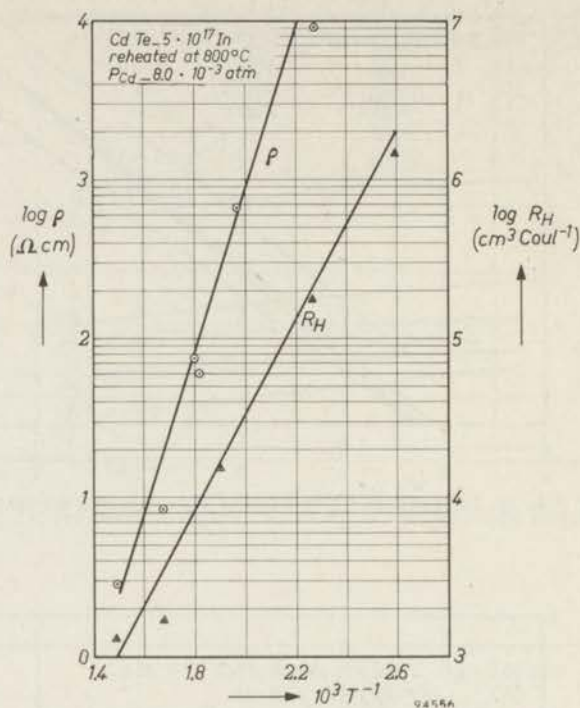
Fig. 25. Temperature dependence of R_H and ϱ of an n-type CdTe – 5.10^{17} In sample.
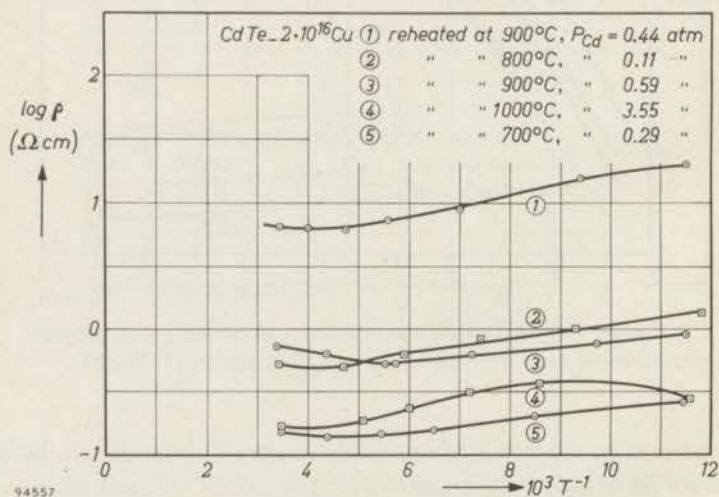
Fig. 26. Temperature dependence of ϱ of various n-type samples.

1.6.4. *Measurement of the resistance*

The resistance r was determined by measuring the voltage drop over two probes by a compensation method when a direct current was passed through the

crystal. By reversing the current the homogeneity of the crystal was checked. From these measurements the specific resistance ϱ was obtained by means of the relation $\varrho = rbd/l$, in which l = distance between the probes, b = width and d = thickness of the sample. The results of some measurements of the resistance of crystals prepared under various conditions are shown as a function of the temperature in figs 26, 27 and 28.
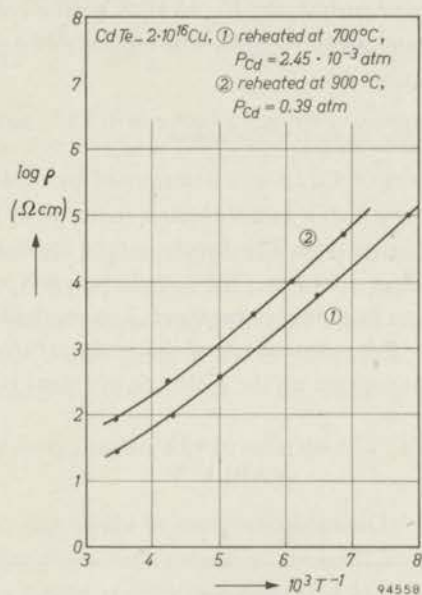
Fig. 27. Temperature dependence of ϱ of various p-type samples.
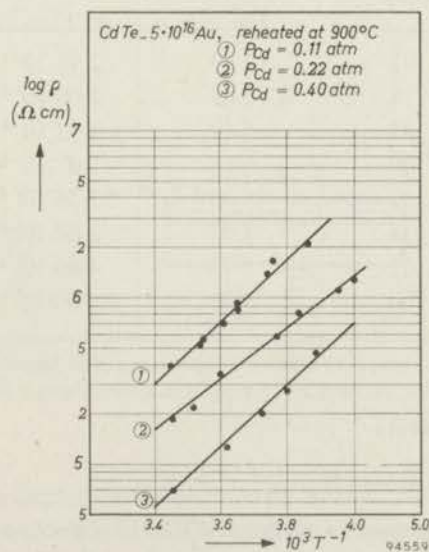
Fig. 28. Temperature dependence of ϱ of various p-type samples.

By combining the data for resistance and Hall-effect measurements, the mobility of the charge carriers could be obtained. For the case of charge carriers of one type only, which applies to CdTe in the temperature range in which our measurements were made, the following relation holds:

$$\mu = R_H \, \varrho^{-1} f^{-1}$$

in which μ = mobility in cm²/V sec, R_H = Hall coefficient in cm³/Coul, ϱ = specific resistance in Ωcm, and $f = 3\pi/8$. The mobility of n- and p-type samples will be discussed in section 2.3.

1.6.5. *Measurement of the dielectric constant*

The dielectric constant of CdTe was determined by measuring the capacity of a condensor containing CdTe as a dielectric material at various frequencies with a bridge of the Schering type. The dimensions of the mono-crystalline piece of CdTe were 9·8 × 9·8 × 1·63 mm. The sample was p-type and had a specific resistance of $1·5.10^3$ Ωcm at room temperature. The results are given in table V; it is seen that $\varepsilon = 11 \pm 0·3$ independent of the temperature and the frequency. An influence of the composition on the dielectric constant is not to be expected.

TABLE V

Dielectric constant of CdTe

T	frequency (kc)	capacity (pF)	tan δ	ε
20 °K	1	5·69	$2·98.10^{-4}$	$10·9 \pm 0·3$
	8	5·69	$4·00.10^{-4}$	$10·9 \pm 0·3$
	32	5·69	$4·92.10^{-4}$	$10·9 \pm 0·3$
	100	5·69	$5·0 .10^{-4}$	$10·9 \pm 0·3$
77 °K	1	5·73	$2·36.10^{-4}$	$11·0 \pm 0·3$
	8	5·73	$3·02.10^{-4}$	$11·0 \pm 0·3$
	32	5·73	$4·66.10^{-4}$	$11·0 \pm 0·3$
	100	5·73	$5·0 .10^{-4}$	$11·0 \pm 0·3$

1.7. Optical measurements

1.7.1. *Spectral transmission*

The spectral transmission of plates of CdTe of a thickness $d = 0·2$ mm was measured as a function of the temperature (fig. 29). The measurements were
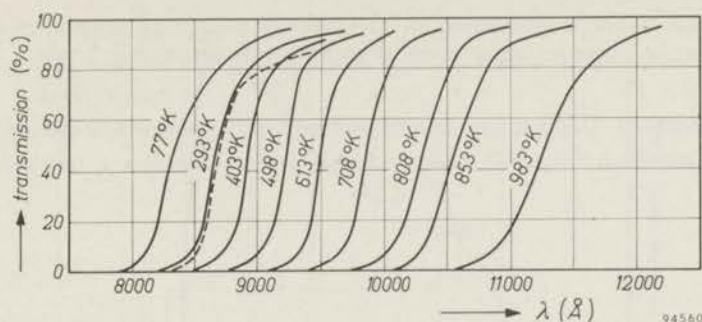
Fig. 29. The transmission of CdTe as a function of the wavelength at various temperatures. The dotted line gives the transmission at 293 °K after cooling down from the highest temperatures of measurement.

performed up to 983 °K. Higher temperatures could not be employed because of the decomposition of CdTe. After measuring the transmission at 983 °K the room temperature measurement was repeated, which did not differ much from the first measurement (dotted curve in fig. 29). This indicated that no irreversible changes had occurred.

1.7.2. *Electromotive force produced by irradiation of a CdTe p–n junction (photo-emf.)*

A photo-emf. cell was made starting with a plate of monocrystalline n-type CdTe. One side of the plate was covered by an $AuCl_3$ solution, which after some minutes produced a p-type surface layer covered by gold. After removing the solution, contacts were made to both the bulk material and the p-type layer, after which the cell could be used (fig. 30).
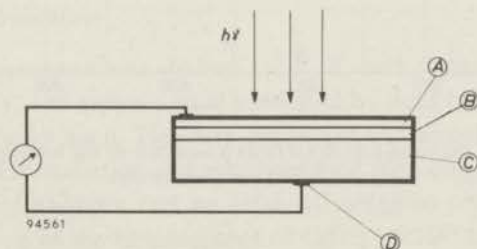
Fig. 30. A CdTe photo-emf. cell, consisting of a piece of n-type CdTe (C), having a p-type region (B) covered with a gold screen (A). Contact to the n-type region is made by an alloyed indium contact (D).

The spectral distribution of the photo-emf. of this cell shows a sharp limit at the long wavelength side (fig. 31). The position of this limit was determined at temperatures between 77 °K and 480 °K (see fig. 32).
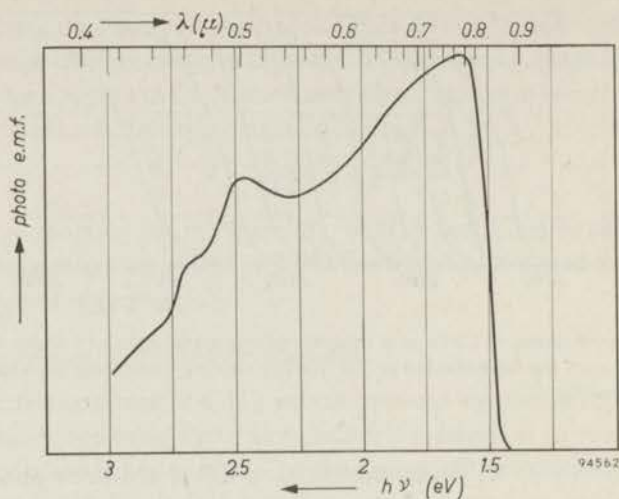
Fig. 31. The photo-emf. (in arbitrary units) of a CdTe photo-emf. cell as a function of the wavelength (or the photon energy) of the irradiating light.
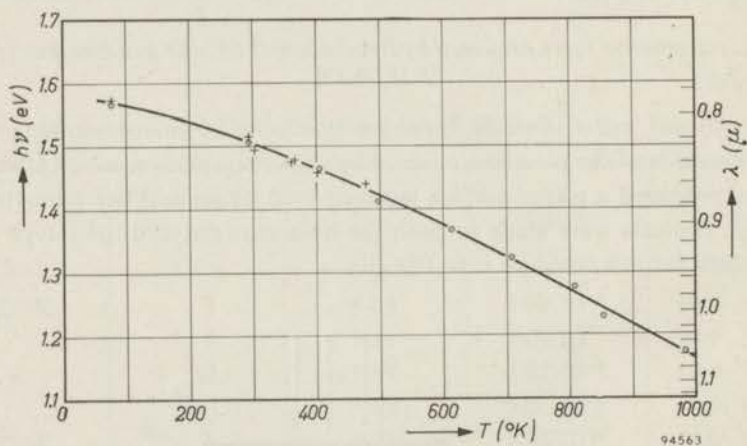
Fig. 32. The value of the band gap of CdTe as a function of the temperature. (⊙ from transmission measurements; + from photo-emf. measurements).

1.7.3. *Emission of light*

1.7.3.1. *Emission of light from a rectifying p–n junction*

Emission of light from a *p–n* junction when biased in the forward direction has been observed in Ge [12,13,14]), Si [17]) and SiC [15,16,18]). The same effect was found with a CdTe *p–n* junction as described in 1.7.2.

At 77 °K the emitted light was very weak by the absorption by the gold layer.

For this reason the gold layer was removed by boiling the crystal in a 10% KCN solution, after which a very thin iridium layer or a gold screen was evaporated onto the *p*-type region.

The spectral distribution could be determined only roughly, because a monochromator with a wide slit (2 mm) had to be used. The result is shown in fig. 33.
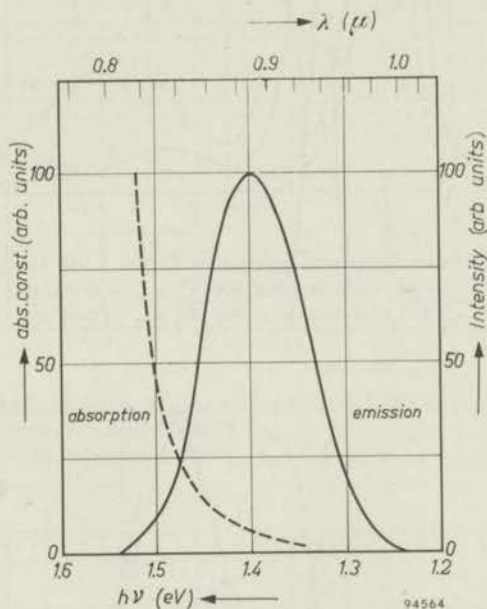
Fig. 33. The emission of a CdTe *p–n* junction biased in the forward direction. The absorption constant is given by a dashed line.

1.7.3.2. *Photoluminescence*

The photoluminescence was studied at 77 °K with crystals prepared under various conditions. The crystals were irradiated by light from a 1000 W super high-pressure mercury lamp. The infra-red radiation was cut off by a saturated $CuSO_4$ solution. The radiation was measured by a recording quartz monochromator with a light chopper and an infra-red sensitive photomultiplier. The spectral distribution of the luminescence of CdTe $- 5.10^{17}$ In crystals at 77 °K is shown in fig. 34. The crystals were prepared at 900 °C under a cadmium pressure of 0·1 atm and 0·01 atm. The crystals prepared under 0·1 atm cadmium pressure showed a large peak at 1·42 eV and a small peak at 1·10 eV. The crystals prepared under 0·01 atm cadmium pressure showed the same large peak at 1·42 eV but a smaller peak at 1·06 eV. The spectral distribution of the luminescence of CdTe $- 5.10^{16}$ Au, reheated at 900 °C under a cadmium pressure of 0·2 atm, is shown in fig. 35.
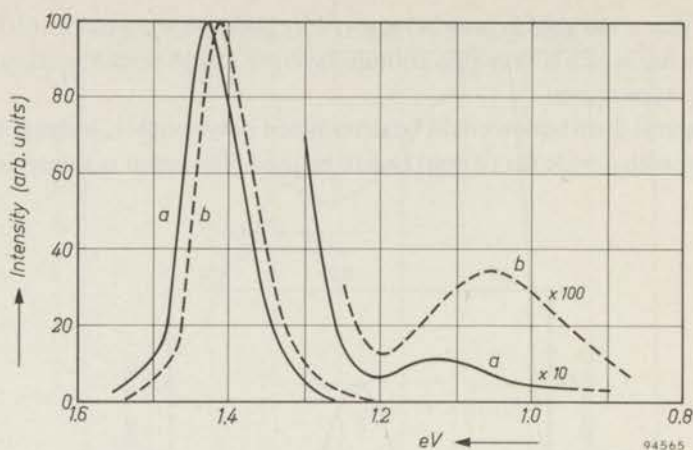
Fig. 34. The luminescence spectrum of CdTe-5.10^{17} In at 77 °K.
(a) CdTe-5.10^{17} In, reheated at 900 °C, $p_{Cd} = 0\cdot1$ atm;
(b) CdTe-5.10^{17} In, reheated at 900 °C, $p_{Cd} = 0\cdot01$ atm.
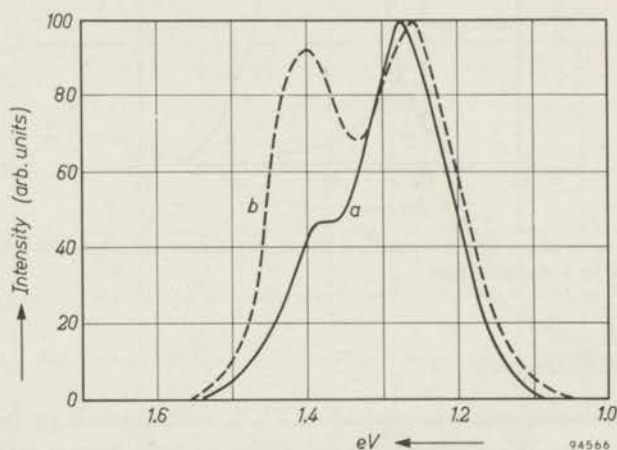
Fig. 35. The luminescence spectrum of CdTe-5.10^{16} Au at 77 °K.
(a) CdTe-5.10^{16} Au, reheated at 900 °C, $p_{Cd} = 0\cdot1$ atm, immediately after preparation;
(b) CdTe-5.10^{16} Au, reheated at 900 °C, $p_{Cd} = 0\cdot1$ atm, after heating at 100 °C for 1 hr (on
an enlarged scale to bring the intensity of the highest peak at 100).

Immediately after preparation of the sample the luminescence spectrum shows
two bands, one at about 1·40 eV and another at 1·27 eV. After reheating the
sample during one hour at 100 °C and cooling to room temperature the peaks
remain at the same place; however the peak at 1·27 eV has decreased in inten-
sity (see fig. 35).

With CdTe doped with Ag or Cu only a peak at about 1·40 eV was found,

independent of the conditions of preparation. A very broad band in the luminescence spectrum of CdTe peaking at 0·54 eV is mentioned by Brown [28]). We could not find any indications of such a band.
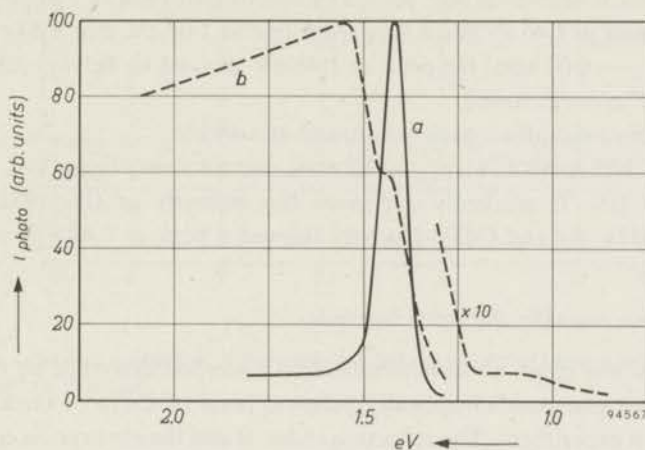
Fig. 36. The photoconductivity spectrum of CdTe−5.10^{17} In at room temperature.
(a) CdTe − 5.10^{17} In, reheated at 900 °C, p_{Cd} = 0·01 atm;
(b) CdTe − 5.10^{17} In, reheated at 900 °C, p_{Cd} = 0·1 atm.
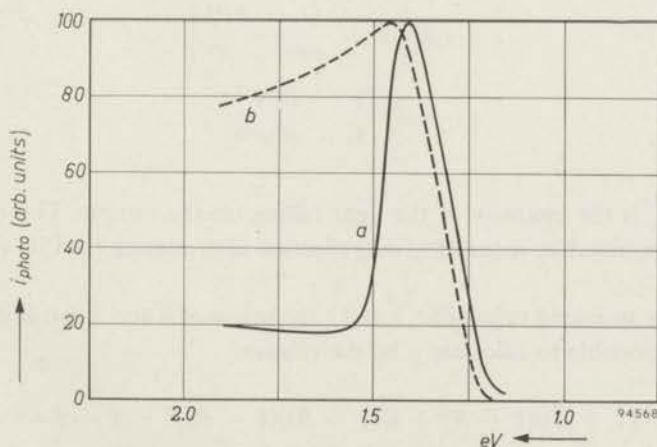
Fig. 37. The photoconductivity spectrum of CdTe−5.10^{16} Au at room temperature.
(a) CdTe−5.10^{16} Au, reheated at 900 °C, p_{Cd} = 0·1 atm, immediately after preparation;
(b) CdTe−5.10^{16} Au, reheated at 900 °C, p_{Cd} = 0·1 atm, after heating at 100 °C for 1 hr (on an enlarged scale to bring the maximum at 100).

1.7.4. *Photoconductivity*

The measurement of the photoconductivity as a function of the wavelength of the exciting light showed one peak at ≈ 1·49 eV which was rather independent

of the way in which the samples were prepared; in addition other peaks appeared which were characteristic for the examined sample.

For CdTe – 5.10^{17} In prepared at 900 °C under $p_{Cd} = 0.1$ atm and $p_{Cd} = 0.01$ atm the spectrum is shown in fig. 36. CdTe – 5.10^{17} In (900 °C, $p_{Cd} = 0.1$ atm) showed a peak at 1.46 eV and a very weak one at 1.07 eV. For CdTe – 5.10^{17} In (900 °C, $p_{Cd} = 0.01$ atm) the peak at 1.46 eV showed to be very large, but no peak at 1.07 eV was found.

In very pure samples a peak was found at 1.49 eV.

CdTe – 5.10^{16} Au (900 °C, $p_{Cd} = 0.2$ atm) showed a very large peak at 1.40 eV. Heating at 100 °C markedly decreased the intensity of this peak (fig. 37). Samples CdTe–Ag and CdTe–Cu only showed a peak at 1.49 eV.

1.7.5. *Measurement of the refractive index*

The refractive index n was determined by a method described by Oswald and Schade [19]. A planparallel optically polished plate of CdTe of thickness d was used for this experiment. The reflection index R and the absorption coefficient K can be determined from the intensity of the reflected light (i_r) and the transmitted light (i_t) at various wavelengths in the infra-red region. Between these quantities the following relations exist:

$$i_r = i_o R \left\{ 1 + \frac{(1 - R)^2}{e^{2Kd} - R^2} \right\},$$

$$i_t = i_o \frac{(1 - R)^2 e^{-Kd}}{1 - R^2 e^{-2Kd}},$$

in which i_o is the intensity of the light falling on the sample. The value of i_o can be determined by measuring the reflection after plating the CdTe slide with silver.

From the measured values of i_r, i_t and i_o the values of K and R can be calculated. Then it is possible to calculate n by the relation

$$n = (1 + R)/(1 - R) \pm [\{(1 + R)/(1 - R)\}^2 - 1 - K\lambda/4\pi]^{1/2}.$$

If $K\lambda/4\pi$ is small this formula simplifies to

$$n = (1 + R^{1/2})/(1 - R^{1/2}).$$

As the transmission in the studied infra-red region showed to be very large, the $K\lambda/4\pi$ term could be neglected and the simplified formula could be used. In fig. 38 the reflection coefficient $R = i_r/i_o$ and the refractive index n are shown
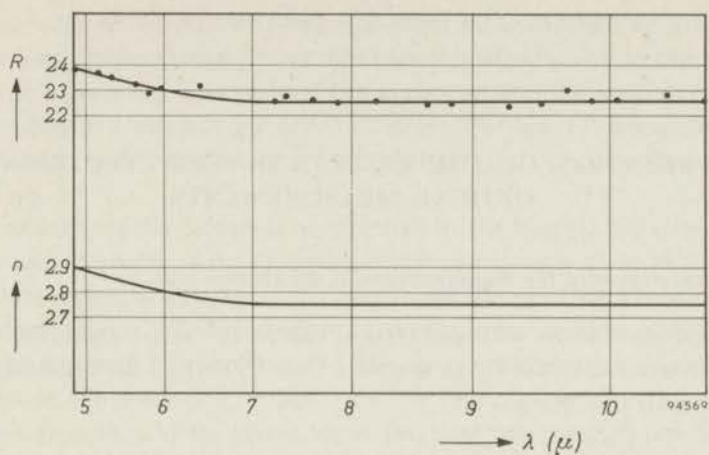
Fig. 38. The reflection coefficient R (in percents) and the refractive index n as a function of the wavelength (in microns). ⟶

as a function of the wavelength. The plates were too thick to carry out measurements at wavelengths smaller than $5\,\mu$, the absorption in this region becoming too large. The value of n in the wavelength region in which it is constant is $2 \cdot 75 \pm 0 \cdot 01$.

CHAPTER 2

INTERPRETATION OF THE RESULTS OF THE ELECTRICAL AND OPTICAL MEASUREMENTS

2.1. Interpretation of the measurements of the thermo-emf.

For semi-conductors with one type of charge carriers, a condition which is almost always fulfilled in CdTe samples, Tauc [20] derived the following simple expression for the thermo-emf:

$$\varphi = -(\varepsilon' + \bar{\varepsilon}_n)/eT \text{ for } n\text{-type semi-conductors};$$ (2.1)

$$\varphi = (\varepsilon'' + \bar{\varepsilon}_p)/eT \text{ for } p\text{-type semi-conductors};$$ (2.2)

in which ε' and ε'' are the distances in the energy diagram from the Fermi level to the conduction and valence band, respectively, and $\bar{\varepsilon}_n$ and $\bar{\varepsilon}_p$ are the mean values of the transport energy of electrons and holes in the conduction and valence band, respectively (fig. 39). The concentration of electrons in the conduction band is given by the formula

$$n = 2(2\pi mkT/h^2)^{3/2}(m_n^*/m)^{3/2} \exp(-\varepsilon'/kT),$$ (2.3)
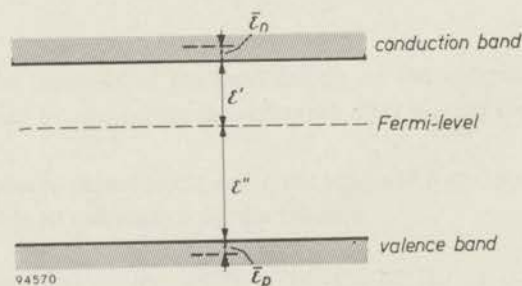
Fig. 39. Electronic energy-band scheme. The mean values of the transport energy of electrons and holes are denoted by $\bar{\varepsilon}_n$ and $\bar{\varepsilon}_p$, respectively.

in which m_n^* is the density-of-states effective-mass of the electrons in the conduction band and m is the free-electron mass. Subtitution of (2.3) in (2.1) leads to

$$\varphi = 2.303(k/e)(\log n - \log n_o^* - \tfrac{3}{2}\log(m_n^*/m) - \bar{\varepsilon}_n/kT)$$ (2.4)

$$\text{with } n_o^* = 2(2\pi mkT/h^2)^{3/2}.$$ (2.5)

When the value of n is known from Hall-effect measurements we are able to calculate the effective mass m_n^* from the experimental values of the thermo-emf. for a given value of $\bar{\varepsilon}_n$. This method is not very accurate, a small deviation in log m_n^* leading to a much larger deviation in m_n^*. Further it is not quite certain what value has to be adopted for $\bar{\varepsilon}_n$ and this incertainty is also reflected in the value of m_n^*.

If the mobility of the carriers is only limited by the thermal vibrations of the lattice, which probably is the case with our measurements of φ in the room temperature region, and the mean free path of the charge carriers is independent of the energy, $\bar{\varepsilon}_n = 2kT$. This has to be expected for covalent crystals [21, 22]. If the mean free path is proportional to the energy, which is the case with purely ionic crystals, the result is $\bar{\varepsilon}_n = 3kT$.

In plotting φ (in μV/°C) versus log n (in electrons per cm³) (see fig. 13) a straight line is obtained with slope 2·303 k/e, whereas the value of log n at $\varphi = 0$ gives the value of m_n^*. In the same way the value of m_n^* can be found from a φ versus log p plot for p-type samples (fig. 14). The results for various values of $\bar{\varepsilon}_n$ and $\bar{\varepsilon}$ are given in table VI.

TABLE VI

Effective mass of electrons and holes in CdTe for various values of $\bar{\varepsilon}_n$ and $\bar{\varepsilon}_p$

	$\bar{\varepsilon}_n$ or $\bar{\varepsilon}_p$		
	$2kT$	$2·5kT$	$3kT$
m_n^*/m	0·13	0·10	0·066
m_p^*/m	0·41	0·30	0·22

2.2. Interpretation of the measurements of the Hall effect as a function of the temperature

The variation of the number of charge carriers as a function of the temperature gives information about the ionization energies of the various centres which donate electrons or holes. An exact determination of these energies is only possible by a careful analysis. In the following n- and p-type samples will be discussed separately.

2.2.1. n-Type samples

In general the situation in an n-type sample at 0 °K can be visualised by fig. 40. In this figure D denotes a donor level, which can be caused by a foreign atom, a tellurium vacancy or an interstitial cadmium atom. D' denotes an ionized donor
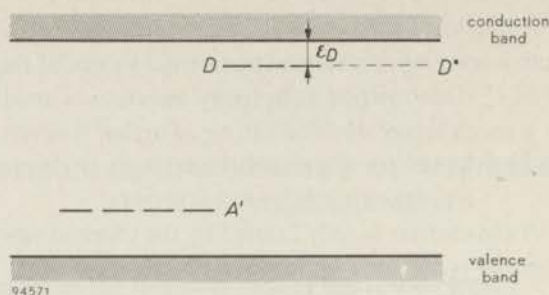
Fig. 40. Electronic energy-band scheme of an *n*-type sample with one donor and one acceptor level.

level and A' an acceptor level, caused by the presence of a foreign atom, a cadmium vacancy or an interstitial tellurium atom. It is assumed throughout this study that tellurium vacancies and interstitial tellurium do not play an important role, excess cadmium being caused by interstitial cadmium and excess tellurium being caused by cadmium vacancies. By applying the law of mass action to the equilibrium between a donor level and the conduction band, viz.

$$D \rightleftarrows D^{\cdot} + e' \tag{2.6}$$

(in which e' denotes a free electron) and keeping in mind that always electrical neutrality is maintained, viz.

$$[A'] + n = [D^{\cdot}], \tag{2.7}$$

(where n is the concentration of free electrons and the brackets stand for concentrations) it can be seen that

$$\frac{n [D^{\cdot}]}{[D]} = \frac{n\{[A']+ n\}}{[D]_{tot}-\{[A']+n\}} = an_{o} \exp(-\varepsilon_{D}/kT), \tag{2.8}$$

in which $[D]_{tot} = [D] + [D^{\cdot}]$, a is a statistical factor, $n_{o} = 2(2\pi mkT/h^{2})^{3/2}$ $(m_{n}^{*}/m)^{3/2}$, and ε_{D} is the ionization energy of the donor level.

When the values of n, $[D^{\cdot}]$ and $[D]$ are known for two temperatures one can calculate ε_{D} and m_{n}^{*}/m.

If the acceptor levels are due to a large quantity of copper or gold, the value of $[D^{\cdot}](=[A']+n)$ can be put equal to the concentration of Au or Cu in samples in which [Au] or [Cu] $\gg n$ and [Au] or [Cu] is much larger than the number of vacancies which can act as acceptor. The value of $[D]$ can be obtained from the value of n at temperatures higher than about 250 °C. In this temperature region n goes to a saturation value. This shows that all donor levels, which are filled at 0 °K, are empty at this temperature (see fig. 22).

This saturation value of n is indicated here as n_{sat}. The value of $[D]$ at a certain

temperature T now is equal to $n_{sat} - n_T$. This analysis was performed for some samples doped with Cu and Au. These samples could be made n-type by reheating at high cadmium pressures. The excess cadmium which cancels the acceptor activity of copper and gold is assumed to go to interstitial positions (Cd_i) (see section 3.1.1). The results of this analysis are summarized in table VII.

TABLE VII

Calculation of the ionization energy and of the effective-mass ratio for some n-type samples

Sample	donor centre	Reheating temp. (°K)	p_{Cd} (atm)	measuring temp. (°K)	n_T	n_{sat}	[D·]	ε_D (eV)	m^*/m	fig.
CdTe – 2.10^{17} Cu	Cd_i	1173	0·86	200	$4·88.10^{15}$	$6·3.10^{15}$	2.10^{17}	0·021	0·187	22
				237	$5·30.10^{15}$	$6·3.10^{15}$	2.10^{17}			
CdTe – 2.10^{17} Cu	Cd_i	1173	1·40	291	$2·4.10^{16}$	$3·4.10^{16}$	2.10^{17}	0·024	0·096	22
				206	$1·7.10^{16}$	$3·4.10^{16}$	2.10^{17}			
CdTe – 5.10^{16} Au	Cd_i	1273	1·45	224	$3·9.10^{14}$	$4·3.10^{14}$	5.10^{16}	0·022	0·126	22
				176	$3·6.10^{14}$	$4·3.10^{14}$	5.10^{16}			

The mean ionization energy of the centre caused by excess interstitial Cd (Cd_i) is found to be 0.022 ± 0.002 eV. The value of the effective-mass ratio of 0.14 ± 0.04 (which is the density-of-states effective-mass ratio) corresponds approximately with the value found from the thermo-electric power for $\bar{\varepsilon}_n = 2kT$ (Table VI), corresponding to a predominantly covalent type of bonding.

However, it has to be noted that the value of ε_D found by this method is very sensitive for slight variations in the saturation value obtained for the concentration of electrons at about 250 °C. This effect is reflected too in the values found for m^*/m.

The value of the ionization energy of the In_{Cd} centre, responsible for n-type conductivity in In-doped samples, cannot be determined in this way because of the unknown concentration of acceptors. As however the slopes in the log n vs $1/T$ diagrams are rather the same for all n-type samples, whether the n-type conductivity is caused by centres formed by excess cadmium (Cd_i) or by In_{Cd} centres, the ionization energy of the latter centre is probably close to that of the Cd_i centre.

The effective-mass ratio can also be calculated by applying a hydrogen-like approximation to the donor centre [23]). In this case the inertial effective-mass ratio $(m_n^*/m)_i$ is found. The ionization energy is then given by

$$E_D = 13.53(m_n^*/m)_i \left\{ \frac{1}{\varepsilon_s} + \frac{5}{16}\left(\frac{1}{\varepsilon_o} - \frac{1}{\varepsilon_s}\right)\right\}^2, \tag{2.9}$$

in which ε_s and ε_o denote the static and the optical dielectric constant, respectively. Inserting the value $E_D = 0.022$ eV as found experimentally and using the values $\varepsilon_o = n^2 = 7.6$ (section 1.7.5) and $\varepsilon_s = 11$ (section 1.6.5) one finds $(m_n^*/m)_i = 0.147$, which is close to the value found for the density-of-states effective mass (see above). Identity between the inertial effective mass and the density-of-states effective mass would be in agreement with a simple band structure for the conduction band (spherical energy surfaces). Such a structure has actually been predicted by Herman [46]).

In contradistinction to the shallow donor levels mentioned above, donor levels with a large ionization energy were found with CdTe–In samples when prepared under a definite cadmium pressure. These samples showed a very high resistance at room temperature (10^6–10^7 Ωcm). Hall-effect measurements were only possible at higher temperatures ($T > 150$ °C). The samples showed n-type conductivity; the variation of the Hall effect as a function of $1/T$ is given in figure 25.

The ionization energy can be calculated from the slope of the curve given in fig. 25 by a method as described for the p-type samples (see section 2.2.2). This leads to an ionization energy of 0.60 eV. It can be seen in figure 25 that at higher temperatures no longer a linear dependence is maintained between log R_H and

$1/T$. Apparently the samples are decomposing, which is confirmed by the change in conductivity of the samples after cooling to room temperature again.

Measurements with other samples showed some fluctuation in the value of the ionization energy. In the following the value of this energy will be approximated by 0.60 ± 0.05 eV. The centre which causes the n-type conductivity in this case is the double negatively charged cadmium vacancy V''_{Cd} (see section 3.3).
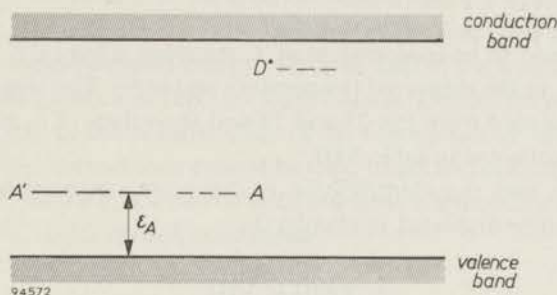
Fig. 41. Electronic energy-band scheme of a p-type sample with one donor and one acceptor level.

2.2.2. p-Type samples

A general energy-band scheme applying to p-type samples is shown in fig. 41. Again A stands for an acceptor and D for a donor which may be either foreign atoms or vacancies. Applying the law of mass action to the equilibrium

$$A \rightleftarrows A' + e^{\cdot} \tag{2.10}$$

in which $e^{\cdot}$ stands for a hole, we obtain

$$p[A']/[A] = a p_o \exp(-\varepsilon_A/kT) \tag{2.11}$$

where a is again a statistical factor, $p = [e^{\cdot}]$ and $p_o = 2(2\pi m k T/h^2)^{3/2}(m_p^*/m)^{3/2}$. Furthermore, $p + [D^{\cdot}] = [A']$. Introducing this into (2.11) one gets

$$\frac{p\{p + [D^{\cdot}]\}}{[A]_{tot} - \{p + [D^{\cdot}]\}} = a p_o \exp(-\varepsilon_A/kT). \tag{2.12}$$

A careful analysis as given for the n-type samples cannot be given here. The reason is that, because of the large depth of the acceptor level, the temperature to which we have to heat the sample in order to obtain the saturation value of the holes, which is equal to $[A]_{tot} - [D^{\cdot}]$ at $0\,°K$, is so high that the sample decomposes. However, this same circumstance makes it possible to simplify (2.12).

Due to the large depth of the acceptor level the hole concentration p is always much smaller than $[D^{\cdot}]$. Therefore $[A'] = [D^{\cdot}]$. Since $[A] = [A]_{tot} - [A']$, equation (2.11) reduces to

$$p/T^{3/2} = 2(2\pi mk/h^2)^{3/2}(m_p^*/m)^{3/2}\frac{[A]_{tot} - [D^{\cdot}]}{[D^{\cdot}]}\exp(-\varepsilon_A/kT). \qquad (2.13)$$

If $[D^{\cdot}]$ is assumed to be independent of T, the slope $d \log (p/T^{3/2})/d(1/T)$ leads to a value of ε_A in the measured temperature region [47]. The slopes for various samples are deduced from figs 23 and 24 and the values of ε_A calculated from the slopes are collected in table VIII.

The notation and the identification of the centres responsible for the hole conductivity will be discussed in chapter 3.

TABLE VIII

Ionization energies of the acceptor centres in various p-type CdTe samples

Sample	acceptor centre	Reheating temp. (°C)	$\log p_{Cd}$ (atm)	ε_A (eV)	fig.
purest CdTe	V_{Cd}	700	−2·73	0·15	23
		900	−0·54	0·15	23
		900	−0·12	0·13	23
		800	−1·26	0·15	23
CdTe − 10^{18} Ag	Ag_{Cd}	950	0·65	0·35	24
		980	0·80	0·30	24
CdTe − 5.10^{17} Cu	Cu_{Cd}	800	0·10	0·34	24
		800	0·05	0·34	24
CdTe − 5.10^{16} Au	Au_{Cd}	900	−0·95	0·35	28
		900	−0·65	0·32	28
		900	−0·40	0·27	28

In some cases where the determination of the hole concentration by Hall effect measurements offered difficulties by the large resistance or inhomogeneities in the samples, the slope of the $\log \varrho$ versus $1/T$ curve had to be used to determine the value of ε_A (fig. 28).

Now $\varrho^{-1} = pe\mu_p$, in which μ_p is the mobility of the holes and e is the charge of the electron. As μ is a slowly varying function of T, the error made is very small.

The fact that various neutral acceptors have different ionization energies sug-

gests that the ionization energy cannot be expressed in terms of a hydrogen-like model. In fact, if we calculate the energy E_A from the expression (2.9) with m_p^* instead of m_n^*, using the average effective-mass ratio of ≈ 0.30 found from the thermoelectric-power measurements (section 2.1), one finds $E_A = 0.045$ eV. This is not surprising, for if there is a difference between the actual state and the hydrogen model we may expect this to be in the direction that the actual level is further from the band than the level calculated with the hydrogen model. The reason is that a more localized wave function of the hole gives rise to deviations from the Coulomb-potential energy, which is used in the hydrogen approximation and so the expression (2.9) no longer holds. Deviations of this kind may, inter alia, be due to the polarizability of the foreign ion or vacancy.

Although this method thus cannot be used to get a check on the value of the effective mass, such a check can be obtained from the mobility ratio. According to Shockley [24], under certain conditions

$$\mu_n/\mu_p = (m_p^*/m_n^*)^{5/2}. \tag{2.14}$$

Although it is not quite certain whether these conditions apply to the present case, we may try how it works out. As will be seen in section 2.3, $\mu_n/\mu_p = 700/65 = 10.8$. Further, we have seen that the best value of $(m_n^*/m)_i = 0.15 \pm 0.02$. Relation (2.14) then leads to $(m_p^*/m)_i = 0.39$.

This value is identical with that of the density-of-states effective mass obtained from the thermo-electric power measurements (section 2.1), using $\bar{\varepsilon}_p \approx 2kT$.

2.3. Mobility of the charge carriers in CdTe

The value of the mobility μ of electrons and holes was determined from the relation existing between the Hall constant R_H and the specific resistance of a sample, viz.

$$\mu = R_H \varrho^{-1} f^{-1} \quad \text{with } f = 3\pi/8.$$

For a large number of samples the mobility was determined at room temperature. The mean value of μ at room temperature was found to be

$$\mu_n = 700 \text{ cm}^2/\text{V sec},$$

$$\mu_p = 65 \text{ cm}^2/\text{V sec}.$$

The variation of μ_n and μ_p as a function of the temperature is given in fig. 42 and fig. 43 (see also figs 21, 23, 26 and 27). From these figures it can be seen that in going from room temperature to lower temperatures the mobility first increases. In this temperature region lattice scattering will be predominant. In going to still
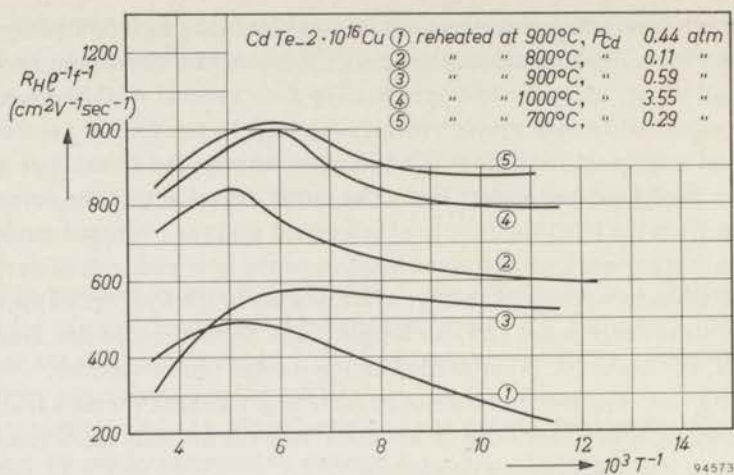
Fig. 42. The mobility of various *n*-type samples as a function of the temperature.
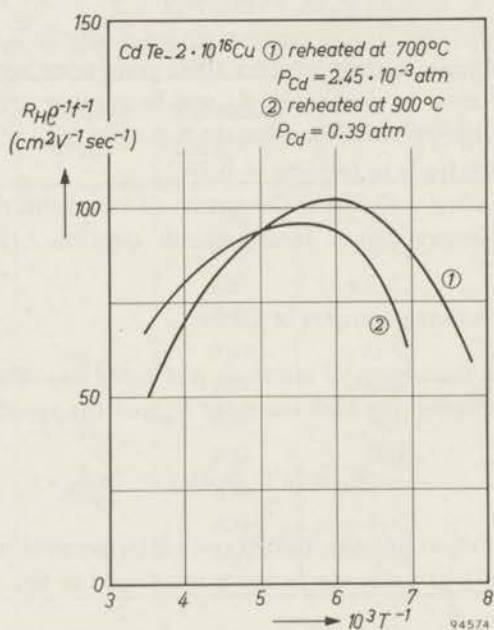
Fig. 43. The mobility of various *p*-type samples as a function of the temperature.

lower temperatures the mobility decreases again as a consequence of the fact that in this temperature region impurity scattering becomes important. Theoretically a $T^{-3/2}$ dependence of the mobility should be expected in the lattice-scattering region, if only the acoustical modes play a role in the non-polar scattering mechanism [25]). The temperature dependence which is observed in our figures is

much smoother. The temperature dependence between the maximum and the room-temperature value approximately can be given by $\mu = aT^{-3/2}$. This flattening may be caused by a contribution in the total scattering mechanism of the polar scattering by optical modes. For CdS [26]) and ZnO [27]) the experimental curves could be explained by a combination of these scattering mechanisms. However, the temperature range in which mobility values are determined is too small in our case to apply such an analysis to CdTe.

2.4. Interpretation of the optical measurements

2.4.1. *Transmission*

In fig. 29 the results of the spectral transmission of CdTe samples (thickness ≈ 0.2 mm) at various temperatures were given. The foot of the curve was taken as a measure of the energy gap. This choice was rather arbitrary, though justified in some way by the thickness of the sample. The value obtained was in good agreement with the values found from the photo-emf. measurements, by which a much sharper limit was obtained (cf. section 2.4.2).

The width of the energy gap as a function of the temperature, determined in this way, is shown in fig. 32. The change of the optical band gap with the temperature varies from $2.34.10^{-4}$ eV/°K at 77 °K to $5.44.10^{-4}$ eV/°K at 800 °K. Bube [6]) concluded from the position of the maximum in the photoconductivity spectrum as a function of T to $3.6.10^{-4}$ eV/°K between 100 °K and 330 °K, which is in fair agreement with our value in this temperature region ($3.2.10^{-4}$ eV/°K).

2.4.2. *Photo-electromotive force*

The sharp limit at the long-wavelength side of the photo-emf. spectrum can also be used to obtain the value of the optical band gap (fig. 31). Its position was measured at various temperatures between 77 °K and 480 °K (fig. 32). The values obtained agree with the values found from the transmission measurements.

2.4.3. *Photo-luminescence*

The interpretation of the results of the luminescence measurements mentioned in section 1.7.3.2 is still very uncertain. Much more experiments will have to be performed before quantitative conclusions can be drawn.

As to the measurements with CdTe -5.10^{17} In samples it can be seen that for samples reheated under a relatively high cadmium pressure (0·1 atm) a large peak at 1·42 eV and a smaller peak at 1·10 eV was obtained (fig. 34). Samples prepared at lower cadmium pressure (0·01 atm) showed the same large peak at 1·42 eV and a very small peak at 1·06 eV (fig. 34).

The large peak at 1·42 eV can possibly be ascribed to a band-to-band transition, the peak at 1·10 (1·06) eV to a centre with a level situated at about 0·34 eV from

the valence band or from the conduction band. This result will be compared with photoconductivity measurements in section 2.4.4. The decrease of the peak at 1·26 eV in CdTe − 5.10^{16} Au samples (fig. 35) by heating at 100 °C must be ascribed to a decrease of the number of centres which are responsible for this luminescence. A possible explanation will be proposed in section 3.7.

2.4.4. *Photoconductivity*

The spectral distribution of the photoconductivity reported in section 1.7.4 showed some resemblance with that of the luminescence (section 1.7.3.2). In CdTe − 5.10^{17} In, prepared at 0·1 atm cadmium pressure, a peak at 1·46 eV and a small peak at 1·07 eV was found (fig. 36). CdTe − 5.10^{17} In prepared at 0·01 atm cadmium pressure showed a very large peak at 1·46 eV, but no indication of a peak at 1·07 eV (fig. 36).

If we ascribe the two peaks found in the photoconductivity spectrum to two centres it is clear that one centre is increasing in concentration (1·07 eV peak) in going from higher to lower cadmium pressures. This is in accordance with the picture which will be developed in the theoretical part of this thesis (section 3.1).

It is assumed that the 1·49 eV peak corresponds to the band-band transition; then the position of the levels of the centres responsible for the other peaks must be at 0·03 eV and at 0·42 eV from either of the bands.

Owing to the Franck-Condon shift, level positions obtained from absorption, luminescence and electrical measurements (so-called "thermal energies") must be expected to differ. Therefore the correlation between levels found from the various experiments is not quite clear. It seems likely that the value of 0·03 eV found in photoconductivity measurements corresponds to the value of 0·34 eV from luminescence measurements, the last value being larger owing to the Franck-Condon effect. As a rough estimate of the thermal ionization energy one might take the average $\frac{1}{2}(0·03 + 0·34) = 0·18$ eV, which corresponds roughly to the thermal value found for the V_{Cd} centre (0·15 eV) (see section 2.2.2). This then would indicate that the absorption peak at 1·46 eV and the luminescence peak at 1·10 eV are due to transitions between the conduction band and the V'_{Cd} level close to the valence band.

As far as the second centre is concerned, one can only say that its ionization energy is larger than 0·42 eV. This centre may possibly be identified with the V''_{Cd} centre (see section 3.3) which has an ionization energy of 0·60 eV. No indication of this centre was found by us in the luminescence spectrum. These V''_{Cd} centres are in fact present in CdTe − 5.10^{17} In in an appreciable concentration and their concentration is increasing and decreasing as a function of p_{Cd} in the way as found in photoconductivity measurements (see section 3.3 and fig. 55).

The decrease of the photoconductivity peak at 1·40 eV in CdTe − 5.10^{16} Au by heating at 100 °C must be ascribed to a decrease of the number of centres causing this peak (see section 3.7).

conduction band

Cd_i In_{Cd}

$\varepsilon_1 = \varepsilon_5 = 0.02\,eV$ $\varepsilon_4 = 0.60\,eV$

$\varepsilon_6 = 1.17\,eV$

$\varepsilon_3 = 1.35\,eV$

V''_{Cd}

0.90 eV

Cu'_{Cd}, Ag'_{Cd}, Au'_{Cd}

0.33 eV

V'_{Cd} 0.15 eV

valence band

94575
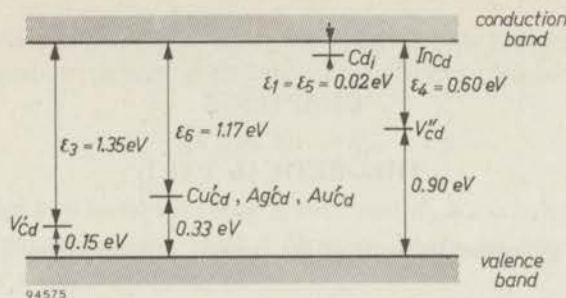
Fig. 44. Electronic energy-band scheme of CdTe, giving the room-temperature values of the thermal ionization energy of the various centres.

2.5 Characteristics of CdTe at room temperature

The quantities characterizing CdTe at room temperature as arrived at in the previous sections are summarized in table IX. An energy-band scheme showing the various thermal energy levels relative to the bands is shown in fig. 44.

TABLE IX

Characteristics of CdTe at room temperature

property	value	see section
effective mass ratio		
(a) m_n^*/m	0.14 ± 0.02	2.1; 2.2.1
(b) m_p^*/m	0.35 ± 0.05	2.1; 2.2.2
mobility		
(a) of electrons	700 cm^2 V^{-1}sec^{-1}	2.3
(b) of holes	65 cm^2 V^{-1}sec^{-1}	2.3
$\bar{\varepsilon}_n/kT$, $\bar{\varepsilon}_p/kT$	≈ 2	2.1; 2.2.2
E_{gap} at 300 °K	1·50 eV	2.4.1
dE_{gap}/dT	$2\cdot3.10^{-4}$ to $5\cdot4.10^{-4}$ eV/°K	2.4.1
$\varepsilon(Cd_i;\ In_{Cd})$	0.022 ± 0.002 eV	2.2.1
$\varepsilon(V'_{Cd})$	0.15 ± 0.02 eV	2.2.2
$\varepsilon(Cu'_{Cd}, Ag'_{Cd}, Au'_{Cd})$	0.33 ± 0.02 eV	2.2.2
$\varepsilon(V''_{Cd})$	0.60 ± 0.05 eV	2.2.1
dielectric constant ε_s	11	1.6.5
refractive index n	2.75 ± 0.01	1.7.5

CHAPTER 3

THEORETICAL PART

3.1. Equilibria governing the state of the crystals at high temperatures

The crystals, which were used in our experiments, were prepared by heating the samples at high temperatures under the controlled vapour pressure of the components. This method of preparation leads to crystals containing several kinds of imperfections. In this chapter first imperfections inherent to the pure CdTe lattice (i.e. the so-called native imperfections) are considered. Then imperfections due to the incorporation of foreign atoms will be discussed. After knowledge of the various disorder equilibria is gained, finally a complete description of the state of the samples at high temperatures will be given.

3.1.1. *Native atomic disorder*

A crystal in equilibrium at very low temperatures will have a purely periodic structure. At higher temperatures atomic disorder may occur involving vacant lattice sites and/or interstitial atoms. Several types of disorder are possible, viz. Schottky disorder, Frenkel disorder, and antistructure disorder. In the Schottky disorder vacancies of both types of atoms are formed in equal concentrations. In Frenkel disorder equal concentrations of interstitial atoms and vacancies at normal lattice positions are formed. In the antistructure disorder finally one type of atom occupies the position of the atom of the other type, and vice versa.

A decision as to which of these types of imperfections actually occur can be arrived at with the aid of various measurements. Thus it has been shown [29] that substances having an antistructure disorder will show n-type electrical conductivity if an excess of the more electronegative component is present, and p-type conductivity in the opposite case. For Schottky and Frenkel disorder on the other hand the opposite holds. As CdTe is found to show n-type conductivity in the presence of an excess of the less electronegative component (Cd) the former type of disorder may be discarded.

In order to decide between Schottky and Frenkel disorder other types of measurement are required. Preliminary measurements of the selfdiffusion using radioactive cadmium indicate Frenkel disorder involving interstitial cadmium and cadmium vacancies. This type of disorder will be assumed in the following. The Frenkel type of disorder can be described by

$$CdTe \rightleftarrows Cd_{(1-\delta)} (V'_{Cd})_\delta (Cd_i^{\cdot})_\delta Te, \tag{3.1}$$
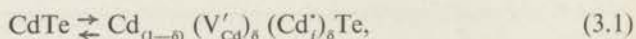
in which δ denotes the molar concentration of the imperfection, $Cd_i^{\cdot}$ indicates

an interstitial cadmium atom which has lost one electron to the cadmium vacancy and V'_{Cd} a cadmium vacancy with a negative effective charge. If $\delta \ll 1$ it is evident that

$$[V'_{Cd}][Cd_i^{\cdot}] = K_F, \qquad (3.2)$$

in which the brackets stand for concentration and K_F is a constant at a definite temperature, indicated as the Frenkel constant. In the following the concentrations will be given in number cm^{-3}.

3.1.2. *Native electronic disorder*

At low temperature the valence electrons in a semiconductor are in the state of lowest energy. At increasing temperatures some electrons are excited to higher states and are able to move in an electric field. These electrons are called free electrons. The unexcited valence electrons are now able to move too in an electric field to a degree determined by the number of missing electrons which behave as particles with a positive electric charge. They are called free holes. The number of holes created by thermal excitation is equal to the number of excited free electrons. This thermal excitation can be described by the quasi-chemical reaction

ground state $\rightleftarrows$ free electron + free hole $- \varepsilon_i$.

Application of the law of mass action to this reaction leads to

$$np = K_i, \qquad (3.3)$$

in which n is the free electron concentration, p is the free hole concentration and K_i is called the intrinsic constant. In the energy-band scheme the thermal excitation is represented as the excitation of an electron from the valence band to the conduction band, leading to a free electron and a free hole (fig. 44).

Another type of electronic native disorder is caused by the ionization of the lattice imperfections, mentioned in section 3.1.1. An interstitial Cd atom can be ionized according to

$$Cd_i^{\times} \rightleftarrows Cd_i^{\cdot} + e' - \varepsilon_1 \qquad (3.4)$$

in which the cross denotes an effective charge zero, the dot indicates the positive charge remaining on the centre after ionization, ε_1 is the ionization energy of the Cd_i centre and e' stands for a free electron. Further ionization leads to

$$Cd_i^{\cdot} \rightleftarrows Cd_i^{\cdot\cdot} + e' - \varepsilon_2. \qquad (3.5)$$

In fig. 45 these processes are visualized, giving the levels an arbitrary position between the energy bands. Solid lines indicate energy levels occupied by an
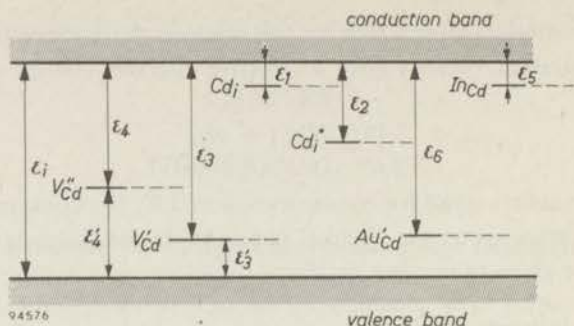
Fig. 45. A possible electronic energy-band scheme of CdTe containing various imperfections.

electron, dashed lines empty levels. All levels, occupied or empty, are designated by the symbol of the centre corresponding to the level when it is occupied. Applying the law of mass action to the equations (3.4) and (3.5) leads to

$$[Cd_i^{\cdot}]\, n/[Cd_i^{\times}] = K_1 \tag{3.6}$$

and

$$[Cd_i^{\cdot\cdot}]\, n/[Cd_i^{\cdot}] = K_2. \tag{3.7}$$

In principle, a process as described by

$$Cd_i + e' \rightarrow Cd_i' \tag{3.8}$$
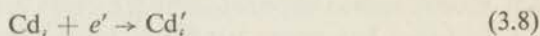
might also be possible. Since cadmium is the less electronegative component of the crystal, the tendency to give off an electron will be more probable. Therefore reaction (3.8) need not to be taken into account.

The V_{Cd} centres can be treated in an analogous way, with the difference that in this case the liberation of a hole (which is identical with the attraction of an electron) is the most probable process. This leads to the equations

$$V_{Cd}^{\times} \underset{\leftarrow}{\rightarrow} V_{Cd}' + e^{\cdot} - \varepsilon_3', \tag{3.9}$$

$$V_{Cd}' \underset{\leftarrow}{\rightarrow} V_{Cd}'' + e^{\cdot} - \varepsilon_4', \tag{3.10}$$
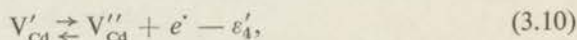
in which $e^{\cdot}$ stands for a free hole.

In fig. 45 possible positions of the levels corresponding to these centres are also given. The notation of the centres is chosen in such a way that the subscript indicates the kind of vacancy and the superscript the effective charge (the effective charge zero being denoted by the superscript $\times$). Ionization of vacancies can also be described in a different way, viz. by the transfer of electrons between the centres and the conduction band:

$$V'_{Cd} \underset{\leftarrow}{\rightarrow} V^x_{Cd} + e' - \varepsilon_3, \tag{3.11}$$

$$V''_{Cd} \underset{\leftarrow}{\rightarrow} V'_{Cd} + e' - \varepsilon_4. \tag{3.12}$$
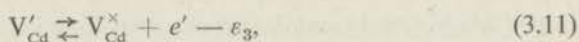
In equilibrium the degree to which the levels are filled is determined by the equilibrium constants of the reactions (3.9) and (3.10) or of the reactions (3.11) and (3.12). Choosing the last set it can be seen that

$$[V^x_{Cd}]\, n/[V'_{Cd}] = K_3, \tag{3.13}$$

$$[V'_{Cd}]\, n/[V''_{Cd}] = K_4. \tag{3.14}$$

3.1.3. *Atomic and electronic disorder caused by the incorporation of foreign atoms*

Foreign atoms can be incorporated in a crystal lattice both at interstitial or at lattice positions. As will be shown, the influence of the foreign atoms on the electrical properties of the crystal can be explained if the incorporation is assumed to take place at normal lattice positions, i.e. so-called substitutional incorporation. As to the lattice site at which the foreign atom is introduced, as a rule the foreign atom tends to choose the position of the lattice atom to which it is nearest in the periodic system, e.g. In, Cu, Au, etc. are supposed to be incorporated at cadmium sites; Cl, I, etc. at tellurium sites. The incorporation of foreign atoms can lead to energy levels between the bands. The position of these levels depends on the number of valence electrons of the substituting atom and the number of valence electrons of the lattice constituent which it replaces. A tendency to give off electrons will be predominant if the foreign atom possesses more valence electrons than the lattice atoms they replace. Foreign atoms with less valence electrons than the lattice atom it replaces tend to bind extra electrons. Thus substitutional In with three valence electrons at a cadmium position will act as a donor of electrons, substitutional Au with one valence electron acts as an acceptor of electrons. This function is illustrated by the equations

$$In^x_{Cd} \underset{\leftarrow}{\rightarrow} In^{\cdot}_{Cd} + e' - \varepsilon_5, \tag{3.15}$$

$$Au^x_{Cd} + e' \underset{\leftarrow}{\rightarrow} Au'_{Cd} + \varepsilon_6, \tag{3.16}$$

in which the notation of the centres is the same as used for the description of the vacancies, viz. the main symbol indicating the atom considered, the subscript denoting its position, and the superscript the effective charge of the centre. In fig. 45 possible positions of these levels are indicated. The equilibrium constants associated with the foregoing equations are given by

$$[In^{\cdot}_{Cd}]\, n/[In^x_{Cd}] = K_5, \tag{3.17}$$

$$[Au^x_{Cd}]\, n/[Au'_{Cd}] = K_6. \tag{3.18}$$

In this description In and Au are chosen as simple examples. However, the same procedure can be followed for other foreign atoms with more ionization steps. In some cases it will be difficult to predict the function of an introduced foreign atom. Thus Sb may act as a donor when introduced at a cadmium site, but as an acceptor when introduced at a tellurium site. In such cases only precise experiments can show at which position the atoms are incorporated.

3.1.4. *Reaction between the atmosphere and the crystal*

When a crystal is heated in an atmosphere containing its components and the partial pressures of these components are different from the partial pressures corresponding to equilibrium at that temperature, a reaction takes place between the crystal and the atmosphere. The introduction of cadmium atoms in the crystal lattice can occur according to the following equations:

$$\text{(a)} \quad CdTe + \delta\,Cd \rightleftarrows CdTe(Cd_i^x)_\delta, \tag{3.19}$$

$$\text{(b)} \quad CdTe + \delta\,Cd \rightleftarrows CdTe(Cd_i^{\cdot})_\delta + \delta\,e', \tag{3.20}$$

$$\text{(c)} \quad CdTe + \delta\,Cd \rightleftarrows CdTe(Cd_i^{\cdot\cdot})_\delta + 2\delta\,e'. \tag{3.21}$$
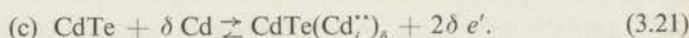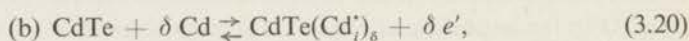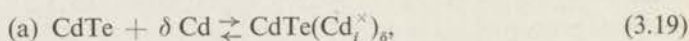
As these reactions are coupled by the equilibria between the Cd_i^x, $Cd_i^{\cdot}$ and $Cd_i^{\cdot\cdot}$ centres within the crystal, one of these equations is sufficient to account for the reaction between the crystal and the vapour.

The experimental curves giving the relation between the logarithm of the number of electrons and the logarithm of the cadmium pressure show that in the high cadmium-pressure region the number of electrons is proportional to $p_{Cd}^{1/2}$ (see fig. 15). As in this region the number of free electrons is equal to the number of $Cd_i^{\cdot}$ centres, reaction (b) appears to be predominant in this region. Therefore in the following reaction (3.20) is chosen. Application of the law of mass action to this reaction leads to

$$[Cd_i^{\cdot}]\,n = K_r p_{Cd}, \tag{3.22}$$

in which K_r is called the reduction constant.

The introduction of tellurium can be described in an analogous way. In the temperature region studied tellurium is present in the gas phase as Te_2 molecules. The reaction which is chosen to describe the incorporation of tellurium in CdTe is

$$(1-\delta)CdTe + \tfrac{1}{2}\delta\,Te_2 \rightleftarrows Cd_{(1-\delta)}Te(V_{Cd}')_\delta + \delta\,e^{\cdot} \tag{3.23}$$
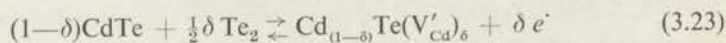
leading to

$$[V_{Cd}']\,p = K_{ox}\,p_{Te_2}^{1/2}, \tag{3.24}$$

where K_{ox} is the oxydation constant. Of course the cadmium and the tellurium pressure over a CdTe crystal are not independent from each other. They are coupled by the relation

$$p_{Cd}\, p_{Te_2}^{1/2} = K_{CdTe}.\tag{3.25}$$

Owing to this relation the equations (3.22) and (3.24) are not independent. Therefore in the further calculations only one of them has to be taken into account.

3.1.5. *The complete equilibrium between the crystal and the vapour at high temperatures*

In the foregoing, the various equilibria governing the state of CdTe at high temperature were described. If the reaction constants of these equilibria were known it should be possible to calculate the concentrations of the various centres, electrons and holes at a definite temperature and cadmium pressure. By a simple transformation of the expressions for the various K values it is possible to express all centre concentrations as a function of K, p_{Cd} and the concentration of one of the imperfections, e.g. that of the electrons.

For the case in which both donor atoms (e.g. indium) and acceptor atoms (e.g. gold) are simultaneously present, this transformation leads to

$$p = K_i/n,\tag{3.26}$$

$$[Cd_i^\times] = K_r p_{Cd}/K_1,\tag{3.27}$$

$$[Cd_i^\cdot] = K_r p_{Cd}/n,\tag{3.28}$$

$$[Cd_i^{\cdot\cdot}] = K_2 K_r p_{Cd}/n^2,\tag{3.29}$$

$$[V_{Cd}^\times] = K_3 K_F/K_r p_{Cd},\tag{3.30}$$

$$[V_{Cd}'] = K_F n/K_r p_{Cd},\tag{3.31}$$

$$[V_{Cd}''] = K_F n^2/K_4 K_r p_{Cd},\tag{3.32}$$

$$[In_{Cd}^\cdot] = K_5 [In_{Cd}^\times]/n,\tag{3.33}$$

$$[Au_{Cd}'] = n\, [Au_{Cd}^\times]/K_6,\tag{3.34}$$

$$[In]_{total} = [In_{Cd}^\times] + [In_{Cd}^\cdot],\tag{3.35}$$

$$[Au]_{total} = [Au_{Cd}^\times] + [Au_{Cd}'].\tag{3.36}$$

To this set of equations a last one has to be added, viz. the equation expressing the conservation of neutrality of the crystal as a whole:

$$2\,[Cd_i^{\cdot\cdot}] + [Cd_i^\cdot] + p + [In_{Cd}^\cdot] = 2\,[V_{Cd}''] + [V_{Cd}'] + n + [Au_{Cd}'].\tag{3.37}$$

It is rather tiresome to calculate the exact solution of this set of equations. It is possible, however, to obtain an approximate solution in a simple way worked out by Brouwer [30]). If one studies the exact solution of the equations (3.26) to

(3.37) in a graph in which $\log K_r p_{Cd}$ is plotted against the centre concentration, it is seen that in some ranges of the $K_r p_{Cd}$ scale only two concentrations of centres with opposite effective charge play a dominant role. In such a region the neutrality condition may be approximated by a simpler equation containing only the two dominating terms, thus neglecting all the other terms. Now it is possible to give the neutrality equation (3.37) a logarithmic form. In doing the same with the equations (3.26) to (3.34) a set of linear equations is obtained and the logarithm of each centre concentration can be expressed as a linear function of $\log K_r p_{Cd}$. This means that we do not only get the value of all the concentrations at one particular value of $K_r p_{Cd}$, but also the variation of these concentrations as $K_r p_{Cd}$ varies. Therefore it can be seen when the approximation applied ceases to be valid and by which approximation it has to be replaced. This method has been found to be very useful in obtaining insight in the relations between $\log K_r p_{Cd}$ and the logarithm of the concentration of the centres, in particular when use is made of the $\log K_r p_{Cd}$ – log concentration plots. In the following this method will be applied to pure CdTe (section 3.1.5.1), to CdTe–In (section 3.1.5.2) and to CdTe–Au (section 3.1.5.3).

3.1.5.1. *Pure CdTe*

The type of imperfections appearing in the solid and the way in which their concentration varies with the conditions of preparation depends on the energy-level diagram and the values of the constants governing the reactions involving the various imperfections.
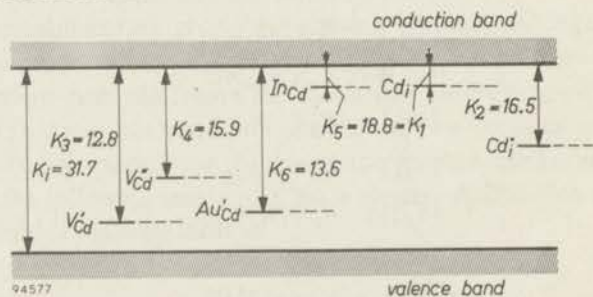
Fig. 46. A possible electronic energy-band scheme of CdTe. In this figure the symbols K denote the logarithms of the various equilibrium constants.

Let us first consider pure CdTe with an energy-level diagram as shown in fig. 46, in which the values chosen for the logarithms of the various constants are inserted.

When CdTe is heated under a high cadmium pressure, cadmium is introduced into the crystal at interstitial sites (Cd_i), which ionize practically completely and thus give rise to an equal concentration of $Cd_i^\cdot$ and free electrons. Hence under these conditions the neutrality condition (3.37) may be simplified to

$$[Cd_i^\cdot] = n.$$

With this approximation the set of equations (3.26) to (3.32) describing the equilibrium crystal-vapour becomes

$$p = K_i \left(K_r p_{Cd}\right)^{-1/2}, \tag{3.26a}$$

$$n = \left(K_r p_{Cd}\right)^{1/2}, \tag{3.26a'}$$

$$[Cd_i^\times] = K_r p_{Cd}/K_1, \tag{3.27a}$$

$$[Cd_i^\cdot] = \left(K_r p_{Cd}\right)^{1/2}, \tag{3.28a}$$

$$[Cd_i^{\cdot\cdot}] = K_2, \tag{3.29a}$$

$$[V_{Cd}^\times] = K_3 K_F/K_r p_{Cd}, \tag{3.30a}$$

$$[V_{Cd}'] = K_F/\left(K_r p_{Cd}\right)^{1/2}, \tag{3.31a}$$

$$[V_{Cd}''] = K_F/K_4. \tag{3.32a}$$
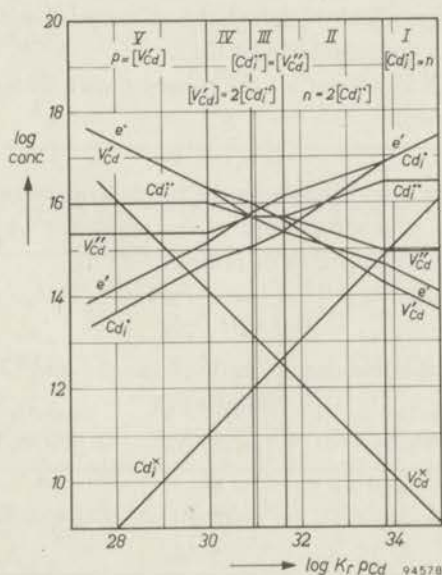
Fig. 47. Concentration of imperfections in pure CdTe at 700 °C (including the $Cd_i^\cdot$ level).

The concentrations of the various imperfections as a function of $K_r p_{Cd}$ are shown at the right-hand side of fig. 47 (range I). This figure, which has been constructed with the aid of a set of constants K, calculated from a plausible energy-level diagram of CdTe (like that of fig. 44) and with the assumption that $K_F \approx K_i$ (cf. the situation with CdS[2] and PbS[3]), where $K_S \approx K_i$). It is seen that the concentration of $Cd_i^{\cdot\cdot}$ is constant in this range with decreasing $K_r p_{Cd}$ and becomes equal to the half of the electron concentration at $\log K_r p_{Cd} = 33.8$. Beyond this point the neutrality condition can no longer be approximated by $[Cd_i^\cdot] = n$ but becomes $n = 2\,[Cd_i^{\cdot\cdot}]$.

With this condition, the set of equations (3.26) to (3.32) can again be solved, which leads to

$$p = K_i/(2K_2K_r p_{Cd})^{1/2}, \tag{3.26b}$$

$$n = (2K_2K_r p_{Cd})^{1/2}, \tag{3.26b'}$$

$$[Cd_i^x] = K_r p_{Cd}/K_1, \tag{3.27b}$$

$$[Cd_i^\cdot] = (K_r p_{Cd})^{1/2}/(2K_2)^{1/2}, \tag{3.28b}$$

$$[Cd_i^{\cdot\cdot}] = (\tfrac{1}{4}K_2K_r p_{Cd})^{1/2}, \tag{3.29b}$$

$$[V_{Cd}^x] = K_3K_F/K_r p_{Cd}, \tag{3.30b}$$

$$[V_{Cd}'] = (2K_2)^{1/2}K_F/(K_r p_{Cd})^{1/2}, \tag{3.31b}$$

$$[V_{Cd}''] = (2K_2)^{1/2}K_F/K_4(K_r p_{Cd})^{1/2}. \tag{3.32b}$$

This is indicated in fig. 47 as range II. This range in its turn is ended as soon as the V_{Cd}'' concentration, which is increasing in range II with decreasing $K_r p_{Cd}$, becomes equal to the concentration of $Cd_i^{\cdot\cdot}$.

Proceeding in this way we get all the ranges shown in fig. 47, ending finally with a range in which

$$[V_{Cd}'] = p.$$

The equations for the lines presenting the concentration of a particular centre as a function of $K_r p_{Cd}$, in some range of the graph for which a special charge compensation holds, are collected in table X.

TABLE X

Concentration of imperfections in various ranges with simplified neutrality conditions.

In all ranges the concentration of $V_{Cd}^x = K_r p_{Cd}/K_3$ and of $Cd_i^x = K_1K_F/K_r p_{Cd}$

concentration of	$n = p$	$n = [Cd_i^\cdot]$	$n = [In_{Cd}^\cdot]$	$[Au_{Cd}'] = p$
$e' =$	$K_i^{1/2}$	$(K_r p_{Cd})^{1/2}$	$[In_{Cd}^\cdot]$	$\dfrac{K_i}{[Au_{Cd}']}$
$e^\cdot =$	$K_i^{1/2}$	$\dfrac{K_i}{(K_r p_{Cd})^{1/2}}$	$\dfrac{K_i}{[In_{Cd}^\cdot]}$	$[Au_{Cd}']$
$Cd_i^\cdot =$	$\dfrac{K_r p_{Cd}}{K_i^{1/2}}$	$(K_r p_{Cd})^{1/2}$	$\dfrac{K_r p_{Cd}}{[In_{Cd}^\cdot]}$	$\dfrac{K_r p_{Cd}[Au_{Cd}']}{K_i}$
$V_{Cd}' =$	$\dfrac{K_FK_i^{1/2}}{K_r p_{Cd}}$	$\dfrac{K_F}{(K_r p_{Cd})^{1/2}}$	$\dfrac{K_F[In_{Cd}^\cdot]}{K_r p_{Cd}}$	$\dfrac{K_iK_F}{[Au_{Cd}']K_r p_{Cd}}$
$V_{Cd}'' =$	$\dfrac{K_FK_i}{K_4K_r p_{Cd}}$	$\dfrac{K_F}{K_4}$	$\dfrac{K_F[In_{Cd}^\cdot]^2}{K_4K_r p_{Cd}}$	$\dfrac{K_FK_i^2}{K_4[Au_{Cd}']^2K_r p_{Cd}}$

TABLE X (continued)

concentration of	$[V'_{Cd}] = p$	$[V'_{Cd}] = Cd^{\bullet}_i$	$[V'_{Cd}] = [In^{\bullet}_{Cd}]$	$[Au'_{Cd}] = [Cd^{\bullet}_i]$
$e' =$	$\left(\dfrac{K_i K_r p_{Cd}}{K_F}\right)^{1/2}$	$\dfrac{K_r p_{Cd}}{K_F^{1/2}}$	$\dfrac{K_r p_{Cd}[In^{\bullet}_{Cd}]}{K_F}$	$\dfrac{K_r p_{Cd}}{[Au'_{Cd}]}$
$e^{\bullet} =$	$\left(\dfrac{K_i K_F}{K_r p_{Cd}}\right)^{1/2}$	$\dfrac{K_i K_F^{1/2}}{K_r p_{Cd}}$	$\dfrac{K_i K_F}{K_r p_{Cd}[In^{\bullet}_{Cd}]}$	$\dfrac{K_i[Au'_{Cd}]}{K_r p_{Cd}}$
$Cd^{\bullet}_i =$	$\left(\dfrac{K_F K_r p_{Cd}}{K_i}\right)^{1/2}$	$K_F^{1/2}$	$\dfrac{K_F}{[In^{\bullet}_{Cd}]}$	$[Au'_{Cd}]$
$V'_{Cd} =$	$\left(\dfrac{K_i K_F}{K_r p_{Cd}}\right)^{1/2}$	$K_F^{1/2}$	$[In^{\bullet}_{Cd}]$	$\dfrac{K_F}{[Au'_{Cd}]}$
$V''_{Cd} =$	$\dfrac{K_i}{K_4}$	$\dfrac{K_r p_{Cd}}{K_4}$	$\dfrac{K_r p_{Cd}[In^{\bullet}_{Cd}]^2}{K_4 K_F}$	$\dfrac{K_F K_r p_{Cd}}{K_4[Au'_{Cd}]^2}$

concentration of	$2[V''_{Cd}] = p$	$2[V''_{Cd}] = [Cd^{\bullet}_i]$	$2[V''_{Cd}] = [In^{\bullet}_{Cd}]$
$e' =$	$\left(\dfrac{K_i K_4 K_r p_{Cd}}{2K_F}\right)^{1/3}$	$\dfrac{K_4^{1/3}(K_r p_{Cd})^{2/3}}{(2K_F)^{1/3}}$	$\left(\dfrac{[In^{\bullet}_{Cd}]K_4 K_r p_{Cd}}{2K_F}\right)^{1/2}$
$e^{\bullet} =$	$\left(\dfrac{2K_i^2 K_F}{K_4 K_r p_{Cd}}\right)^{1/3}$	$\dfrac{K_i(2K_F)^{1/3}}{K_4^{1/3}(K_r p_{Cd})^{2/3}}$	$\left(\dfrac{2K_i^2 K_F}{[In^{\bullet}_{Cd}]K_4 K_r p_{Cd}}\right)^{1/2}$
$Cd^{\bullet}_i =$	$\left(\dfrac{2K_F K_r^2 p_{Cd}^2}{K_i K_4}\right)^{1/3}$	$\left(\dfrac{2K_F K_r p_{Cd}}{K_4}\right)^{1/3}$	$\left(\dfrac{2K_F K_r p_{Cd}}{[In^{\bullet}_{Cd}]K_4}\right)^{1/2}$
$V'_{Cd} =$	$\dfrac{(\frac{1}{2}K_i K_4 K_F^2)^{1/3}}{(K_r p_{Cd})^{2/3}}$	$\left(\dfrac{K_4 K_F^2}{2K_r p_{Cd}}\right)^{1/3}$	$\left(\dfrac{[In^{\bullet}_{Cd}]K_4 K_F}{2K_r p_{Cd}}\right)^{1/2}$
$V''_{Cd} =$	$\frac{1}{2}\left(\dfrac{2K_i^2 K_F}{K_4 K_r p_{Cd}}\right)^{1/3}$	$\frac{1}{2}\left(\dfrac{2K_F K_r p_{Cd}}{K_4}\right)^{1/3}$	$\frac{1}{2}[In^{\bullet}_{Cd}]$

In a similar way we can also find a solution with the aid of a slightly simpler model, viz. for a model in which Cd_i gives rise to only one level within the forbidden gap and can occur only in two forms, viz. as $Cd^{\times}_i$ and as $Cd^{\bullet}_i$.

Taking for the constants the same values as assumed in the preceding calculation, one gets the result shown in fig. 48. Comparing fig. 47 and fig. 48 it is seen that the omission of the $Cd^{\bullet}_i$ level leads not only to the disappearance of the line giving the $Cd^{\bullet\bullet}_i$ concentration, but also to a marked change in the variation of the concentrations of the other imperfections with $K_r p_{Cd}$. Such a change is not caused by the omission of the V''_{Cd} level from the model, as the V'_{Cd} con-
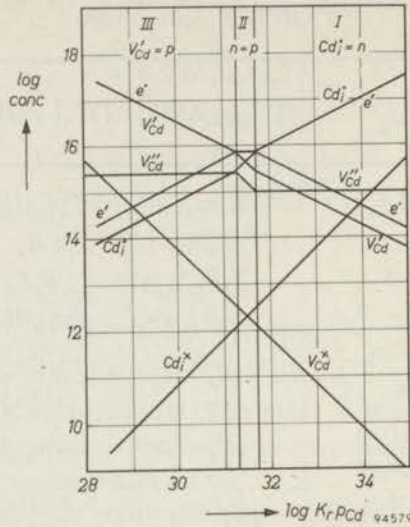
Fig. 48. Concentration of imperfections in pure CdTe at 700 °C (omitting the Cd_i level).

centration does not play a dominant role in the concentration versus $K_r p_{Cd}$ graph. This statement only holds for the combination of constants used. For other values of the constants the introduction or omission of V''_{Cd} may have a marked effect.

3.1.5.2. *CdTe–In*

For CdTe samples doped with indium, which was taken here as a typical foreign atom giving rise to donor levels, a procedure similar to that described for pure CdTe to obtain the log $K_r p_{Cd}$ versus log concentration graph can be followed. The drawing of such a diagram is always started with the right hand or the left hand range which are the same for pure and for doped samples. The equations which hold in the various ranges can be easily derived from the equations (3.26) to (3.33), inserting the simplified neutrality condition holding in each range. In table X the results of this procedure are summarized. If in drawing a log $K_r p_{Cd}$ diagram one is led to assume a particular simplified form of the neutrality condition, the equation of the line presenting the variation of the concentration of a special centre as a function of log $K_r p_{Cd}$ can be taken from this table.

In fig. 49 and fig. 50 diagrams are shown for two different models. In fig. 49, next to the neutral and singly charged centres, the V''_{Cd} centres are taken into account; in fig. 50 these centres are omitted. It can be seen that the variation of the concentration of the other centres is markedly influenced by the choice of the model. Further these figures show that the Cd" centres do not play a dominant role in any part of the diagram.
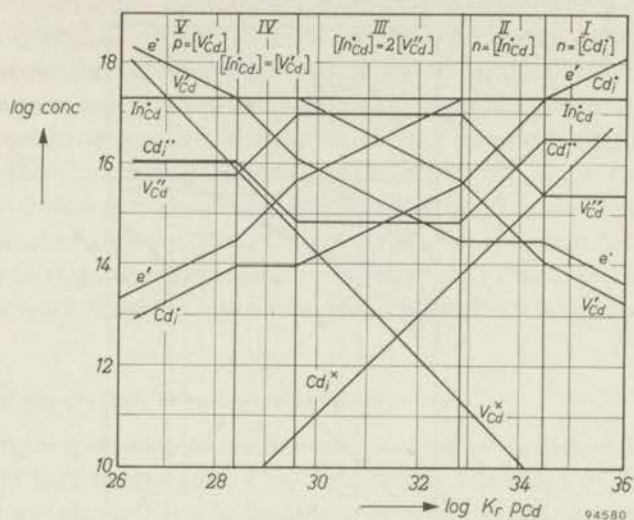
Fig. 49. Concentration of imperfections in CdTe − 2.10¹⁷ In at 700 °C (including the V''_{Cd} level).
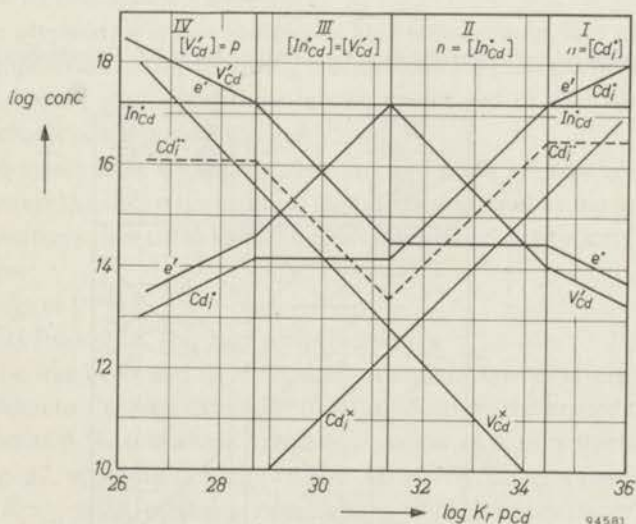
Fig. 50. Concentration of imperfections in CdTe − 2.10¹⁷ In at 700 °C (omitting the V''_{Cd} level).

3.1.5.3. *CdTe–Au*

Similar calculations can also be carried out for CdTe containing foreign atoms which act as acceptors, e.g. Au. Using the same values as before, and accepting the energy levels as shown in fig. 46, one gets the $\log K_r p_{Cd}$ versus log concentration graphs as presented in fig. 51 and fig. 52. The latter figure applies to the case in which double charged Cd''_i centres are omitted; fig. 51 shows the situation im-
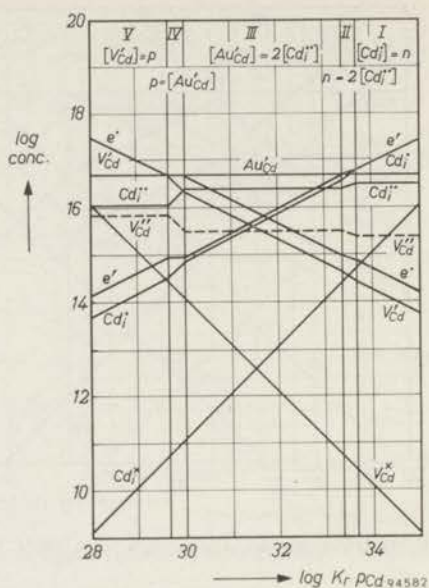
Fig. 51. Concentration of imperfections in CdTe−5.10^{16} Au at 700 °C (including the Cd$_i'$ level).
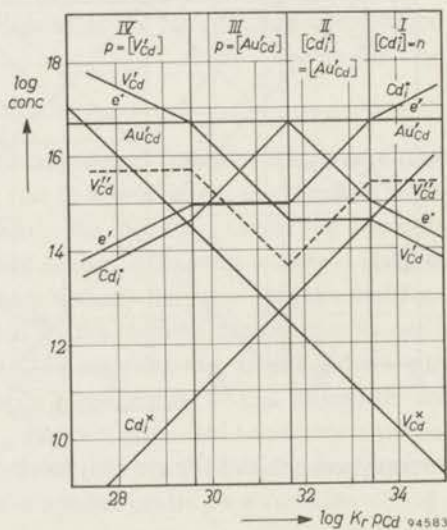
Fig. 52. Concentration of imperfections in CdTe−5.10^{16} Au at 700 °C (omitting the Cd$_i'$ level).

plicating these centres. In studying these figures it can be seen that the choice of our model markedly influences the variation of the concentration of the various centres in the log $K_r p_{Cd}$ graph. The V$_{Cd}''$ centres shown as a dashed line in figs 51 and 52 do not play a dominant role in any part of the diagram.

So far, we have studied the variation of the various imperfections as a function of the atmosphere. In our considerations we have assumed a certain model by ascribing certain energy levels to these imperfections. This model could be tested by comparison of experimental data (electrical and optical), measured as a function of the cadmium pressure, with the variation of measurable entities (such as electron and hole concentration) as deduced from the $\log K_r p_{Cd}$ graphs. However, measurements have not been carried out at the temperatures of preparation for which the graphs have been drawn (700–1000 °C), but at or near room temperature. In the next chapter the question what happens to the crystals when they are cooled down from high temperatures to room temperature will be considered.

3.2. State of the crystals at room temperature

In the foregoing chapter the concentrations of the various imperfections were calculated at high temperatures (700–1000 °C) as a function of the cadmium pressure. It was assumed that at these temperatures the various centres are not associated with each other. To which extent this assumption is true will be discussed in section 3.7.

After the preparation of the samples at high temperatures they are quenched to room temperature. In the following it is assumed that this quenching happens so quickly that all atomic positions remain unchanged so that no association or cluster effects occur during the quenching.

A second assumption is that the electrons and holes are able to redistribute themselves over the various centres, so that electronic equilibrium is maintained at all temperatures. For the sake of simplicity the quenching process is discussed in two stages:

(a) quenching to 0 °K;

(b) reheating from 0 °K to room temperature.

At 0 °K no free holes and electrons are left and the energy levels between the bands are filled to a certain extent. In order to illustrate the procedure by which the situation at 0 °K is derived from the situation at high temperature, let us consider fig. 52, applying to CdTe– 5.10^{16} Au at 700 °C. At a particular point, e.g. at $\log K_r p_{Cd} = 34$, certain concentrations of the various imperfections are present.

In going from high temperatures to 0 °K a small fraction of the electrons is required to annihilate the holes. After this the $V_{Cd}^{\times}$ and V_{Cd}' levels are filled. This leads to a number of V_{Cd}'' centres almost equal to the original number of V_{Cd}'' centres as the number of $V_{Cd}^{\times}$ and V_{Cd}' centres is very small.

As Au_{Cd}' represents a level filled with an electron, the remaining number of electrons are used to fill a number of the empty levels due to the $Cd_i^{\cdot}$ centres, leading to an equal number of $Cd_i^{\times}$ centres. The number of $Cd_i^{\cdot}$ levels which remain empty at 0 °K will be equal to the sum of the Au_{Cd}' and the double of the

Fig. 53. Concentration of imperfections at 0 °K (fully drawn lines) and of electrons and holes at room temperature (dashed lines) of pure CdTe (including the Cd_i' level).
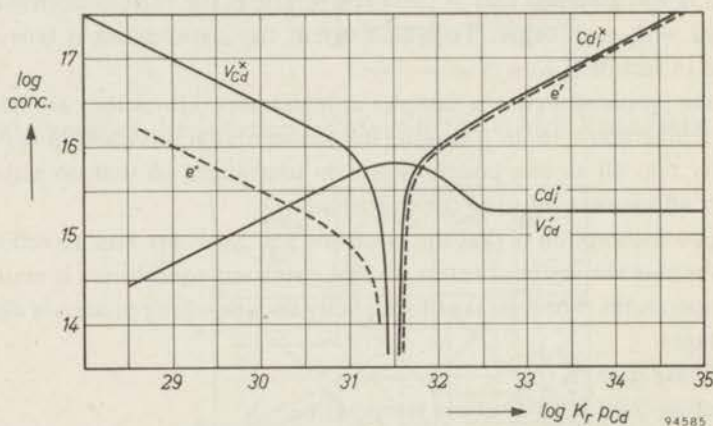
Fig. 54. Concentration of imperfections at 0 °K (fully drawn lines) and of electrons and holes at room temperature (dashed lines) of pure CdTe (omitting the Cd_i' level).

concentration of V_{Cd}'' centres. As the last concentration is rather small, $[Cd_i'] \approx [Au_{Cd}']$.

The total result thus is, that for $\log K_r p_{Cd} = 34$ at 0 °K we have a concentration of $Cd_i^\times$ almost equal to the concentration of electrons at 700 °C, a concentration of Cd_i' almost equal to $[Au_{Cd}']$ at 700 °C and a concentration of V_{Cd}'' almost equal to $[V_{Cd}'']$ at 700 °C (see fig. 58).

In doing the same at other $K_r p_{Cd}$ values a complete $\log K_r p_{Cd}$ vs log concentration graph for the situation at 0 °K can be constructed. The figures 53 to 58 present this situation for pure CdTe, CdTe–In and CdTe–Au, for both models assumed in 3.1.5. From the situation at 0 °K the number of free electrons and
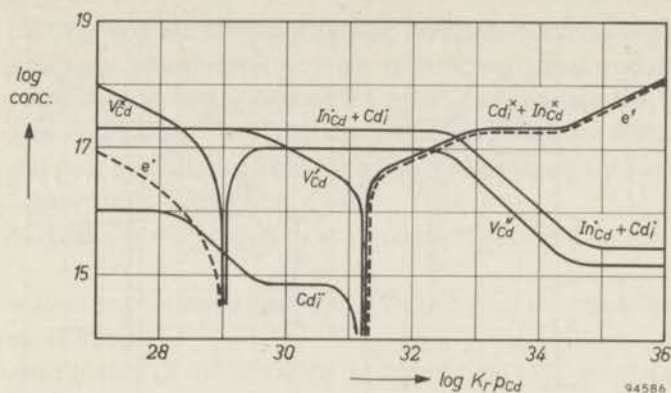
Fig. 55. Concentration of imperfections at 0 °K (fully drawn lines) and of electrons and holes at room temperature (dashed lines) of CdTe − 2.10^{17} In (including the V_{Cd}'' level).
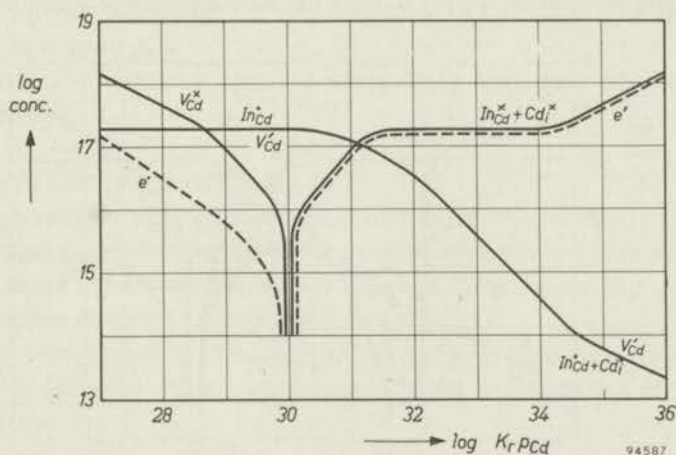
Fig. 56. Concentration of imperfections at 0 °K (fully drawn lines) and of electrons and holes at room temperature (dashed lines) of CdTe − 2.10^{17} In (omitting the V_{Cd}'' level).

holes at room temperature can be calculated. For centres having a small ionization energy, ionization will be almost complete at room temperature. This is the case for Cd_i and In_{Cd} centres, which have an ionization energy of 0·02 eV. For centres having a large ionization energy, only a fraction of the centres will be ionized at room temperature. This applies to V_{Cd} and Au_{Cd} centres, which in our model have an ionization energy of 0·15 eV and 0·33 eV, respectively. In the figures the number of free electrons and free holes at room temperature is indicated by dashed lines. In the section of fig. 55 and fig. 57, where the double charged Cd_i'' or V_{Cd}'' centres are present in appreciable concentrations, a number of electrons or holes can be released from these centres. As the levels correspond-

72
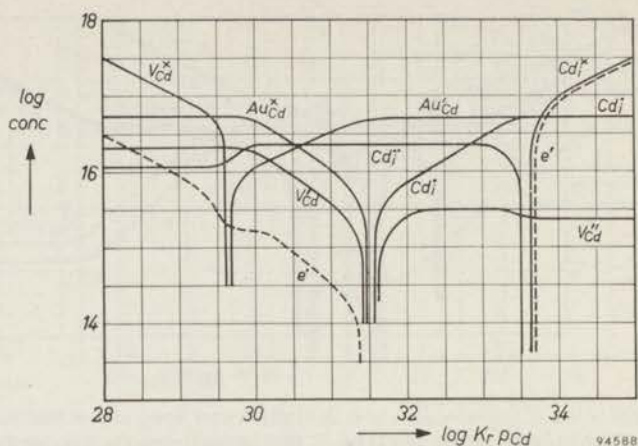
Fig. 57. Concentration of imperfections at 0 °K (fully drawn lines) and of electrons and holes at room temperature (dashed lines) of CdTe – 5.10¹⁶ Au (including the Cd_i level).
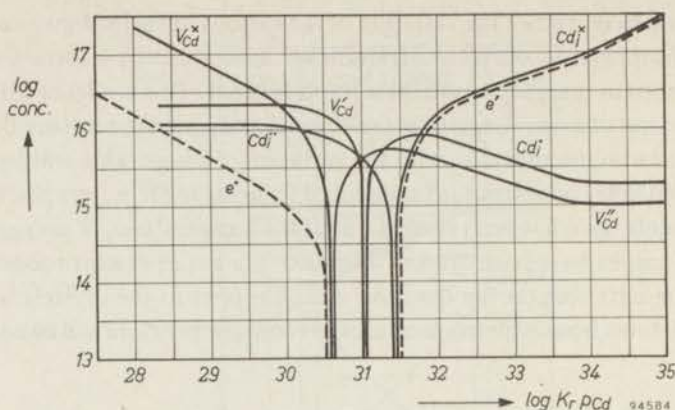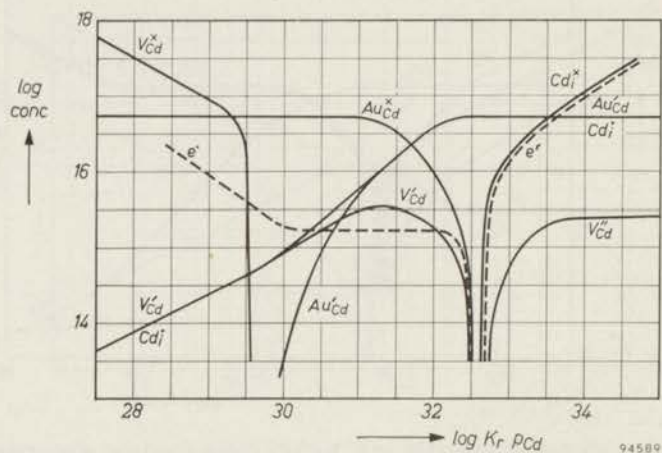

Fig. 58. Concentration of imperfections at 0 °K (fully drawn lines) and of electrons and holes at room temperature (dashed lines) of CdTe – 5.10¹⁶ Au (omitting the Cd_i level).

ing to these centres are situated at a rather large distance from the bands, this number will be small, leading to crystals with a high resistance (10^6–10^7 Ωcm).

3.3. Determination of the correct model

If we want to see whether the experimental data can be explained on the basis of the theory outlined above, this has to be done in two steps.

First we have to find out which model is best to describe the state of pure and doped CdTe, or in other words, what are the imperfections playing a part and

what are the approximate positions of their energy levels. This can be done by comparing the most saliant features of the experimental curves with those shown by the theoretical curves calculated on the basis of various models, using arbitrarily chosen values of the constants. Once this has been done the comparison has to be put on a quantitative basis. From this comparison the correct values of the constants can be determined.

The most characteristic properties of the experimental curves are:

(1) *CdTe without foreign atoms* (see figure 15 which gives the graph for the purest CdTe obtained by us).

(a) The concentration of free electrons is proportional to $p_{Cd}^{1/2}$ over a wide range of pressures.

(b) Similarly the concentration of free holes is going to be proportional to $p_{Cd}^{-1/2}$ in the small part of the p-type region which could be covered experimentally. In a narrow intermediate range the concentrations of holes and electrons depend more strongly upon p_{Cd}.

(c) There is no appreciable range in which CdTe has a very small number of charge carriers.

(2) *CdTe–In* (see figures 16, 17 and 18).

(a) At high values of p_{Cd} the concentration of free electrons is equal to the indium concentration and is independent of p_{Cd} (range of controlled conductivity).

(b) This range is followed by another range at lower values of p_{Cd} where the number of free electrons is proportional to $p_{Cd}^{1/2}$.

(c) At a certain value of p_{Cd} the concentration of free electrons decreases suddenly. This is followed by a range in which the concentration of carriers is extremely low.

(3) *CdTe–Au* (see fig. 19).

(a) At low values of p_{Cd} there is a range in which the concentration of holes is independent of p_{Cd}, but proportional to the gold concentration (range of controlled conductivity). Towards higher values of p_{Cd} the concentration of free holes drops to a very low value in a narrow range of cadmium pressures.

(b) The change in conductivity from p- to n-type happens without the occurrence of a range of appreciable width in which the concentration of charge carriers is very low.

(c) At high values of p_{Cd} the concentration of free electrons is proportional to $p_{Cd}^{1/2}$.

Comparing the curves for pure CdTe and CdTe–In it is seen that the cadmium pressure at which n-type conduction is suppressed is lower for CdTe–In than for pure CdTe (see figs 16, 17, 18 and 15). For CdTe–Au, on the contrary, this cad-

mium pressure is higher (fig. 19). Similarly the p_{Cd} at which p-type conduction is suppressed is highest for CdTe–Au and lowest for CdTe–In (with CdTe–In it is even so low that p-type conduction is not observed at all).

Comparing now the experimental curves with the calculated ones (figs 53 to 58), paying attention in particular to the characteristics mentioned above, it can be seen that:

(1) The experimental curve for pure CdTe (fig. 15) can only be explained by the model of 3.1.5.1 (figs 48 and 54). If Cd_i should give rise to a level near the middle of the gap (figs 47 and 53) in a observable range of cadmium pressures the crystals should show a large resistivity owing to the small number of charge carriers in this range. This is not the case as is shown in fig. 15.

(2) The occurrence with CdTe–In of a range of cadmium pressures in which the concentration of charge carriers is extremely low (figs 16, 17 and 18) can only be explained by a model in which V_{Cd} gives rise to two levels within the forbidden gap, one (viz. that of V''_{Cd}) lying near the middle of the gap. In the absence of such a doubly charged centre, this high resistivity range would not occur (fig. 56). Also the range of cadmium pressures in which the concentration of electrons is proportional to $p_{Cd}^{1/2}$ can only be explained by applying the model mentioned above.

(3) The absence with CdTe–Au of a range of pressures in which the concentration of carriers is extremely low (see fig. 19) indicates that Cd_i does not give rise to a level near the middle of the gap. As Cd_i gives a level close to the conduction band, this indicates that Cd_i gives rise to only one level within the forbidden gap.

On the basis of these facts we feel confident that the energy-level diagram as shown in fig. 44 applies to the situation existing in CdTe. This model therefore will be used in the following calculations. Now we can proceed to discuss the results more quantitatively. This can best be done by deriving expressions for characteristic points in the various graphs.

3.4. Characteristic points in the concentration-pressure graphs

3.4.1. *Pure CdTe*

The only sharp characteristic point which can be indicated for pure CdTe is the p_{Cd} value at which the samples change from n- to p-type. This transition will happen in range II of fig. 48 at the point where $[V'_{Cd}] = [Cd_i^{\cdot}]$. The value of $K_r p_{Cd}$ at this particular point can be evaluated from the expressions for $[V'_{Cd}]$ and for $[Cd_i^{\cdot}]$ which hold in this range (see table X). This leads to

$$K_F K_i^{1/2}/K_r p_{Cd} = K_r p_{Cd}/K_i^{1/2}$$

or

$$K_r p_{Cd} = (K_i K_F)^{1/2}. \qquad (3.38)$$

3.4.2. CdTe–In

In the CdTe–In graphs the following characteristic points occur (see figs 49 and 55).

(a) *The limit of the range of controlled conductivity at the high p_{Cd} side*. The position of this point is determined by the requirement that at this particular point the concentration of free electrons due to the incorporation of an excess of cadmium is equal to the concentration of electrons donated by In_{Cd}^{x}. Equalizing $n = [In_{Cd}^{\cdot}] = [In]_{total}$ or $[K_r p_{Cd}]^{1/2} = [In]_{total}$ (see table X) leads to

$$K_r p_{Cd} = [In]_{total}^2. \tag{3.39}$$

(b) *The limit of the range of controlled conductivity at the low p_{Cd} side*. The end of the range of controlled conductivity at the low p_{Cd} side is determined by the point at which the concentration of V_{Cd}'' centres becomes equal to the half of the concentration of $In_{Cd}^{\cdot}$ centres:

$$2[V_{Cd}''] = [In_{Cd}^{\cdot}] = [In]_{total}.$$

Combining this equality with the expression for $[V_{Cd}'']$ as holding in range II (fig. 49, table X) one gets $2K_r [In]_{total}^2 / K_4 K_r p_{Cd} = [In]_{total}$ or

$$K_r p_{Cd} = 2K_F [In]_{total} / K_4. \tag{3.40}$$

(c) *The end of the n-type region*. The *n*-type region will end at a value of p_{Cd} at which all free electrons present at high temperature either recombine with holes or are trapped at deep lying levels during the quenching process. The imperfections which trap electrons are the V_{Cd}' centres. This leads to the condition for this particular point:

$$n = p + [V_{Cd}'].$$

Using the expressions for these quantities in range III of fig. 49 (see table X) we obtain

$$\left(\frac{[In]K_4 K_r p_{Cd}}{2K_F} \right)^{1/2} = \left(\frac{2K_i^2 K_F}{[In]K_4 K_r p_{Cd}} \right)^{1/2} + \left(\frac{[In]K_4 K_F}{2K_r p_{Cd}} \right)^{1/2}$$

or after some rearrangement

$$K_r p_{Cd} = K_F (1 + 2K_i / [In]K_4). \tag{3.41}$$

If $2K_i \ll K_4 [In]$ this expression simplifies to

$$K_r p_{Cd} = K_F. \tag{3.42}$$

Under this condition a simple expression can be derived for the difference $\Delta \log K_r p_{Cd}$ between $\log K_r p_{Cd}$ at the end of the controlled conductivity range at the low p_{Cd} side and $\log K_r p_{Cd}$ at the end of the n-type region. From (3.40) and (3.42) one obtains

$$\Delta \log K_r p_{Cd} = \log ([\text{In}]/K_4). \qquad (3.43)$$

(d) *The beginning of the range in which the samples show p-type conductivity*. The n-type region is followed by a range in which the samples show very high resistances (10^6–10^7 Ωcm). This is caused by the fact that in this range the V''_{Cd} centres play a dominant role in the high-temperature diagram (fig. 49), functioning as traps for the holes during the quenching process. The ionization energy of these V''_{Cd} levels is too large to lead to an appreciable n-type conductivity at room temperature.

Hole conductivity begins to show when the number of holes which is increasing in going to lower $K_r p_{Cd}$ values has become larger than the number of V''_{Cd} centres. Thus the point at which appreciable p-type conductivity sets in (by ionization of $V^{\times}_{Cd}$ centres) is the point where

$$p = [V''_{Cd}].$$

Inserting the expressions for these quantities holding in range IV of fig. 49 (see table X) it can be seen that

$$K_i K_F / K_r p_{Cd} [\text{In}] = K_r p_{Cd} [\text{In}]^2 / K_F K_4$$

or

$$K_r p_{Cd} = (K_i K_F^2 K_4 / [\text{In}]^3)^{1/2}. \qquad (3.44)$$

3.4.3. *CdTe–Au*

In the concentration-pressure graph for CdTe–Au (figs 52 and 58) the following characteristic points can be observed:

(a) *The p_{Cd} at which the samples change from n- to p-type conductivity*. This change in conductivity type will happen in range II of fig. 52 as soon as the number of electrons is equal to the number of holes. Inserting the expressions for these quantities holding in this range (table X) leads to

$$K_r p_{Cd} / [\text{Au}'_{Cd}] = K_i [\text{Au}'_{Cd}] / K_r p_{Cd}$$

or

$$K_r p_{Cd} = K_i^{1/2} [\text{Au}'_{Cd}]. \qquad (3.45)$$

The Au'_{Cd} concentration can be put equal to the total gold concentration as can

be shown by the following argument. The concentration of Au'_{Cd} centres can be evaluated from the equilibrium constant of $Au'_{Cd} \rightleftarrows Au^{\times}_{Cd} + e'$, viz.

$$K_6 = [Au^{\times}_{Cd}]n/[Au'_{Cd}].$$

At 700 °C, $K_6 \approx 4.10^{13}$. As at this characteristic point $n = p = K_i^{1/2} = 7 \cdot 1.10^{15}$, $[Au'_{Cd}] = 1 \cdot 8.10^2 [Au^{\times}_{Cd}]$. Thus at 700 °C, $[Au'_{Cd}]$ can be put equal to the total gold concentration. At 900 °C, $[Au'_{Cd}] = 20 [Au_{Cd}]$. Even at this temperature the approximation $[Au'_{Cd}] = [Au]_{total}$ is fairly good.

(b) *The limit of the controlled conductivity range at the high p_{Cd} side (figs 52 and 58).* From fig. 52 it can be seen that the controlled conductivity range begins as soon as the concentration of holes becomes equal to the concentration of Au'_{Cd} centres. Inserting the expressions of table X for these concentrations leads to

$$K_i [Au'_{Cd}]/K_r p_{Cd} = [Au'_{Cd}]$$

or

$$K_r p_{Cd} = K_i. \tag{3.46}$$

(c) *The limit of the controlled conductivity range at the low p_{Cd} side (figs 52 and 58).* The controlled conductivity range will end as soon as, in going to lower p_{Cd} values, the number of vacancies becomes equal to the number of foreign atoms:

$$[V'_{Cd}] = [Au'_{Cd}].$$

Inserting the expressions for these quantities holding in range III of fig. 52 (see table X) we get

$$(K_F K_i/K_r p_{Cd})^{1/2} = [Au'_{Cd}]$$

or

$$K_r p_{Cd} = K_F K_i/[Au'_{Cd}]^2. \tag{3.47}$$

Just as shown sub (a), the Au'_{Cd} concentration can be put almost equal to the total gold concentration.

3.5. Determination of the equilibrium constants

The equilibrium constants used in the foregoing chapters can be determined in various ways.

(a) From optical data (see sections 1.7 and 2.4);

(b) from the position of the energy levels as determined from the temperature dependence of the Hall effect (see section 2.2);

(c) by a detailed comparison between theoretical and experimental concentration-pressure diagrams, i.e. from the positions of the characteristic points calculated in section 3.4.

3.5.1. *The intrinsic constant K_i*

The constant K_i which is equal to the product of hole and electron concentration is very important in semiconductor physics. The evaluation of this constant can be achieved in various ways.

(a) By determination of the concentration of intrinsic charge carriers. The concentration of intrinsic charge carriers is determined by the electrons and holes generated in equal numbers by transition of electrons from the valence band to the conduction band. Their concentration can only be determined exactly when this concentration is so high that it is outnumbering the concentration of charge carriers produced by transitions from levels between the bands to one of the bands. So it has to be measured in very pure and nearly stoichiometric samples or at higher temperatures, because the number of intrinsic carriers increases exponentially with the temperature while the number of extrinsic charge carriers is limited by the concentration of foreign atoms or vacancies. As to CdTe; the temperature, to which we have to heat the sample to satisfy the mentioned condition, is so high that CdTe already decomposes. At 600 °K, at which decomposition starts to occur, the number of intrinsic carriers is only of the order of 10^{12} cm^{-3}, which is very low compared with the number of foreign atoms present even in the purest samples (10^{15}–10^{16} foreign atoms per cm^3).

(b) From the experimental value of the band gap. The intrinsic constant K_i is related to the thermal band gap ΔE by

$$K_i = n_i p_i = n_o p_o T^3 \exp\left[-\Delta E/kT\right] \tag{3.48}$$

in which n_i and p_i are the numbers of intrinsic electrons and holes and

$$n_o = 2(2\pi m_n^* k/h^2)^{3/2}, \quad p_o = 2(2\pi m_p^* k/h^2)^{3/2}. \tag{3.49}$$

As to the value of ΔE, the band gap, we only have at our disposal the value of the optical band gap as a function of the temperature (see section 2.4.1). The value of thermal band gap may differ from the value of the optical band gap, if indirect transistions between the bands are involved. The difference between the two is of the order of $\hbar\omega_t$ (ω_t = frequency of the transversal lattice vibrations) [31]). As $\omega_t = 2\cdot8.10^{13}$ rad sec^{-1} ($\lambda' = 67$ μ; see appendix) this difference, viz. $1\cdot85.10^{-2}$ eV, can be neglected.

If in the expression for K_i the values of the optical band gap (section 2.4.1) and the values of m_n^* and m_p^* determined in section 2.1 are inserted, the values of log K_i shown in table XI are obtained.

(c) The value of K_i can also be calculated from a characteristic point in the log n (or p) versus log p_{Cd} graph for CdTe–Au. As was shown in section 3.4.3, the p_{Cd} at which the range of controlled conductivity begins in CdTe–Au samples is given by the relation

$$p_{Cd} = K_i/K_r. \tag{3.46}$$

TABLE XI

Values of K_i as a function of the temperature

T (°C)	$\log K_i$ (cm^{-6})
700	31·7
800	32·5
900	33.2
1000	33·8

Inserting the value of K_r, which is determined in an independent way (3.5.4), the value of K_i at the temperature at which the samples are prepared can be calculated from the experimental value of this characteristic p_{Cd} at the given temperature.

Though the beginning of the region of controlled valency is not a very sharp limit, this method gives a good check on the optical values for K_i calculated in (b). The results are shown in table XII; for comparison the values of table XI are also given.

TABLE XII

Calculation of the value of K_i by means of expression (3.46)

T (°C)	$\log p_{Cd}$	$\log K_r$	$\log K_i$	$\log K_i$ (table XI)
700	—2·3	34·1	31·8	31·7
900	—0·4	33·4	33·0	33·2

It is seen that the $\log K_i$ values obtained are in close agreement with the values obtained from the optical band gap.

3.5.2. *Determination of the equilibrium constants for the various ionization processes*

The equilibrium constant of the reaction describing the ionization of a certain centre, e.g.

$$Cd_i^x \rightleftarrows Cd_i^{\cdot} + e',$$

can be expressed in the form of partition functions

$$K = \frac{Z(Cd^{\cdot})\, Z(e')}{Z(Cd_i^x)}\ \exp\left[-\varepsilon/kT\right]$$

in which Z expresses the partition function of the electron in the centres or in the conduction band. In the mentioned example, $Z(e')$ can be expressed by

$$Z(e') = 2(2\pi m_n^* kT/h^2)^{3/2} = n_o.$$

$Z(Cd_i^\cdot)$ will be equal to 2, as two orientations for the spin of the electron are available for the remaining electron. $Z(Cd_i^\times)$ is equal to 1, as only one configuration is possible for the two electrons present in the centre.

In the same way, $Z(e^\cdot) = 2(2\pi m_p^* kT/h^2)^{3/2} = p_o$, $Z(V_{Cd}^\times) = 1$, $Z(V_{Cd}') = 2$ and $Z(V_{Cd}'') = 1$.

Applying these values, the equilibrium constants mentioned in section 3.1 can be written as

$$K_1 = 2n_o \exp(-\varepsilon_1/kT), \tag{3.50}$$
$$K_2 = \tfrac{1}{2}n_o \exp(-\varepsilon_2/kT), \tag{3.51}$$
$$K_3 = \tfrac{1}{2}n_o \exp(-\varepsilon_3/kT), \tag{3.52}$$
$$K_4 = 2n_o \exp(-\varepsilon_4/kT), \tag{3.53}$$
$$K_5 = \tfrac{1}{2}n_o \exp(-\varepsilon_5/kT), \tag{3.54}$$
$$K_6 = \tfrac{1}{2}n_o \exp(-\varepsilon_6/kT). \tag{3.55}$$

So far, only the spin contribution to the statistical factor was considered. There may be however other factors influencing this factor. One of these is illustrated by fig. 59, which shows the ionic presentation of a V_{Cd}' centre. If the remaining electron of the V_{Cd}' centre is assumed to describe a hydrogen-like orbit, it can have some preferential position, e.g. at one of the Te^{2-} ions, each possibility giving rise to a contribution in the statistical factor. Such a preferred position of the electron should lead at low temperatures to relaxation effects, as studied by Volger in Fe_2O_3 [32]). With CdTe no indications of such effects could be found experimentally. In our calculations the expressions (3.50) to (3.55) were used.
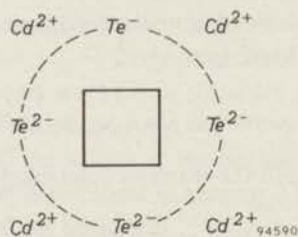

Fig. 59. Ionic representation of a V_{Cd}' centre.

The ionization energies of the various centres which were determined from the temperature dependence of the Hall effect (section 2.2) are almost equal to the ionization energies at $0\ °K$, as the $\log n$ (or p) vs $1/T$ graphs show a nearly

straight line in the temperature range from 77 °K to 300 °K. This indicates that there exists only a small variation in the ε-values, or that this variation is smaller than the experimental accuracy. At higher temperatures the ionization energy may be assumed to depend on temperature according to

$$\varepsilon_T = \varepsilon_o - aT, \tag{3.56}$$

in which a is a constant, the value of which is unknown. As an approximation we have assumed that a is proportional to the variation of the band gap with the temperature (a_{gap}) in such a way that

$$a_{level} = \frac{\varepsilon_o \text{ of the level}}{(\Delta E)_o \text{ of the energy gap}} \, a_{gap}. \tag{3.57}$$

It should be noted that this assumption is rather arbitrary, as nothing is known about the real variation of the ionization energy with the temperature. As a value of a_{gap} we have taken $a_{gap} = 5 \cdot 4.10^{-4}$ eV/°K, a value which holds in the high temperature region. Extrapolation of ΔE from high temperatures to 0 °K gave $1 \cdot 7$ eV (fig. 32) as a value for $(\Delta E)_o$. With these assumptions the value of ε_T was calculated at various temperatures.

Inserting the value of ε_T, obtained in this way, in the expressions for the various equilibrium constants leads to the values which are given in table XIII.

TABLE XIII

Values of ε and log K for various centres as a function of temperature

Centre	ε	K	ε_0(eV)	700 °C ε(eV)	700 °C log K	800 °C ε(eV)	800 °C log K	900 °C ε(eV)	900 °C log K	1000 °C ε(eV)	1000 °C log K
$Cd_i^{\times}$	ε_1	K_1	0·02	0·02	18·8	0·02	18·8	0·02	18·8	0·02	18·8
$In_{Cd}^{\times}$	ε_5	K_5	0·02	0·02	18·2	0·02	18·2	0·02	18·2	0·02	18·2
V_{Cd}'	ε_3	K_3	1·43	1·08	13·3	1·03	14·0	0·98	14·6	0·94	15·2
V_{Cd}''	ε_4	K_4	0·60	0·51	16·2	0·50	16·5	0·49	16·7	0·48	16·9
Au_{Cd}'	ε_6	K_6	1·25	0·96	13·9	0·90	14·6	0·87	15·0	0·84	15·6

3.5.3. *The Frenkel-equilibrium constant K_F*

The constant which determines the Frenkel-equilibrium

$$CdTe \rightleftarrows Cd_{(1-\delta)}Te(Cd_i^{\cdot})_{\delta}(V_{Cd}')_{\delta} \tag{3.58}$$
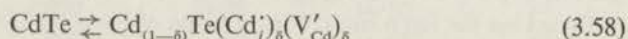
can be expressed by

$$K_F = [Cd^{\cdot}] \, [V_{Cd}']. \tag{3.59}$$

No direct method for the determination of this constant is known at present. The calculation of this value by estimating the number of vacancies at the melting point, worked out by Mott [33]), is only a very rough approximation. The high-temperature values of K_F can, however, be evaluated from the position of a characteristic p_{Cd} in the $\log n$ (or p) versus $\log p_{Cd}$ graph for CdTe–In samples. In section 3.4.2 it is seen that the p_{Cd} at which the range of controlled conductivity ends in these samples is given by

$$p_{Cd} = 2K_F \, [\text{In}]/K_4 K_r. \tag{3.40}$$

As K_r and K_4 can be determined in an independent way (sections 3.5.4 and 3.5.5) the value of K_F can be calculated for the temperature at which the samples are prepared. The results of such a calculation are given in table XIV.

TABLE XIV

Calculation of the values of K_F at various temperatures with the aid of expression (3.40)

T (°C)	$\log$ [In]	$\log K_r$	$\log K_4$	$\log p_{Cd}$	$\log K_F$
700	17·3	34·1	15·9	−1·1	31·3
800	17·3	33·7	16·1	−0·4	31·8
900	17·3	33·4	16·3	0·1	32·2
1000	17·3	33·3	16·4	0·5	32·6

3.5.4. *The equilibrium constant* K_r

The constant K_r which determines the equilibrium between a crystal and the atmosphere via the reaction

$$\text{CdTe} + \delta \, \text{Cd} \rightleftarrows \text{CdTe}(\text{Cd}_i^{\cdot})_\delta + \delta \, e' \tag{3.60}$$
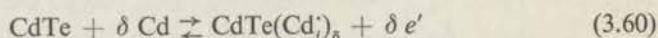
can be expressed as

$$K_r = [\text{Cd}_i^{\cdot}]n/p_{Cd}. \tag{3.61}$$

A direct method to determine this constant is not known. However, K_r can be determined indirectly for various temperatures from the $\log n$ (or p) versus $\log p_{Cd}$ diagram for pure CdTe (see fig. 15). It has been shown that for high cadmium pressures $\log K_r p_{Cd} = 2 \log n$ (3.26a).

By taking for $\log n$ the arbitrary value of $\log n = 17·0$ and taking the corresponding value of $\log p_{Cd}$ from fig. 15, $\log K_r$ can be evaluated from (3.26a). This leads to table XV.

TABLE XV

Calculation of K_r at various temperatures from expression (3.26a)

T (°C)	$\log n$ (cm^{-3})	$\log p_{Cd}$ (atm)	$\log K_r$
700	17·0	—0·1	34·1
800	17·0	+0·3	33·7
900	17·0	+0·6	33·4
1000	17·0	+0·7	33·3

3.5.5. Determination of K_4 from the log n (or p) versus log p_{Cd} graphs

The value of the equilibrium constant K_4 of the reaction

$$V''_{Cd} \underset{\leftarrow}{\rightarrow} V'_{Cd} + e'$$
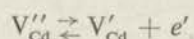
plays an important role in the CdTe–In diagrams. As has been shown in section 3.4.2, the constant K_4 forms an integral part of the expression for the end of the controlled conductivity region at the low cadmium-pressure side and of the expression for the end of the n-type range in indium doped crystals. It was indicated that when $2K_i/[\text{In}]K_4 \ll 1$ (section 3.4.2) a simple expression was found for the difference $\Delta \log K_r p_{Cd}$ between the two characteristic points mentioned above, viz.

$$\Delta \log K_r p_{Cd} = \log ([\text{In}]/K_4), \tag{3.43}$$

which relation enables us to calculate K_4. However, for the indium concentrations which were applied and inserting the values of K_i for various temperatures, it can be shown that the condition $2K_i/[\text{In}]K_4 \ll 1$ only holds at temperatures $\leqslant 800$ °C. For various indium concentrations this calculation leads to the values of table XVI.

TABLE XVI

Calculation of K_4 at various temperatures with the aid of expression (3.43)

	T (°C)	$\Delta \log p_{Cd}$	$\log K_4$	fig.
CdTe–1·3.10^{17} In	700	1·25	15·85	16
	800	0·95	16·15	16
CdTe–2.10^{17} In	700	1·40	15·90	17
	800	0·20	16·10	17
CdTe–5.10^{17} In	700	1·90	15·85	18
	800	1·60	16·10	18
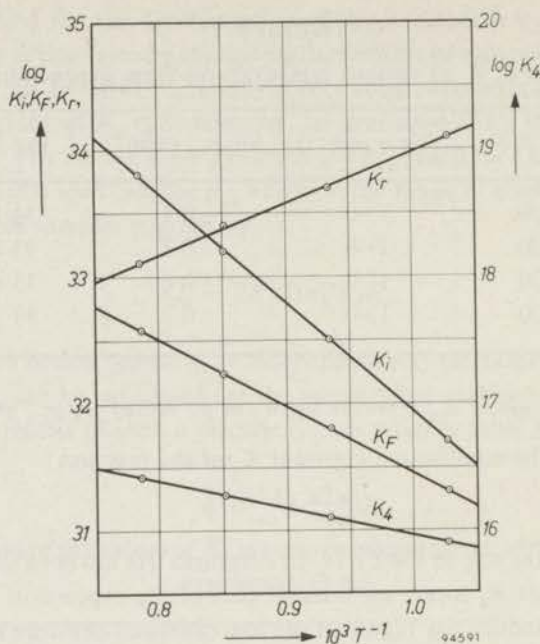
Fig. 60. The values of the constants K_i, K_F, K_r and K_4 as a function of the temperature.

The values of log K_4 for temperatures > 800 °C were determined by extrapolation of the low-temperature values in a log K_4 versus $1/T$ plot (fig. 60). In table XVII these values are collected and for comparison the values of log K_4 as calculated from the experimental values of the ionization energy of the V''_{Cd} centre (see section 3.5.2) are also given.

TABLE XVII

Comparison of the values of K_4 at various temperatures as calculated by eqs (3.43) and (3.53)

T (°C)	log K_4 (this section)	log K_4 (section 3.5.2)	log K_4 ($a = 6 \cdot 5.10^{-4}$eV/°K)
700	15·9	16·2	15·9
800	16·1	16·5	16·2
900	16·3	16·7	16·4
1000	16·4	16·9	16·6

It can be seen that, though the absolute values of log K_4 determined by the mentioned methods are in good agreement, the variation with the temperature is not the same. The values in the second column of table XVII were calculated

with an ionization energy ε_o of the V_{Cd}'' centre of 0·60 eV. Calculation of an ionization energy from the values given in the first column leads to a value of 0·5 eV in this temperature region.

In the third column of table XVII the values of log K_4 calculated with $a = 6·5.10^{-4}$ eV/°K (see section 3.5.2, in which $a = 5·4.10^{-4}$ eV/°K is used) are given. A good agreement between the semi-experimental values of the first column and the calculated values in the last column can be observed.

3.6. Comparison between theory and experiment

The results obtained from the preceding theoretical considerations and the experimentally determined values can be compared in two ways.

(a) By a graphical method, viz. by constructing the log n (or p) versus log $K_r p_{Cd}$ diagram at room temperature and comparing the obtained diagram with the experimental log n (or p) versus log p_{Cd} diagram (compare e.g. figs 17 and 55).

(b) From the way in which the high-temperature graphs are used to construct the graphs applying to low temperature it is clear that several characteristic points of the high-temperature graph occur also in the low-temperature graph and vice versa. Examples of such characteristic points are the point at which a sample will change from n- to p-type at room temperature, the point at which a controlled conductivity region ends, etc. The comparison between theoretical and experimental values of p_{Cd} at these characteristic points can serve as a test for the agreement between theory and experiment.

The former more or less qualitative method is the best if one wants to determine which model has to be chosen to describe the properties of CdTe. In fact this method has already been used in section 3.3.

The latter method is the best if one wants to put the theory on a quantitative basis. This method is used both to evaluate equilibrium constants not known from other experiments (e.g. K_F and K_r) and to check the correctness of other constants determined by experimental methods (e.g. K_i).

In the following sections the characteristic points obtained in the experimental log n (or p) versus log p_{Cd} graphs will be compared with the values calculated from the expressions for these points, using the values of the various equilibrium constants derived in the preceding section 3.5. Of course such a comparison only makes sense in so far as these points have not been used in determining the constants.

3.6.1. *Pure CdTe*

The values of p_{Cd} at which the purest CdTe (which was obtained after segregating CdTe 40 times) changes from p- to n-type at various temperatures of preparation can be seen in fig. 15. In table XVIII the experimental values of p_{Cd} are compared with the p_{Cd} values calculated with eq. (3.38).

TABLE XVIII

Comparison between experimental values (fig. 15) and calculated values (3.38)
of the p_{Cd} at which CdTe changes from n-type to p-type

T (°C)	$\log K_i$	$\log K_F$	$\log K_r$	calc. $\log p_{Cd}$	exp. $\log p_{Cd}$
700	31·7	31·3	34·1	−2·6	−1·9
800	32·5	31·8	33·7	−1·5	−1·1
900	33·2	32·2	33·4	−0·6	−0·4
1000	33·8	32·6	33·3	0·0	0·0

It is seen that there is good agreement between theory and experiment at
900 °C and at 1000 °C. The discrepancy at lower temperatures can be explained
by the presence of impurities. At higher temperatures (1000 °C) these impurities
loose their influence on the position of the transition value of p_{Cd}, as at this
temperature the intrinsic electrons and holes outnumber the concentration of
impurity atoms and the sample behaves as pure CdTe. The impurities start to
influence the electrical properties when their concentration is higher than $K_i^{1/2}$.
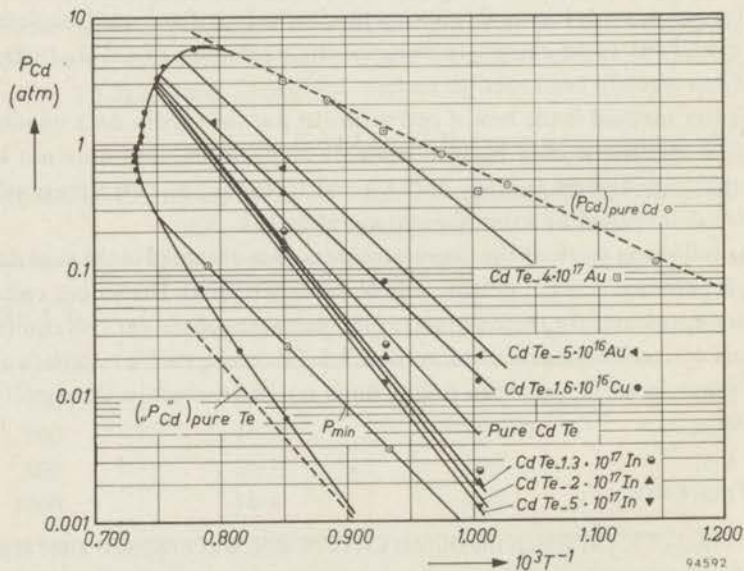

Fig. 61. The $\log p_{Cd}$ vs $10^3 T^{-1}$ diagram of CdTe. The drawn lines in the solid-state region give
the theoretical values at which CdTe of various compositions ceases to be n-type. The experi-
mental values of this characteristic p_{Cd} are denoted by symbols given in the text of the figure.

Hence it may be concluded that the impurity concentration is of the order of $K_i^{1/2}$ at 900 °C, i.e. 4.10^{16} cm^{-3}. It will be seen in section 3.6.3 that the impurity responsible for the discrepancy is probably copper, present in a concentration of about 2.10^{16} cm^{-3}.

3.6.2. *CdTe–In*

As to the agreement between experimental and theoretical values of the characteristic points in the log n (or p) versus log p_{Cd} graphs, it has to be noted that the values of K_F and K_4, which play a dominant role in the theoretical value

TABLE XIX

Comparison of experimental and calculated values of p_{Cd} for characteristic points in the CdTe–In graphs

T (°C)	log K_r	log K_F	log K_4	log [In]	log K_i	end of controlled conduct. range (log p_{Cd})		end of n-type range (log p_{Cd})		beginning of p-type range (log p_{Cd})	
						theor.	exp.	theor.	exp.	theor.	exp.
700	34·1	31·3	15·9	17·1	31·7	−1·3	−1·3	−2·7	−2·6	−4·8	—
800	33·7	31·8	16·1	17·1	32·5	−0·7	−0·6	−1·7	−1·6	−3·4	—
900	33·4	32·2	16·3	17·1	33·2	−0·2	−0·1	−0·8	−0·7	−2·3	—
700	34·1	31·3	15·9	17·3	31·7	−1·1	−1·1	−2·8	−2·8	−5·1	—
800	33·7	31·8	16·1	17·3	32·5	−0·4	−0·4	−1·8	−1·7	−3·7	—
900	33·4	32·2	16·3	17·3	33·2	+0·1	+0·1	−0·9	−0·8	−2·6	—
700	34·1	31·3	15·9	17·7	31·7	−0·8	−0·9	−2·9	−2·9	−5·7	—
800	33·7	31·8	16·1	17·7	32·5	0·0	−0·2	−1·9	−1·9	−4·3	—
900	33·4	32·2	16·3	17·7	33·2	0·5	0·3	−0·9	−0·8	−3·2	—

of the cadmium pressure at which the controlled conductivity ends and at which the n-type region ends, were derived from the experimental values of these characteristic points. Hence, agreement between theoretical and experimental values for these two characteristic points has to be expected. The fact that this agreement is maintained for various indium concentrations inspires confidence in the method used. The various values are collected in table XIX. In fig. 61 the theoretical values of the end of the n-type range are given by drawn lines; the experimental values are also inserted in this diagram.

The theoretical value of p_{Cd} at which the p-type range begins is also given in table XIX. Experimentally, this point could not be reached, however, as the calculated values of p_{Cd} lie outside the solid-state region of the phase diagram (see fig. 61).

3.6.3. CdTe–Au and CdTe–Cu

The results obtained with CdTe samples doped with a small amount of Au $(5.10^{16}$ Au cm$^{-3})$ (fig. 19) are in fair agreement with the theory. A comparison between theory and experiment is given in table XX.

TABLE XX

Comparison of the experimental and the calculated values of p_{Cd}
for the characteristic points in the CdTe – Au graphs

T (°C)	log K_r	log K_i	log K_F	log [Au]	change of sign ($\log p_{Cd}$)		begin controlled cond. range ($\log p_{Cd}$)		end controlled conduct. range ($\log p_{Cd}$)	
					calc.	exp.	calc.	exp.	calc.	exp.
700	34·1	31·7	31·3	16·7	—1·6	—1·7	—2·4	—2·3	—3·5	—
900	33·4	33·2	32·2	16·7	—0·1	—0·2	—0·2	—0·4	—1·4	—
1000	33·1	33·8	32·6	16·7	+0·5	+0·1	+0·7	—	—0·1	—

The agreement between theory and experiment at 700 °C and 900 °C is fairly good. The end of the controlled conductivity range could not be reached experimentally as the p_{Cd} at which this transition takes place is situated near to the P_{min} line (fig. 61), which fact causes sublimation of the samples. The discrepancy at 1000 °C is caused by the fact that at this temperature CdTe–5.10^{16} Au behaves as pure CdTe ($K_i^{1/2} >$[Au]), so that the special expressions derived for CdTe–Au do not hold any longer.

For CdTe with higher gold content ([Au] $= 4.10^{17}$ cm^{-3}) only the p_{Cd} at which

the samples change from n- to p-type was determined. The results are compared in table XXI with the p_{Cd} values calculated with (3.45).

TABLE XXI

Experimental and calculated values of p_{Cd}
at which $CdTe - 4.10^{17}$ Au changes from n- to p-type

T (°C)	$\log K_r$	$\log K_i$	$\log$ [Au]	change of type ($\log p_{Cd}$)	
				calc.	exp.
700	34·1	31·7	17·6	− 0·6	−0·4
800	33·7	32·5	17·6	0·1	0·1
900	33·4	33·2	17·6	0·8	0·5

The theoretical values of p_{Cd} at which the samples change sign are given as drawn lines in fig. 61, in which the experimental values are also given.

As was indicated in section 3.6.1, the purest CdTe which was obtained still appeared to have an impurity concentration of the order of 4.10^{16} cm^{-3}. Spectrochemical analysis showed an amount of copper of this order. This impurity concentration presents itself by a shift of the transition cadmium-pressure at 700 °C and 800 °C (see table XVIII). The copper concentration can be evaluated from (3.45); the result of this calculation is given in table XXII.

TABLE XXII

Calculation of the copper concentration
in very pure CdTe with the aid of expression (3.45)

T (°C)	$\log K_r$	$\log K_i$	$\log p_{Cd}$	$\log$ [Cu]
700	34·1	31·7	−1·9	16·3
800	33·7	32·5	−1·1	16·3

The purest CdTe obtained by us thus contained still 2.10^{16} Cu cm^{-3}.

3.7. Association and clustering effects

In the preceding chapters it was assumed that, when CdTe crystals are reheated at higher temperatures (700 °C–1000 °C) under various cadmium pressures followed by quenching to room temperature, all atomic positions of vacancies

and foreign atoms remain unchanged while only the electrons and the holes are supposed to redistribute themselves over the various centres. This can only be realized by infinitely rapid quenching. We have tried to approximate this in our experimental set up.

If the cooling takes place more slowly vacancies and foreign atoms are able to move to energetically more favourable positions. This may lead to the formation of centres consisting of a few imperfections (associates) or of many imperfections (clusters). When a cluster becomes so large that it adopts its own characteristic structure and properties, we are dealing with the formation of a separate phase.

The most probable associates are those between oppositely charged centres. An associate between neutral centres will have a small dissociation energy, associates between centres having a charge of the same sign being rather improbable.

3.7.1. Calculation of the association equilibrium

Several attempts have been made to calculate the amount of associates at a given temperature. These calculations are restricted to associates of two oppositely charged centres. When two centres with opposite effective charge associate according to the reaction

$$A^+ + B^- \rightleftarrows (A^+ \, B^-), \tag{3.62}$$

the equilibrium constant of this reaction can be written as

$$K_a = [(A^+B^-)]/[A^+][B^-] = C \exp(-E_{AB}/kT). \tag{3.63}$$

The constant C contains a weight factor of the associate, viz. the number of positions A^+ can have relative to B^- (in the ZnS structure this will be four), and a factor to convert mole fractions into molecules per cm^3, viz. $6 \cdot 45.10^{-23}$ for CdTe.

The energy E_{AB} is the association energy. If it is assumed to be mainly due to electrostatic attraction,

$$E_{AB} = -z_A z_B e^2/\varepsilon \, r_{AB}. \tag{3.64}$$

The cell-constant a of CdTe is $6 \cdot 41$ Å; the distance between two nearest neighbours can be calculated to be $\frac{1}{4}a\sqrt{3} = 2 \cdot 77$ Å and the dielectric constant ε is equal to 11. Thus the energy $E_{AB} = 0 \cdot 61$ eV. However the actual association energy is often smaller. Teltow [34]) showed that for the alkali halides the association energy is 10–40% smaller than the Coulomb value. There may be several reasons for this difference. In calculating the Coulomb term the charged centres are thought as point charges and the polarisation of the medium, which is thought

as a continuum, is introduced by the macroscopic value of the dielectric constant, which assumptions can lead to a too large value of the energy. So E_{AB} has to be replaced by $E'_{AB} = E_{AB} - \alpha$, in which α is a still unknown correction term.

Another factor which may influence the association energy will be demonstrated for a particular example, viz. the $(In_{Cd}^{\cdot} V'_{Cd})$ associate which may occur in indium doped samples. The V'_{Cd} centre is a V''_{Cd} centre which has trapped one hole. This hole will have some position outside the vacancy. If it is situated at one of the tellurium atoms surrounding the vacancy, its distance from the vacancy is small enough to have a polarizing effect on the cadmium vacancy, which effect will give a contribution in the total association energy.

This polarization effect tends to increase the energy E'_{AB} by a term β. The total expression now becomes

$$E''_{AB} = E_{AB} - \alpha + \beta. \tag{3.65}$$

Another associate that may occur in CdTe–In is $(V_{Cd} In_{Cd})'$. The last term of (3.65), however, is not present in the energy of this associate in which no hole is caught by the V''_{Cd} centre. So the energy of this associate will be

$$E'''_{AB} = 2E_{AB} - \alpha', \tag{3.66}$$

in which α' will not be the same as α in (3.65). The absolute values of α and β are unknown. However, we can approximate these values by giving α and β a value which can explain some experimental facts which are found in indium doped samples.

3.7.2. *Clustering effects in CdTe–In*

CdTe crystals doped with a large amount of indium (5.10^{17} In cm^{-3}), and prepared at high temperatures (700 °C–1000 °C) showed in a small p_{Cd} region a remarkable influence of the velocity of quenching to room temperature. This is illustrated by fig. 18. It can be seen from this figure that slow quenching extends the p_{Cd} range in which the samples are *n*-type to lower values of p_{Cd}. In the same way slow cooling may extend the *p*-type region to higher p_{Cd} values so that now *p*-type conductivity is observed, which was not the case for rapidly quenched samples. Thus by slow quenching the range in which the samples have a very high resistance will be narrowed from both sides.

(a) *The n-type range.* From a comparison between the experimental $\log p_{Cd}$ vs $\log n$ graph (fig. 18) and the $\log K_r p_{Cd}$ graph (fig. 62) showing the concentration of the various centres at high temperature (e.g. at 700 °C) we have already seen before that the *n*-type range ends when the number of electrons present at high
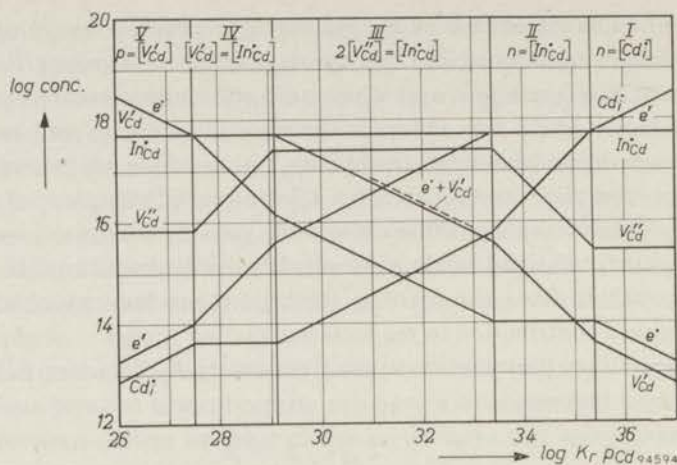
Fig. 62. Concentration of the various imperfections in CdTe–5.10^{17} In at 700 °C. The dashed line gives the sum of hole and V$'_{Cd}$-centre concentrations.

temperature is equal to the number of holes and electron traps (viz. V$'_{Cd}$ centres).

For rapidly quenched samples, where all centres may be assumed to remain unchanged, this was found to happen when

$$n = [\mathrm{V}'_{Cd}] + p.$$

This condition is fulfilled at log $K_r p_{Cd} = 31 \cdot 3$ (log $p_{Cd} = -2 \cdot 8$; fig. 62). The fact that slow cooling extends the n-type region to much lower Cd pressures indicates that the trapping V$'_{Cd}$ centres disappear for the greater part.

In order to diminish the V$'_{Cd}$ concentration in this range, to such an extent that electrons are no longer trapped, the V$'_{Cd}$ concentration must have become smaller than the electron concentration. From fig. 62 it is seen that the V$'_{Cd}$ concentration has to decrease to about 5% of its original value to explain the prolongation of the n-type range. A simple association of V$'_{Cd}$ and In$^{.}_{Cd}$ centres cannot solve this problem as this associate will also act as a trapping centre, its level lying probably even lower than that of the V$'_{Cd}$ centre due to the presence of the neighbouring In$^{.}_{Cd}$ centre.

Only large clusters or segregation as a separate phase can remove the V$'_{Cd}$ centres without forming new traps. The segregation will give rise here to an InTe$_2$ cluster or separate phase.

(b) *The p-type range.* The crystals will show p-type conductivity when the number of holes at high temperature is larger than the number of hole traps, viz. V$''_{Cd}$

centres. According to fig. 62, for rapidly quenched samples this condition is fulfilled at $\log K_r p_{Cd} = 28.5$ ($\log p_{Cd} = -5.6$). When the samples show p-type conductivity at higher cadmium pressures, as is the case upon slow cooling, these hole traps must have disappeared in some way during the cooling from high temperature to room temperature. The inactivation of the V''_{Cd} hole traps can be explained by segregation of V''_{Cd} and $In^{·}_{Cd}$ centres as a separate phase (In_2Te_3 phase).

The degree to which these clustering effects occur at a certain temperature is determined by the following factors:

(1) The vacancies and foreign atoms must be able to move sufficiently quickly to make possible the formation of clusters in the time the crystals are at this temperature. When the temperature decreases the rate of diffusion of these centres will decrease and below a certain temperature will become negligible. In fig. 63 the rate of diffusion of the centres is indicated qualitatively by the dashed line.
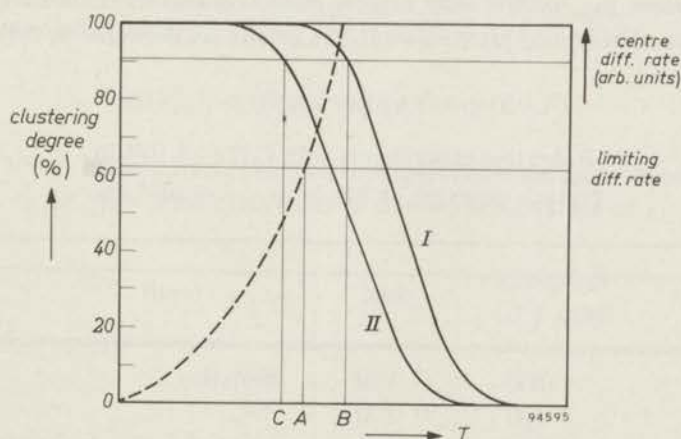

Fig. 63. The clustering degree (fully drawn lines) and the centre-diffusion rate (dashed line) as a function of the temperature. The clustering degree of a highly doped sample is given by curve I, that of a sample with a smaller concentration by curve II. At diffusion rates smaller than the limiting diffusion rate, no associates can be formed in a reasonable time; clustering degrees smaller than about 90% do not lead to the observed effects.

(2) The number of primary associates $(V_{Cd}In_{Cd})$ or $(V_{Cd}In_{Cd})'$ has to be very large at this temperature (of the order of 90%) in order to lead to results as were mentioned before. This number must be expected to increase with decreasing temperatures. In fig. 63 this is indicated by the curves I and II. Curve I represents the association in crystals with a higher, curve II the association in crystals with a lower indium content.

Combination of (1) and (2) leads to a more or less narrow temperature range

in which clustering effects are effective. In fig. 63 clustering is effective in the temperature range AB. Above the upper limit of this range (indicated by B in fig. 63) the degree of association is too small, below the lower limit (indicated by A in fig. 63) the diffusion rate of the centres is too small. It can be seen from this figure that with small indium concentrations (curve II in fig. 63) the upper limit (indicated by C in fig. 63) will pass the lower limit (indicated by A in fig. 63); then clustering effects will not occur at all. For higher indium concentrations (curve I in fig. 63) the upper limit will be displaced to higher temperatures. These considerations are confirmed by the following experiments.

Some CdTe – 5.10^{17} In crystals were reheated at 700 °C under a cadmium pressure of 5.10^{-4} atm. By rapidly quenching these crystals became insulating, slowly quenching giving rise to n-type conductivity as mentioned before. After the crystals had been made insulating they were reheated at various temperatures lower than 700 °C in a stream of dry inert gas, during a time which was short enough to avoid the crystals to come into equilibrium with the atmosphere. After this treatment the crystals were rapidly quenched and the number of charge carriers was determined after etching. The results are collected in table XXIII.

TABLE XXIII

Reheating experiments with CdTe – 5.10^{17} In
crystals prepared at 700 °C, $p_{Cd} = 5.10^{-4}$ atm

Reheating temp. (°C)	time	result
600	1 hr	insulating
590	1 hr	,,
580	1 hr	n-type; log $n = 16.7$
580	10 min	,, log $n = 16.5$
570	1 hr	,, log $n = 16.7$
540	1 hr	,, log $n = 16.6$
530	1 hr	insulating
530	3 hr	,,
500	1 hr	,,
500	10 hr	,,

From table XXIII it can be seen that for CdTe – 5.10^{17} In samples clustering effects occur in the small temperature range between 530 and 590 °C (see curve I, fig. 63).

CdTe crystals with a smaller amount of indium (2.10^{17} In cm^{-3}) did not show

these effects. As the degree of clustering is smaller the smaller the indium content, the large amount of clusters can only be reached here in a range in which the diffusion rate of the ions is no longer large enough (fig. 63 curve II).

In order to explain these experimental facts we require the presence of a considerable amount of elementary associates $(In_{Cd}V_{Cd})$ at about 550 °C. It is not necessary that all V'_{Cd} centres present in the sample are associated at this temperature. When the $(In_{Cd}V_{Cd})$ associates present unite to larger clusters the equilibrium
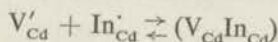
$$V'_{Cd} + In^{\cdot}_{Cd} \rightleftarrows (V_{Cd}In_{Cd})$$

is shifted to the right-hand side, which fact results into the association of the still remaining free V'_{Cd} and $In^{\cdot}_{Cd}$ centres.

At higher temperatures (600 °C and higher), however, the number of associates $(V_{Cd}In_{Cd})$ has to be very low, in order to explain the fact that the crystals remain insulating by rapidly quenching from these temperatures to room temperature. By assuming the value of $E(In_{Cd}V_{Cd})$ to be 0·5 eV ($E_{Coulomb} = 0·6$ eV) the concentration of associates $x = [(V_{Cd}In_{Cd})]$ with $\log [In^{\cdot}_{Cd}] = 17·7$ is determined by

$$x/([V'_{Cd}]-x)([In^{\cdot}_{Cd}]-x) = C \exp(E/kT)$$

with $E = 0·5$ eV. In the extreme case that the centres have the same concentration, viz. $[V'_{Cd}] = [In^{\cdot}_{Cd}] = 5.10^{17}$, this leads to the following values of x:

T (°C)	x
700	0·15 $[V'_{Cd}]$
500	0·50 $[V'_{Cd}]$

The chosen value of 0·5 eV for $E(In_{Cd}V_{Cd})$ thus leads to values of x which can explain the experimental facts.

The number of associates $(In_{Cd}V_{Cd})'$ has to be rather low at 700 °C too. In the preceding chapters it was assumed that the V''_{Cd} and $In^{\cdot}_{Cd}$ centres were completely free at this temperature. This may be not completely correct. However, when the number of associates is much smaller than the number of free V''_{Cd} centres, there will be little change in the position of the characteristic points in the $\log K_r p_{Cd} - \log n$ graphs. If however the V''_{Cd} centres are almost completely associated, these diagrams change completely as a new set of constants has to be added to describe the equilibria between the levels belonging to these associates and the energy bands. As to the value of $E(V_{Cd}In_{Cd})'$, we have to take 0·7 eV for this in order not to come in conflict with the fact that we can explain our

experimental $\log p_{Cd}$ versus $\log n$ graphs only by assuming that the V_{Cd}'' and $In_{Cd}^{\cdot}$ centres are almost completely free at 700 °C. With an indium concentration of 5.10^{17} cm^{-3} this leads to the following values for $y = [(V_{Cd}In_{Cd})']$:

T (°C)	y
700	0·24 $[V_{Cd}'']$
500	0·95 $[V_{Cd}'']$

It can be seen that the amount of these associates present at 700 °C and higher is not negligible, but not high enough to influence markedly the position of the characteristic points in the $\log p_{Cd}$ versus $\log n$ graphs.

In choosing the values of $E(In_{Cd}V_{Cd})' = 0·7$ eV and $E(In_{Cd}V_{Cd}) = 0·5$ eV, and assuming that $\alpha' = 2\alpha$, we have to take $\alpha = 0·25$ eV and $\beta = 0·15$ eV (see (3.65) and (3.66)).

3.7.3. *Anomalous effects in CdTe–Au*

With CdTe–Au an irreversible decrease in the number of holes in the *p*-type crystals can be observed upon heating at temperatures as low as 100 °C. This effect was observed in all *p*-type CdTe–Au crystals, independent of the cadmium pressure at which the crystal was made *p*-type. This is illustrated in the following example.

A freshly prepared CdTe single crystal, containing 5.10^{16} Au cm^{-3}, showed at room temperature a number of holes equal to $p = 2·5.10^{15}$ cm^{-3}.

After reheating 30 minutes at 300 °C in N$_2$, $p = 1·6.10^{14}$ cm^{-3},
,, ,, 30 ,, ,, 400 °C ,, ,, , $p = 1·6.10^{15}$ cm^{-3},
,, ,, 30 ,, ,, 500 °C ,, ,, , $p = 2·5.10^{15}$ cm^{-3},
,, ,, 30 ,, ,, 600 °C ,, ,, , $p = 2·5.10^{15}$ cm^{-3}.

The reheating time was chosen so short that equilibrium with the atmosphere was not reached. From these observations it may be concluded that some effect producing a decrease in the number of holes occurs at temperatures below 400 °C. Firing at higher temperatures apparently annihilates this effect again. After the treatment at 600 °C, a reheating at 100 °C again caused a decrease in the hole concentration:

1 hr at 100 °C in N$_2$, $p = 4.10^{14}$ cm^{-3},
3 hr at 100 °C in N$_2$, $p = 6·3.10^{13}$ cm^{-3}.

Subsequent reheating at 500 °C again increased the hole concentration to $p = 2 \cdot 5.10^{15}$ cm^{-3}.

This irreversible process is seen to occur at low temperatures. Since in the case of CdTe–In the diffusion via normal lattice sites has been found to be negligible at temperatures $T < 530$ °C, one might think of a different diffusion mechanism, viz. diffusion over interstitial sites. Such a diffusion has been observed with Cu and Ni in Ge [35]) and in PbS [36]), and has been found to be indeed much faster than the diffusion over normal lattice sites. If the equilibrium

$$Au_{Cd} \underset{\leftarrow}{\rightarrow} Au_i^{\cdot} + V'_{Cd}$$
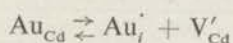
is assumed to lie at the right-hand side at 100 °C, which is the case with Cu in Ge (private communication Ir. P. Penning), the gold atoms which remained at lattice positions after quenching go to the energetically more favourable interstitial positions. By the disappearance of Au_{Cd} centres the ionization equilibrium

$$Au'_{Cd} + e^{\cdot} \rightarrow Au^{\times}_{Cd}$$
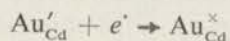
will also be shifted to the right-hand side, resulting in a decrease of the number of free holes.

Apparently, reheating of the crystals at 500 °C drives the interstitial gold again to lattice positions, restoring the original number of charge carriers. The decrease in the number of Au'_{Cd} centres is confirmed by the decrease of the peak value in the photoconductivity spectrum of these crystals after heating at 100 °C (see fig. 37).

3.8. Calculation of the solidus curve in the T–x diagram

When the constants governing the state of CdTe at high temperatures are known it is possible to calculate the deviation from stoichiometry for pure CdTe in the whole solid-state region at a given temperature and cadmium pressure. As we know the values of p_{Cd} and T belonging to the three-phase line (see fig. 5) the deviation from stoichiometry at this line, corresponding to the solidus curve in the T–x diagram, can be calculated too.

Information about the deviation from stoichiometry can be drawn from the graphs showing the concentration of centres at high temperature. From fig. 48, showing the situation for pure CdTe at 700 °C, it can be seen that three ranges can be distinguished.

Range I: In the left-hand part of the figure the concentration of V'_{Cd} centres is much larger than the concentration of the other centres. The deviation from stoichiometry (here an excess of tellurium) hence is approximately equal to this concentration.

Range III: In the right-hand part the concentration of $Cd_i^{\cdot}$ centres is much larger than the concentration of the other centres. The deviation from stoichiometry (here an excess of cadmium) is practically equal to this concentration.

Range II: In the middle part of the figure the concentrations of the V_{Cd}' and $Cd_i^{\cdot}$ centres are approximating each other and at one $K_r p_{Cd}$ value $[V_{Cd}'] = [Cd_i^{\cdot}]$. At this particular $K_r p_{Cd}$ the sample is stoichiometric.

As can be shown from the conditions at the boundaries of these ranges, in range I $K_r p_{Cd} > K_i$, in range III $K_r p_{Cd} < K_F$, the stoichiometric point being situated at $K_r p_{Cd} = (K_i K_F)^{1/2}$ (see section 3.1.5).

If a definite temperature, e.g. 900 °C, is considered in the log p_{Cd} vs $1/T$ diagram (fig. 5) the limits of the solid-state region can be seen to be situated at $p_{Cd} = 3 \cdot 4$ atm and $p_{Cd} = 6 \cdot 5.10^{-3}$ atm. As the value of log $K_r = 33 \cdot 38$ and log $K_i = 33 \cdot 22$ at this temperature, log $K_r p_{Cd} = 33 \cdot 91$ for $p_{Cd} = 3 \cdot 4$ atm, which indicates that at the upper limit $K_r p_{Cd} > K_i$ and the sample thus has an excess of cadmium (range I). The amount of this excess can be calculated from the concentration of $Cd_i^{\cdot}$, which concentration is determined by $[Cd_i^{\cdot}] = (K_r p_{Cd})^{1/2} = 8 \cdot 9.10^{16}$ cm^{-3} (table X). As to the position of the second value of p_{Cd}, viz. $p_{Cd} = 6 \cdot 5.10^{-3}$ atm, it can be shown in the same way that the sample contains an excess of tellurium as log $K_r p_{Cd} = 31 \cdot 20$, which is smaller than log K_F (range III). In this range the excess of tellurium is equal to $[V_{Cd}'] = (K_i K_F / K_r p_{Cd})^{1/2}$ (table X), which leads to $[V_{Cd}'] = 1 \cdot 6.10^{17}$ cm^{-3}.

In the middle range II the excess of cadmium or tellurium can be calculated by the expressions for the concentrations of V_{Cd}' and $Cd_i^{\cdot}$ centres in this region, viz. $[V_{Cd}'] = K_F/[Cd_i^{\cdot}]$ and $[Cd_i^{\cdot}] = K_r p_{Cd}/K_i^{1/2}$ (see table X). This procedure can be applied for various temperatures; the result is collected in table XXIV.

There are two points which deserve particular attention, viz. the maximum melting point and the point at the three-phase line where stoichiometry is obtained.

At the maximum melting point ($T = 1363$ °K), $p_{Cd} = 0 \cdot 75$ atm and log $K_r = 32 \cdot 88$, which leads to log $K_r p_{Cd} = 32 \cdot 75$. As log $K_r p_{Cd}$ is smaller than log $K_F = 32 \cdot 85$, at the maximum melting point we have an excess of tellurium approximately equal to $[V_{Cd}'] = 1 \cdot 4.10^{17}$ cm^{-3}.

According to section 3.1.5, in the stoichiometric point $K_r p_{Cd} = (K_i K_F)^{1/2}$. In the log p_{Cd} vs $1/T$ plot (fig. 61) the values of log p_{Cd} corresponding to this expression for various temperatures are represented as a straight line. Extrapolation of this line to the three-phase line shows that the stoichiometric point at the three-phase line is situated at $T = 1335$ °K and $p_{Cd} = 3 \cdot 1$ atm. Thus it is seen that stoichiometric CdTe melts about 28 °K below the maximum melting point. In fig. 61 it can be seen that the lines, which connect the cadmium pressures at which CdTe doped with a small amount of copper or indium stops to be n-type, approach this particular cadmium pressure if they are extrapolated to the phase boundary.

TABLE XXIV

Calculation of the deviation from stoichiometry at the three-phase line in the *T–x* diagram

| $T(^{\circ}K)$	10^3T^{-1}	$\log K_i$	$\log K_F$	$\log p_{Cd}$	$\log\ K_r$	deviation from stoichiometry	
						excess cadmium (cm⁻³)	excess tellurium (cm⁻³)
1000	1·000	31·94	31·45	−3·13	33·97		1·86.10¹⁶
				−0·22		7·45.10¹⁶	
1112	0·900	32·78	31·96	−2·92	33·56		1·13.10¹⁷
				0·28		9·35.10¹⁶	
1173	0·852	33·22	32·40	−2·18	33·38		1·62.10¹⁷
				0·53		8·92.10¹⁶	
1250	0·800	33·65	32·50	−1·42	33·16		1·63.10¹⁷
				0·78		8·85.10¹⁶	
1333	0·750	34·08	32·76	−0·57	32·96		1·66.10¹⁷
				0·53		7·76.10¹⁶	
1343	0·745	34·13	32·79	−0·47	32·79		2·00.10¹⁷
				0·40			3·24.10¹⁶
1350	0·740	34·18	32·82	−0·38	32·92		1·70.10¹⁷
				0·20			5·13.10¹⁶
1363	0·732	34·26	32·85	−0·13	32·88		1·45.10¹⁷

3.9. Calculation of the energies involved in the transfer of cadmium between crystal and vapour

The knowledge of the values of K_r and K_F as a function of the temperature (fig. 60) enables us to calculate the energies involved in the transfer into the vapour phase of an interstitial cadmium atom and of a cadmium atom at a lattice position.
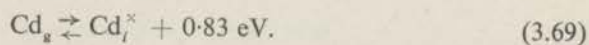
The constant K_r is the reaction constant of the reaction

$$Cd_g \rightleftarrows Cd_i^{\cdot} + e' - E_r. \tag{3.67}$$

Since $K_r = a \exp(-E_r/kT)$, E_r is the slope of $\log K_r$ vs $1/T$ and is found to be equal to —0·81 eV. According to table IX (fig. 44),
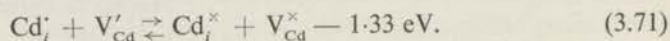
$$Cd_i^{\cdot} + e' \rightleftarrows Cd_i^{\times} + 0.02 \text{ eV}. \tag{3.68}$$
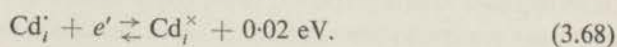
Combination of (3.67) and (3.68) leads to

$$Cd_g \rightleftarrows Cd_i^{\times} + 0.83 \text{ eV}. \tag{3.69}$$
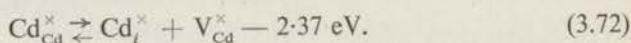
Thus 0·83 eV is required to transfer a neutral cadmium atom from an interstitial site to the vapour phase. The constant K_F is defined by the reaction

$$Cd_{Cd}^{x} \rightleftarrows Cd_{i}^{\cdot} + V_{Cd}' - E_F. \tag{3.70}$$
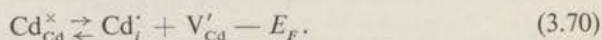
From the slope of log K_F vs $1/T$ it is found that $E_F = 1·04$ eV. From fig. 44 it is seen that

$$Cd_{i}^{\cdot} + V_{Cd}' \rightleftarrows Cd_{i}^{x} + V_{Cd}^{x} - 1·33 \text{ eV}. \tag{3.71}$$

Combination of (3.70) and (3.71) leads to

$$Cd_{Cd}^{x} \rightleftarrows Cd_{i}^{x} + V_{Cd}^{x} - 2·37 \text{ eV}. \tag{3.72}$$

Thus the energy required to transfer a cadmium atom from a lattice position to an interstitial position with the formation of neutral V_{Cd}^{x} and Cd_{i}^{x} centres is 2·37 eV. Combination of (3.69) and (3.72) gives

$$Cd_{Cd}^{x} \rightleftarrows Cd_{g} + V_{Cd}^{x} - 3·20 \text{ eV}.$$
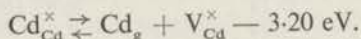
Hence an energy of 3·20 eV is required to transfer a neutral cadmium atom from a lattice site to the vapour phase with the formation of a neutral vacancy.

APPENDIX

THE TYPE OF BONDING IN CdTe

Though no accurate measurements of the type of bonding in CdTe have been performed till now, some speculations can be made about the amount of covalent or ionic character of the bonds in CdTe. Appel [8]) estimated the amount of covalent contribution in the bonds higher than in ZnS for which 65% of covalent contribution is mentioned by Winkler [37]). The high polarizability of the tellurium ions leads to a deformation of the electron sphere which leads to an increased electron density between the cadmium and the tellurium atoms, leading to a covalent contribution in the Cd–Te bond.

Some information about the covalent or ionic character of the bonds can be obtained from the values of $\varepsilon_o = n^2$ and ε_s. A large difference between these constants indicates a large ionic, a small difference a large covalent contribution to the bonding. In the group IV elements like germanium or silicon the difference between ε_s and ε_o is zero. For compounds like NaCl and AgCl the difference between ε_s and ε_o is very large, which indicates a large amount of ionic bonding.

	ε_o	ε_s
NaCl	2·2	5·7
AgCl	4·04	12·3

Compounds with a mixed character show a smaller difference between ε_o and ε_s, e.g.

	ε_o	ε_s
ZnS	5·07	8·3
CdTe	7·6	11·0

Szigeti [38]) derived an expression which holds for crystals with a simple cubic structure and which gives a relation between the dielectric constants, the transversal optical vibration frequency and the so-called "dynamic effective charge" of the ions q:

$$\varepsilon_s = \varepsilon_o + 4\pi N q^2 (\varepsilon_o + 2)^2 / 9 M \omega_t^2, \tag{A.1}$$

in which N is the number of molecules per unit of volume and M is the reduced mass of the ions. The value of $M\omega_t^2$ can be calculated from the expression

$$1/\varkappa = \tfrac{1}{3}R^2 N M\omega_t^2(\varepsilon_s + 2)/(\varepsilon_o + 2) \tag{A.2}$$

in which $\varkappa$ is the compressibility and R is the distance between two nearest neighbours.

With the known values $\varkappa = 23\cdot3.10^{-7}$ cm²/kg [39]), $\varepsilon_s = 11\cdot0$ (section 1.6.5) and $\varepsilon_o = 7\cdot6$ (section 1.7.5) it is possible to calculate $M\omega_t^2 = 7\cdot85.10^4$ dyne cm⁻¹ (or $\omega_t = 2\cdot81.10^{13}$ rad sec⁻¹ or $\lambda_t = 67$ μ). Now q can be calculated to be

$$q = 3\cdot7.10^{-10} = 0\cdot76\ e = 0\cdot38 \times 2e.$$

For ionic compounds the following values are given by Szigeti [38]):

compound	q
LiF	$0\cdot87\ e$
NaF	$0\cdot93\ e$
NaCl	$0\cdot74\ e$
KCl	$0\cdot80\ e$

Compounds with a mixed character show the following values of q:

compound	q	q/ze
ZnS	$0\cdot96\ e$ [39])	$0\cdot48$
SiC	$1\cdot28\ e$ [39])	$0\cdot32$
SiC	$1\cdot00\ e$ [40])	$0\cdot25$

As a rule the value of q does not differ much from unity. The value of q/ze, in which ze is the charge of the ions when the compound would be purely ionic, can be seen to decrease the more the compound shows a covalent character.

Unfortunately, this method does not allow us to determine which atom has attracted the charge, i.e. in our case whether cadmium is positive and tellurium is negative or vice versa. Therefore the exact amount of covalent character cannot be determined. Another method to estimate the amount of covalent character is to calculate the experimental lattice energy by a Haber-Born cycle and to

compare the value obtained with the theoretical value of the lattice energy calculated with the assumption that the lattice is purely ionic. The Haber-Born cycle leads to

$$U_{\text{H.B.}} = \Delta H_f^0 + S_{\text{Cd}} + S_{\text{Te}} + \tfrac{1}{2}D_{\text{Te}_2} + I_{\text{Cd}^{2+}} - E_{\text{Te}^{2-}},$$

in which

$U = $ lattice energy;

$\Delta H_f^0 = $ standard heat of formation which is —24·30 kcal/mole at 25 °C [10]);

$S_{\text{Cd}} = $ heat of sublimation of cadmium (the published values [10]) are 28 kcal/g.at. at 0 °K and 26·28 kcal/g.at. at the melting point (320·9 °C);

$S_{\text{Te}} = $ heat of sublimation of tellurium, for which was taken the heat of melting + the heat of vaporisation at the melting point $= 4·28 + 13·3 = 17·6$ kcal/g.at. at 450 °C;

$D_{\text{Te}_2} = $ dissociation energy of Te_2. The value which is published is 53·0 kcal/mole [41]);

$I_{\text{Cd}^{2+}} = $ ionization energy of $\text{Cd}^{2+} = 593$ kcal/g.at. [42]);

$E_{\text{Te}^{2-}} = $ electron-affinity of $\text{Te}^{2-} = $ —82 kcal/g.at. [43]).

Using these values with consideration of some uncertainty in the values of S_{Cd}, S_{Te} and $E_{\text{Te}^{2-}}$ the value of U is calculated to be

$$U_{\text{H.B.}} = 24·30 + 28\ (\pm 5) + 20\ (\pm 5) + 26·5 + 593 + 80\ (\pm 40) = 768 \pm 50 \text{ kcal mole}^{-1}.$$

The theoretical value of U can be calculated by making use of

$$U = (1-1/n)ANz^2e^2/r \qquad\qquad (A.3)$$

in which $n = 9$, the $1-1/n$ term taking into account the Born repulsion forces; $A = $ the Madelung constant, being 1·639 for CdTe; $N = $ the Avogadro number; and $r = $ the nearest neighbour distance, being $\tfrac{1}{4}a\sqrt{3}$ ($a = $ cell constant $= 6·41$ Å). This leads to $U = 695$ kcal/mole.

The values of $U_{\text{theor.}}$ and $U_{\text{H.B.}}$ of the other cadmium chalcogenides are given in Landolt-Börnstein:

	$U_{\text{theor.}}$ (kcal/mole)	$U_{\text{H.B.}}$ (kcal/mole)
CdO	873	910
CdS	771	808
CdSe	747	800
CdTe	695	768 $\pm$ 50

The difference between $U_{\text{theor.}}$ and $U_{\text{H.B.}}$ shows a slight tendency to increase in the sequence CdO–CdTe. Since for purely ionic compounds both methods lead to nearly the same value, e.g.

	$U_{\text{theor.}}$ (kcal/mole)	$U_{\text{H.B.}}$ (kcal/mole)
NaCl	180·3	184·7
LiF	244·3	246·0
CsF	172·7	177·2

it may be concluded that the deviation found with CdTe (and to a smaller degree also with CdSe and CdS) indicates a certain amount of covalent bonding.

A comparison between the observed internuclear distances and the calculated ionic or covalent distances leads to an analogous effect in a definite sequence of compounds, e.g. [44]

	$d_{\text{ion}} - d_{\text{exp}}$	$d_{\text{cov}} - d_{\text{exp}}$
CdO	0·05	—
CdS	0·17	0·05
CdSe	0·21	0·00
CdTe	0·24	0·00

The deviation of the experimental values of d from the calculated ionic internuclear distance becomes the more pronounced the more we descend in this sequence.

REFERENCES

[1]) C. Wagner and W. Schottky, Z. physik. Chem. B **11**, 163-210, 1931.
 W. Schottky, Z. Elektrochem. **45**, 33, 1939.
[2]) F. A. Kröger, H. J. Vink and J. van den Boomgaard, Z. phys. Chem. **203**, 1-74, 1954.
[3]) J. Bloem, Philips Res. Repts **11**, 273-335, 1956.
[4]) M. Kobayashi, Z. anorg. Chem. **69**, 1-11, 1911.
[5]) R. W. Smith, Semiconducting Materials, Butterworths Publications, London, 1951, p. 202.
[6]) R. H. Bube, Phys. Rev. **98**, 431-433, 1955.
[7]) D. A. Jenny and R. H. Bube, Phys. Rev. **96**, 1190-1191, 1954.
[8]) J. Appel, Z. Naturf. **9a**, 265-267, 1954.
 J. Appel and G. Lautz, Physica **20**, 1110-1114, 1954.
[9]) W. G. Pfann, J. Metals, N.Y. **4**, 747-753, 1952; **4**, 861-865, 1952.
[10]) Selected Values of Chem. Thermodynamic Properties, Circ. Nat. Bur. Stand. 500.
[11]) J. Bloem and F. A. Kröger, Z. phys. Chem. **7**, 15-26, 1956.
[12]) J. R. Haynes and H. B. Briggs, Bull. Amer. phys. Soc. **2**, 14, 1952.
[13]) R. Newman, Phys. Rev. **91**, 1313-1314, 1953.

[14]) J. R. Haynes, Phys. Rev. **98**, 1866-1868, 1955.
[15]) O. V. Losev, Phys. Z. **34**, 397, 1933.
[16]) O. V. Losev, C. R. Acad. Sci. U.R.S.S. **29**, 363-364, 1940.
[17]) K. Lehovec, C. A. Accardo and E. Jamgochian, Phys. Rev. **83**, 603-607, 1951.
[18]) K. Lehovec, C. A. Accardo and E. Jamgochian, Phys. Rev. **89**, 20-25, 1953.
[19]) F. Ostwald and R. Schade, Z. Naturf. **9a**, 611-617, 1954.
[20]) J. Tauc, Czech. J. Phys. **3**, 282-302, 1953.
[21]) A. I. Anselm and V. I. Klachkin, J. exp. theor. Phys. **22**, 297-302, 1952.
[22]) T. A. Kontorova, J. techn. Phys., Moscow **24**, 1291-1297, 1954.
[23]) J. H. Simpson, Proc. roy. Soc. A **197**, 269-281, 1949.
[24]) W. Shockley, Electrons and holes in semiconductors, van Nostrand Cy., N.Y., 1950, p. 278.
[25]) F. Seitz, Phys. Rev. **73**, 549-564, 1948.
[26]) F. A. Kröger, H. J. Vink and J. Volger, Philips Res. Repts **10**, 39-76, 1955.
[27]) A. R. Hutson, Rep. 17th Ann. Conf. Phys. Electron. 1957, p. 76.
[28]) P. F. Browne, J. Electronics **2**, 154-165, 1957.
[29]) F. A. Kröger and H. J. Vink, Solid State Physics, Academic Press Inc., N.Y., 1956, volume 3, pp. 307-435.
[30]) G. Brouwer, Philips Res. Repts **9**, 366-377, 1954.
[31]) L. H. Hall, J. Bardeen and F. J. Blatt, Phys. Rev. **95**, 559-560, 1954.
   G. G. Macfarlane and V. Roberts, Phys. Rev. **97**, 1714-1716, 1955.
[32]) J. Volger, Disc. Faraday Soc. **23**, 63-71, 1957.
[33]) N. F. Mott and R. W. Gurney, Electronic processes in ionic crystals, Clarendon Press, Oxford, 1953, p. 29.
[34]) J. Teltow, Halbleiterprobleme, Fr. Vieweg, Braunschweig, 1956, Bd. III, pp. 26-58.
[35]) F. van der Maessen and J. A. Brenkman, J. electrochem. Soc. **102**, 229-234, 1955.
   F. C. Frank and D. Turnbull, Phys. Rev. **104**, 617-618, 1956.
[36]) J. Bloem and F. A. Kröger, Philips Res. Repts **12**, 281-302, 1957; **12**, 303-308, 1957.
[37]) H. G. F. Winkler, Struktur und Eigenschaften der Kristalle, J. Springer, Berlin, Göttingen, 1950.
[38]) B. Szigeti, Trans. Faraday Soc. **45**, 155-166, 1949; Proc. roy. Soc. A **204**, 51-62, 1950.
[39]) E. Burstein and J. Egli, Adv. electron. and electr. Phys., Academic Press, N.Y., 1955, volume VII, pp. 1-77.
[40]) F. A. Kröger and J. Lely, to be published.
[41]) Gmelin's Handbuch der anorganischen Chemie, Verlag Chemie Berlin, 1940, System No. **11**, p. 165.
[42]) A. E. van Arkel and J. H. de Boer, La Valence et l'Electrostatique, Libr. F. Alcan, Paris, 1936, p. 64.
[43]) K. Doerffel, Z. anorg. alg. Chem. **281**, 212-216, 1955.
[44]) O. K. Rice, Electronic structure and chemical binding, McGraw Hill Book Co., N.Y. and London, 1940, p. 335.
[45]) P. Goldfinger and C. Drowart, Final technical Report, ARDC, AF 61 (514)-868, Oct. 1956.
[46]) F. Herman, J. Electronics **1**, 103, 1955.
[47]) Y. Haven and J. H. van Santen, Philips Res. Repts **7**, 474, 1952.

Summary

In this thesis the relation is studied between the electrical and optical properties of single crystals of cadmium telluride and the conditions of preparation.

In chapter 1 the p–T–x diagram of the system cadmium-tellurium is described. This study shows that the maximum melting point of the compound cadmium telluride is situated at 1090 °C ($p_{Cd} = 0.75$ atm). Cadmium telluride contains an excess tellurium at this point, viz. $1.45.10^{17}$ at. cm^{-3} ($= 1.03.10^{-3}$ at. %). Stoichiometric cadmium telluride melts at 1062 °C ($p_{Cd} = 3.1$ atm). In this chapter a description is given of the way in which cadmium telluride is purified by the method of zone refining, of the zone levelling of foreign atoms into pure cadmium telluride and of the growing of single crystals (section 1.4). The reheating of single crystals in the temperature region of 700-1000 °C at various cadmium pressures, followed by quenching to room temperature, is an important part of this study. Various electrical and optical measurements were performed with these reheated samples (section 1.6). The thermo-electromotive force was measured as a function of the number of charge carriers; the Hall effect as a function of the cadmium pressure at which the samples were reheated. The Hall effect of various samples was also measured as a function of the temperature in combination with measurements of the resistance.

The optical measurements are described in section 1.7. Transmission measurements at various temperatures, photo-luminescence and photo-conductivity measurements were performed with samples prepared at differing conditions.

In chapter 2 an interpretation is given of the measurements of chapter 1. Interpretation of the thermo-emf. measurements leads to a value of the density-of-states effective mass. The value of the effective-mass ratio varies between $m_n^*/m = 0.13$-0.066 for electrons and $m_p^*/m = 0.41$-0.22 for holes, depending on the value of the transport energy of electrons and holes in the conduction or valence band, respectively.

An analysis of the Hall effect as a function of the temperature leads to values for the ionization energies of the various centres in cadmium telluride (table IX). For n-type samples with shallow donors the density-of-states effective-mass ratio can also be calculated from this analysis. This leads to $m_n^*/m = 0.14 \pm 0.04$.

A hydrogen-like approximation for the shallow donor level leads to a value for the inertial effective mass, viz. $(m_n^*)_i = 0.147$.

Transmission measurements lead to a value for the band gap of 1.50 eV at room temperature. The variation of the band gap as a function of the temperature is found to be $2.34.10^{-4}$ to $5.44.10^{-4}$ eV/°K between 77 °K and 800 °K.

The interpretation of the photoluminescence and the photoconductivity measurements is still uncertain (section 2.4). In the spectra obtained, next to a peak which is independent of the composition of the samples and which can be ascribed to a band-band transition, other peaks are found which can be brought qualitatively in agreement with transitions between levels caused by known centres present in cadmium telluride and one of the bands.

In chapter 3 a theoretical discussion is given of the various equilibria which determine the state of cadmium telluride at high temperature. When the equilibrium constants are known, it is possible to calculate the concentration of charge carriers and centres at room temperature as a function of the cadmium pressure at which the samples are reheated. Various band schemes were assumed, and the room-temperature situation resulting from each scheme is given in diagrams showing the number of charge carriers at room temperature as a function of the cadmium pressure at which the samples were reheated.

A qualitative comparison between the experimental and theoretical diagrams leads to the adoption of a definite band scheme. In this scheme two levels are ascribed to the cadmium vacancy; one level is ascribed to interstitial cadmium and to indium (as a specific donor) and to gold (as a specific acceptor). A quantitative discussion of some characteristic points in the experimental and theoretical diagram leads to values of some equilibrium constants which cannot be measured directly, viz. the Frenkel constant K_F and the reduction constant K_r, which describes the equilibrium crystal-vapour.

The variation of these constants with the temperature leads to values of the energy required to transfer a cadmium atom from a lattice site to an interstitial position and of the energies

required to bring a cadmium atom at a lattice site or an interstitial cadmium to the vapour phase (section 3.9).

Association effects play an important role during the quenching of the samples to room temperature. In section 3.7 an analysis of these effects is given for CdTe–In, CdTe–Au, CdTe–Ag and CdTe–Cu crystals. For CdTe–In crystals the occurrence of these effects is dependent on the concentration and only takes place in a narrow temperature region. The effects with CdTe–Au, CdTe–Ag and CdTe–Cu samples occur at much lower temperature.

In an appendix a qualitative discussion is given of the type of bonding in cadmium telluride.

Samenvatting

In dit proefschrift wordt het verband bestudeerd, dat er bestaat tussen de elektrische en de optische eigenschappen van eenkristallen van cadmium telluride en de omstandigheden waaronder deze kristallen gemaakt en nabehandeld zijn.

In hoofdstuk 1 wordt beschreven op welke wijze het p–T–x diagram van het systeem cadmium-telluur bepaald wordt. Dit onderzoek toont aan, dat het maximum smeltpunt van de verbinding cadmium telluride bij 1090 °C ($p_{Cd} = 0.75$ atm) ligt. In dit punt blijkt cadmium telluride een overmaat telluur te bevatten en wel $1.45 \cdot 10^{17}$ at. cm^{-3} ($= 1.03 \cdot 10^{-3}$ at. %), terwijl stoichiometrisch cadmium telluride smelt bij 1062 °C ($p_{Cd} = 3.1$ atm). Verder wordt in dit hoofdstuk beschreven hoe cadmium telluride met de "zone-refining" methode gezuiverd wordt, hoe aan het zuivere materiaal met de "zone-levelling" methode homogeen een bepaalde hoeveelheid vreemde bestanddelen kan worden toegevoegd en hoe uit dit materiaal eenkristallen kunnen worden verkregen (section 1.4).

Het temperen van eenkristallen in het temperatuurgebied van 700 °C-1000 °C onder verschillende cadmium drukken, gevolgd door afschrikken naar kamertemperatuur vormt een belangrijk onderdeel van het gehele onderzoek. Aan deze getemperde kristallen werden verschillende elektrische en optische metingen verricht, die in paragraaf 1.6 worden beschreven. De thermokracht werd bepaald als functie van het aantal ladingsdragers; het Hall-effect als functie van de cadmium druk, waaronder de kristallen bij een bepaalde temperatuur getemperd werden. Van verschillende kristallen werd het Hall-effect bepaald als functie van de temperatuur, welke laatste metingen gecombineerd werden met weerstandsmetingen.

Van de optische metingen, die in paragraaf 1.7 worden beschreven, zijn te noemen: transmissiemetingen bij verschillende temperaturen, photo-luminescentie, photo-geleidingsmetingen en het bepalen van de brekingsindex van cadmium telluride.

In hoofdstuk 2 wordt getracht een interpretatie te geven van de metingen uit hoofdstuk 1. Interpretatie van de thermokracht-metingen leidt tot een waarde voor de effectieve massa ("density-of-states effective mass"). Afhankelijk van bepaalde onderstellingen leidt dit voor elektronen tot een massaverhouding $m_n^*/m = 0.13$-0.066 en voor gaten (holes) tot $m_p^*/m = 0.41$-0.22. Een analyse van het Hall-effect als functie van de temperatuur leidt tot waarden voor de ionisatie energieën van de verschillende centra, die in cadmium telluride kunnen voorkomen (tabel IX).

Voor n-type kristallen met een geringe donordiepte is het mogelijk uit deze analyse ook te concluderen tot een effectieve massaverhouding (density-of-states effective mass ratio), nl. tot $m_n^*/m = 0.14 \pm 0.04$. Toepassing van een waterstofachtige benadering op het ondiepe donor niveau geeft een waarde voor de verhouding der trage effectieve massa's (m_n^*/m_t) = 0.147.

Uit de transmissie-metingen werd geconcludeerd tot een bandafstand van 1.50 eV bij kamertemperatuur. Van 77 °K tot 800 °K varieert de bandafstand met $2.34 \cdot 10^{-4}$ tot $5.44 \cdot 10^{-4}$ eV/°K. De interpretatie van de photo-luminescentie en de photo-geleidingsmetingen is nog zeer onzeker (paragraaf 2.4).

In de verkregen spectra worden naast een piek, die onafhankelijk is van de samenstelling der kristallen en die daarom toegeschreven wordt aan een band-band overgang, andere pieken gevonden, die kwalitatief in overeenstemming zijn te brengen met overgangen tussen niveaus veroorzaakt door bepaalde centra in cadmium telluride en een der banden.

In hoofdstuk 3 wordt een theoretische beschouwing gegeven over de evenwichten, die, tijdens het temperen op hoge temperatuur onder de dampdruk van een der componenten, de toestand bepalen van zuiver cadmium telluride en van cadmium telluride waaraan indium (als specifieke donor) of goud (als een specifieke acceptor) is toegevoegd. Kennis van de evenwichtsconstanten

maakt het mogelijk om de concentratie bij kamertemperatuur van de verschillende centra, die in cadmium telluride kunnen optreden, als functie van de cadmium druk, waaronder getemperd werd, te berekenen. Voor verschillende modellen van het bandenschema van cadmium telluride is het nu mogelijk het aantal ladingsdragers bij kamertemperatuur als functie van de cadmium-druk, waaronder getemperd werd, weer te geven in een diagram. Een kwalitatieve vergelijking met de experimentele diagrammen leidde tot aanname van een bepaald bandenschema voor cadmium telluride. In dit model worden aan de cadmium-vacature twee niveaus tussen de banden toegeschreven; aan interstitieel cadmium, indium en goud elk één niveau.

Een kwantitatieve beschouwing van enkele karakteristieke punten in de theoretische en experimentele diagrammen leidt tot de waarden van enkele evenwicht-constanten, die langs andere weg niet bepaald kunnen worden (o.a. de Frenkel constante K_F en de reductie constante K_r, die het evenwicht kristal-damp bepaalt). Het verloop van deze constanten als functie van de temperatuur maakt het mogelijk om de energie te berekenen, die nodig is om een cadmium atoom van een roosterplaats naar een interstitiële plaats te brengen en om de energieën te berekenen, die nodig zijn om een cadmium atoom van een roosterplaats, respectievelijk interstitiële plaats, naar de gasfase te brengen (paragraaf 3.9).

Associatie-effecten blijken een grote rol te spelen tijdens het afschrikken van kristallen naar kamertemperatuur. In paragraaf 3.7 wordt een analyse gegeven van de effecten, die bij CdTe–In, CdTe–Au, CdTe–Ag en CdTe–Cu geconstateerd werden. Bij CdTe–In kristallen blijkt het optreden van deze effecten sterk afhankelijk te zijn van de concentratie en slechts in een bepaald temperatuur traject voor te komen. De effecten bij CdTe–Au, CdTe–Ag en CdTe–Cu kristallen treden bij veel lagere temperatuur op.

In een aanhangsel wordt tenslotte een kwalitatieve beschouwing gegeven over het karakter van de binding in cadmium telluride.
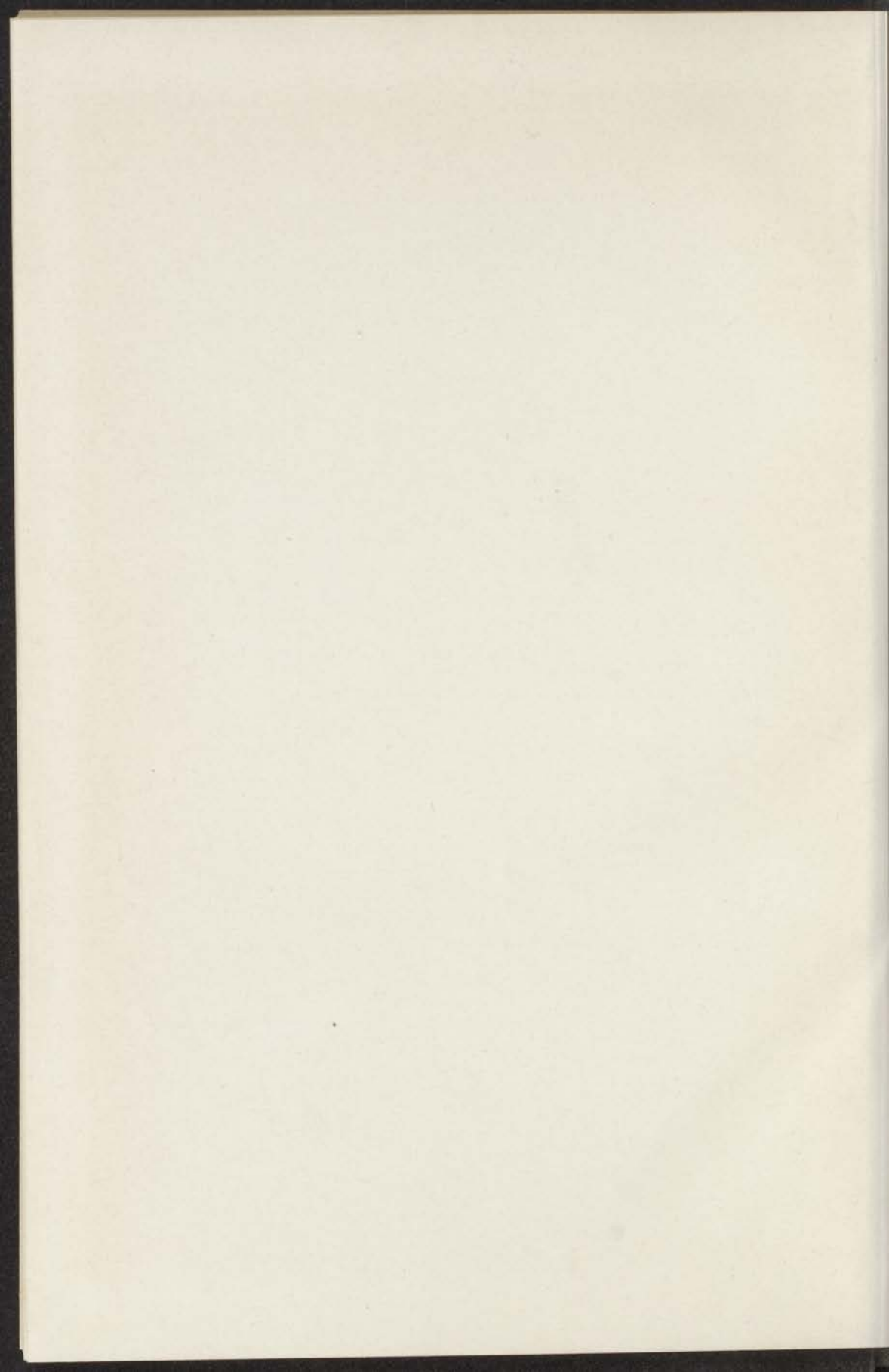
Op verzoek van de Faculteit der Wis- en Natuurkunde volgen hier enige persoonlijke gegevens.

Na het behalen van de onderwijzers-acte aan de Christelijke Kweekschool te Leiden in 1934 (hoofdacte 1937) opende de toenmalige situatie bij het onderwijs zo weinig perspectieven, dat ik door de commissie T.O.W.O. in staat gesteld werd het onderwijs aan de M.T.S. ,,Amsterdam" te volgen. In 1940 deed ik eindexamen in de afdelingen Chemische Techniek en Suikertechniek. In hetzelfde jaar trad ik in dienst bij de Staatsmijnen in Limburg, waar ik werkzaam was op het Stikstofbindingsbedrijf. In 1946 werd ik door de Directie der Staatsmijnen door mijn overplaatsing naar het Verkoopkantoor der Staatsmijnen te 's Gravenhage in de gelegenheid gesteld aan de Rijksuniversiteit te Leiden te studeren. Onder leiding van de hoogleraren Dr. C. J. F. Böttcher, bij wie ik de laatste jaren van mijn studie als hoofd-assistent werkzaam was, Dr. A. E. van Arkel, Dr. E. Havinga, Dr. H. A. Kramers en Dr. L. J. Oosterhoff, beeindigde ik in april 1952 mijn studie door het afleggen van het doctoraal examen (hoofdvak physische scheikunde, bijvak theoretische natuurkunde).

In januari 1953 trad ik in dienst bij de N.V. Philips' Gloeilampenfabrieken, waar ik op het Natuurkundig Laboratorium het in dit proefschrift beschreven onderzoek mocht verrichten.

STELLINGEN

I

De door Browne aan tellurium vacatures toegeschreven brede emissieband in het emissie-spectrum van cadmium telluride kan beter geïnterpreteerd worden als te worden veroorzaakt door de aanwezigheid van cadmium vacatures of vreemde atomen.

P. F. Browne, J. of Electronics **2**, 154–165, (1957)

II

Uit het feit, dat met behulp van de Clausius-Mosotti vergelijking polariseerbaarheden aan ionen kunnen worden toegekend, die voor een bepaald ion in verschillende verbindingen slechts een spreiding van 5% vertonen, volgt niet dat de polariseerbaarheid van een ion onafhankelijk zou zijn van de omgeving waarin het zich bevindt.

S. Roberts, Phys. Rev. **76**, 1215–1220, (1949)
77, 258–263, (1950)
81, 865–868, (1951)

III

De verschijnselen, die door Hirschberg gevonden worden bij het photochemisch bleken van spiropyranen, kunnen verklaard worden door aan te nemen, dat in het reactiemengsel, dat uit de ongekleurde verbinding ontstaat door instralen met ultraviolet licht, twee verbindingen voorkomen van verschillende structuur.

Y. Hirshberg, J. Am. Chem. Soc. **78**, 2304–2312, (1956)

IV

De door Hauffe en Wagner afgeleide formules voor de berekening van het verloop van de thermodynamische potentiaal als functie van de samenstelling van een stof, hebben geen algemene geldigheid.

K. Hauffe en C. Wagner, Z. Elektrochem. **46**, 160–170, (1940)
C. Wagner, Thermodynamics of alloys, Addison-Wesley Press, Cambridge, U.S.A. 1952, pg. 71.

V

De door Satterthwaite en Ure uit Hall-effect metingen berekende afwijking van de stoechiometrie in Bi_2Te_3, berust op een eenzijdige interpretatie van deze metingen.

C. B. Satterthwaite en M. W. Ure, Phys. Rev. **108**, 1164–1170, (1957)

VI

Het verband, dat door Kruh gelegd wordt tussen de temperatuur afhankelijkheid van de oppervlakte spanning en de structuur van gesmolten glas, verdient nadere overweging bij het structuur onderzoek van glas.

R. F. Kruh, J. Chem. Phys. **25**, 1085–1086, (1956)
R F. Kruh en A. B. Bestul, J. Chem. Phys. **27**, 319–320, (1957)

VII

De door K. P. Sinha en A. P. B. Sinha beschreven structuur voor γ-Fe_2O_3 is onjuist.

K. P. Sinha en A. P. B. Sinha, Z. anorg. Chem. **293**, 228–232, (1957)
G. W. van Oosterhout en C. J. M. Rooymans, Nature **181**, 44, (1958)

VIII

De methode, die door Weiser toegepast wordt voor het bepalen van p-T diagrammen van ontledende stoffen, kan aanleiding geven tot ernstige fouten.

K. Weiser, J. phys. Chem. **61**, 513–515, (1957)

IX

De afwijking, die Hartmann en Svendsen vinden in de ionisatieenergie van dureen, ten opzichte van de verwachtingswaarde, moet toegeschreven worden aan een foutieve meting.

H. Hartman en M. B. Svendsen, Z. phys. Chem. **11**, 16–29, (1957)
C. v. d. Stolpe, Solvatie van jodium in organische oplosmiddelen. Dissertatie Amsterdam 1953.

X

De door Hueter en Bolt gegeven formules voor de stralingsdruk en de impedantie van een cilindervormige stralingsbron, worden ten onrechte door hen gebruikt onder condities, waaronder deze formules niet gelden.

T. F. Hueter en R. H. Bolt, Sonics, Chapman & Hall, London 1955, pp. 54–59.
P. M. Morse, Vibration and sound, McGraw Hill, New York 1948.

XI

De opvatting van Kröger, Diemer en Klasens betreffende de natuur van een metaal-halfgeleider contact, dat aan de wet van Ohm voldoet, verdient de voorkeur boven die van Smith en Rose.

F. A. Kröger, G. Diemer en H. A. Klasens, Phys. Rev. **103**, 279, (1956)
R. W. Smith en A. Rose, Phys. Rev. **97**, 1531, (1955)

XII

Door het vroegtijdig afbreken van de reeksontwikkeling voor de magnetische potentiaal geeft Fereday in feite een berekening voor een magneet met constante dH/dx, inplaats van een berekening voor een constante H dH/dx, zoals door hem beoogd wordt.

R. A. Fereday, Proc. phys. Soc., London, **42**, 251–263, (1930)